UNIVERSITY OF ALBERTA

A Laboratory Study of Aqueous Colloidal Gas Aphrons for Enhanced Oil Recovery Applications

by

Shivana Rhea Samuel

A thesis submitted to the Faculty of Graduate Studies and Research in partial fulfillment of the requirements for the degree of

Master of Science

in

Petroleum Engineering

Department of Civil and Environmental Engineering

Spring 2012

Edmonton, Alberta

Examining Committee

Dr. Hassan Dehghanpour, Chair and Examiner, Civil and Environmental Engineering

Dr. Ergun Kuru, Supervisor, Civil and Environmental Engineering

Dr. Japan Trivedi, Co-Supervisor, Civil and Environmental Engineering

Dr. Phillip Choi, External Examiner, Chemical and Materials Engineering

ABSTRACT

Aqueous colloidal gas aphrons (CGAs) have previously been used as drilling fluids because of their pore blocking ability which significantly reduces formation damage. The aim of this study is to generate aqueous colloidal gas aphrons, to examine its stability and rheology as well as to investigate its suitability as an enhanced oil recovery fluid.

Different polymers and surfactants were tested to create the most stable aphrons. To determine the optimum formulation; (aphron) bubble size over time, bubble size distribution over time and fluid rheology were examined.

To determine the CGA fluid suitability for enhanced oil recovery applications, experiments were conducted using a visual cell and radial cell filled with porous media. Flooding experiments were performed using the CGA fluid as well as other comparable fluids. The pressure drop, total recovery data and breakthrough time were measured for both cells while time lapse images were taken for the visual cell.

ACKNOWLEDGEMENTS

It is a pleasure to extend my sincere gratitude and appreciation to my supervisors, Dr. Ergun Kuru and Dr. Japan Trivedi, whose valuable advice, guidance, encouragement and support made this thesis possible.

I am also grateful to Mr. Stephen Gamble for his technical support and patience.

I would also like to show my gratitude to my colleagues for their continuous support and encouragement throughout my graduate program.

Lastly, I would like thank Halliburton for donating samples used in this research study.

TABLE OF CONTENTS

LIST OF TABLES

LIST OF FIGURES

1. INTRODUCTION

1.1 Overview and Background of Problem

The increasing demand for energy coupled with declining global oil production and more stringent environmental policies have resulted in the need for reducing cost while improving oil recovery. This has led to an increased need for improved oil recovery and drilling technologies. During the past fifty years an array of improved/enhanced oil recovery (EOR) methods have been developed and applied to mature and mostly depleted oil reservoirs. These methods improve the efficiency of oil recovery compared with primary and secondary recovery mechanisms. In primary recovery oil is displaced from the reservoir and into the wellbore using its own reservoir energy such as natural water drive, gascap drive or gravity drainage. In secondary recovery a fluid (most commonly water) is injected into the reservoir via injection wells in order to maintain reservoir pressure and continue oil displacement into the wellbore. Upon the completion of secondary recovery much of the original oil in place (OOIP) still resides in the reservoir. Enhanced oil recovery methods are then aimed at recovering this residual oil.

EOR methods can be loosely classified into three areas: gas injection, chemical flooding and thermal flooding. There are a variety of different methods that fall under these three categories. Chemical flooding is comprised of alkaline, polymer and polymer/surfactant methods. Colloidal gas aphrons are described as micro-bubbles which are 10-100 microns in size with a gas containing inner core encapsulated by a thin surfactant film. Aqueous CGA fluids are comprised of water as a base fluid, polymer as a viscosifier and stabilizer and surfactant to generate the micro-bubbles. According to Sebba (1987) CGA fluids differ from conventional bubbles as conventional bubbles are surrounded by a surfactant monolayer while CGA fluids are surrounded by three surfactant layers. The addition of surfactants introduces an energy barrier to coalescence therefore micro-bubbles generated in the presence of surfactants tend to maintain their size. The use of CGA as an alternative chemical EOR technique is proposed in this study.

1.2 Statement of the Problem

As mentioned above the role of EOR is to produce residual oil which remains in place after primary and secondary recovery. The problems associated around chemical flooding technologies are based around inadequate sweep efficiencies and mobility ratios which leave much of the recoverable oil left untouched in the pores of the reservoir. Sweep efficiency refers to the efficacy of an enhanced oil recovery technique. This efficacy is measured by the reservoir coverage of the injected recovery fluid. Therefore a recovery fluid is thought to have good sweep efficiency if it makes contact with most of the reservoir. The volumetric sweep efficiency is the result of a number of factors, such as reservoir fractures, reservoir thickness, placement of injection wells, flow rate and mobility ratios. The mobility of a fluid is the ratio of the formation permeability to a fluid divided by the viscosity of the fluid. Mobility ratios are described as the mobility of the displacing fluid (recovery fluid) divided by the mobility of the displaced fluid (oil). These ratios are important in determining the volume of the reservoir contacted by the recovery fluid. To address the problem of inadequate sweep efficiencies and mobility ratios the use of colloidal gas aphron (CGA) as a recovery fluid rather than its more conventional use as a drilling fluid was investigated.

1.3 Objectives and Scope of the Study

The objective of this experimental study was to generate stable aqueous colloidal gas aphrons and to evaluate its ability to function as an improved oil recovery method. There were two main stages of this study: development and characterization of the aqueous CGA fluid and the evaluation of its stability and performance as an enhanced recovery fluid. The first stage of the project focused on testing different surfactant and polymer concentrations to determine the optimum combination of these chemicals. This was done by examining stability using yield tests and micro-bubble diameter sizing with respect to time. The second stage of the project was to evaluate the performance of the aqueous CGA fluid as an enhanced recovery fluid firstly using a visual cell and later using a radial core holder.

These two main objectives were accomplished by dividing them into the tasks below:

1. Literature Review of the research area.
    - A review of the prior studies and applications of aphrons

- A review of the surfactants and polymers suitable for the generation of aqueous colloidal gas aphrons

2. Generation of Aqueous CGAs
    - Identify a lab procedure for aphron generation
    - Test different surfactants to determine if aphrons are produced
3. Characterization of Aqueous CGAs
    - Determine optimum polymer concentration and type to generate stable CGAs using rheological parameters
    - Investigate the effect of surfactant type and concentration on the yield of aphrons, average CGA bubble size and rheology
    - Analyse the effect of time on aphron yield, average bubble size and bubble size distribution using the various surfactants and concentrations
    - Determine the optimal formulation of CGAs for use as a recovery fluid using the previous data
4. Performance of this CGA fluid as a recovery fluid in visual cell experiments
    - Analyse the results with respect to total oil recovery, breakthrough and injected fluid retention time
    - Observe the pressure profile of the CGA fluid across the visual cell
    - Observe the behaviour of the CGA fluid through the use of time lapse photos showing frontal displacement patterns

5. Performance of this CGA fluid as a recovery fluid in radial core experiments
    - Analyse the results with respect to total oil recovery, breakthrough and injected fluid retention time
    - Observe the pressure profile of the CGA fluid across the radial core

1.4 Methodology of the Research

This study started off with research into colloidal gas aphrons and its uses as a drilling fluid. Through this research polymers and surfactants were identified which were known to produce CGAs. These polymers and surfactants were then screened using rheological tests and parameters to determine the most suitable surfactant and polymer as well as the optimum concentration of each. Stability tests were also employed and these included micro-bubble size with respect to time and bubble size distributions with respect to time. After the optimum formulation was chosen visual cell and radial core tests were done to investigate how CGAs behaved as a recovery fluid. Total recovery, breakthrough, injected fluid retention time and pressure data was recorded to determine this.

1.5 Contributions of the Current Research

This investigation has provided a stable optimum formulation for aqueous colloidal gas aphrons. The oil recovery experiments conducted using this optimum formulation has shown good oil recovery which was on par with the oil recovered using only polymer. Therefore this colloidal gas aphron fluid has proven to be a viable EOR technique. This study should encourage further investigation into the use of colloidal gas aphrons as an alternative EOR technique. This can further lead to designing an EOR process as an alternate to polymer, polymer-surfactant or WAG (Water Alternating Gas) methods. This method can also very significant to carbon sequestration as carbon dioxide or flue gas can also be used in micro-bubble generation instead of air. This way the aqueous CGA fluid can act as a recovery fluid while also providing a way for carbon dioxide or flue gas disposal.

1.6 Structure of the Thesis

Chapter 1 gives an introduction to the thesis. This includes a look at the overview and background of the problem as well as the objectives and scope of the study.

Chapter 2 presents a literature review of the study area. In this chapter previous work completed on CGAs is discussed to provide the foundation for this project.

Chapter 3 describes the experimental set-up, material and procedures used in this study. Specific information about the chemicals and equipment used is provided.

Chapter 4 details the polymer and surfactant screening procedures as well as the results of the rheological characterization studies of aphron fluids.

Chapter 5 shows the procedures and results involved in the visual cell experiments. The time lapse photos for these experiments is shown here.

Chapter 6 describes oil recovery experiments conducted by injecting CGAs through oil saturated porous media packed into a radial cell.

Chapter 7 concludes the thesis and gives recommendations for future work.

Chapter 8 contains the references.

2. LITERATURE REVIEW

The colloidal gas aphron was first introduced conceptually by Felix Sebba (1971). In 1987 Sebba published his book entitled Foams and Biliquid Foams-Aphrons which detailed the characteristics and properties of aphrons (Sebba, 1987). However, it was not until 1998 that the petroleum industry began exploring the potential of colloidal gas aphrons. The aphron system was first applied to a horizontal re-entry well in West Texas, U.S.A. where this new system performed quite well and showed great promise (Brookey, 1998). Other projects followed in different geologic formations such as sand, shale and dolomite and all exhibited excellent drilling conditions and no formation damage or invasion (Brookey, 1998). The use of the CGA system was mainly targeted at balanced drilling.

The term “at balance” refers to drilling techniques which produce a fluid density near the formation pressure gradient but not so low that formation fluids enter the well bore (Brookey, 1998). Colloidal gas aphrons have been used to maintain at balance drilling due to their lower fluid densities and pore sealing abilities.

2.1 CGA as a drilling fluid

Aphrons are described as a novel new drill-in fluid used to drill horizontal and high angle wells through damage prone reservoirs (Brookey 1998). These aphrons are also described as resisting coalescence while being able to recirculate and so reused. Their small size allows them to be recirculated even while solids control systems are being used. This aphron system is used to drill at balance to enhance drilling rates while preventing formation damage. To stabilize the aphron in a drilling fluid a high yield stress, shear thinning polymer is thought to be most effective (Brookey 1998). Aphrons are incorporated into the drilling fluid at the surface using conventional mud mixing equipment, though at shallow depths they may also be created at the drill bit. The micro-bubble size created and size distribution play an important part in how well they can seal a permeable formation. The aphron system is designed to incorporate 8 to 15 percent air volume (Growcock et al. 2003).

Colloidal gas aphrons have proven successful in solving many of the problems associated with low pressure reservoirs such as fluid loss control, formation damage, stabilization of multipressure sequences with one fluid and differential sticking (Gaurina-Medimuric and Pasic, 2009). Depleted reservoirs in mature oil and gas fields are also categorized as low pressure reservoirs. Table 2-1 gives detailed data about these field cases including the location and the benefits gained using this type of fluid.

Table 2-1 Field application data of aphron based fluids (Gaurina-Medimuric, 2009)

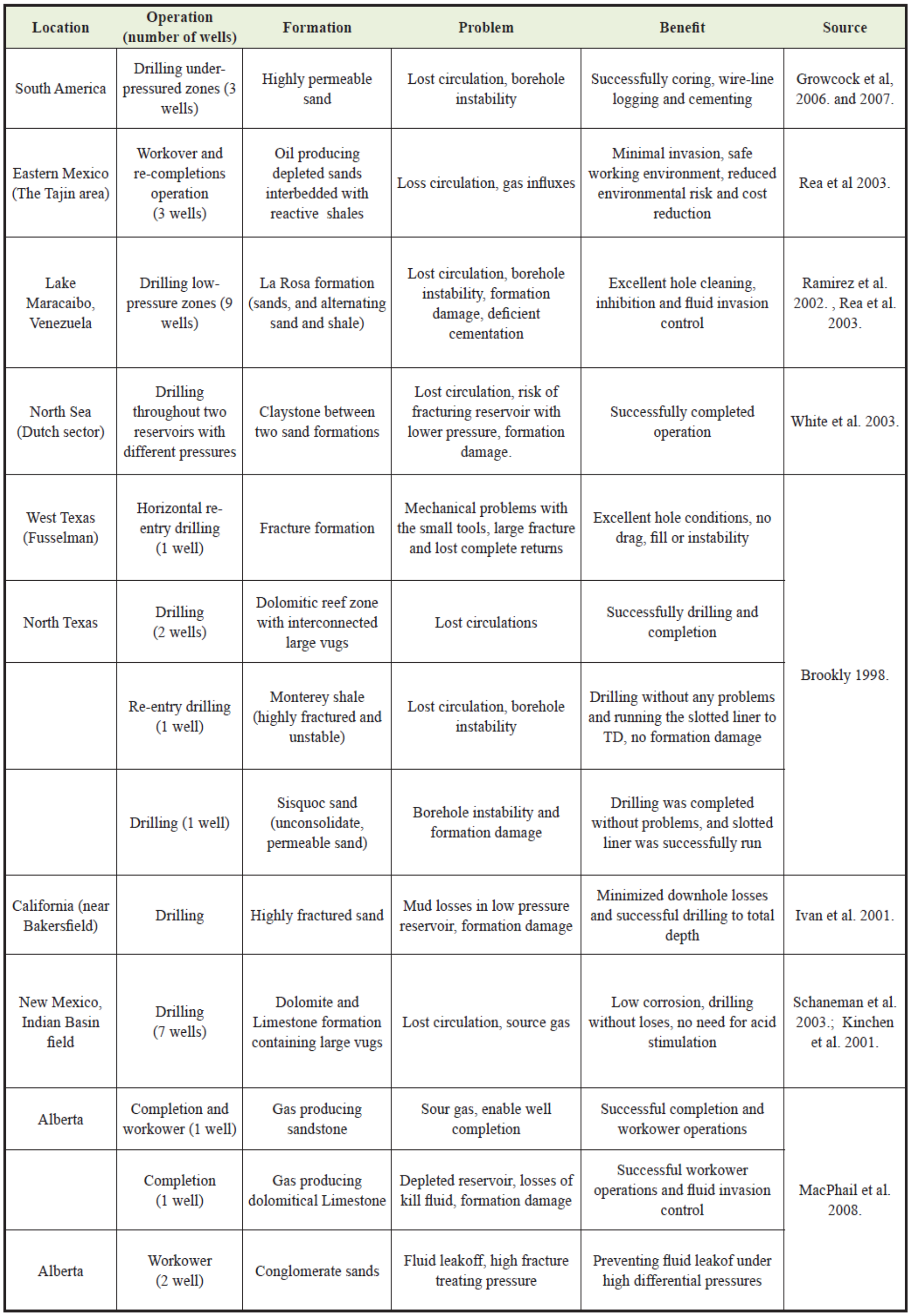

Location	Operation (number of wells)	Formation	Problem	Benefit	Source
South America	Drilling under-pressured zones (3 wells)	Highly permeable sand	Lost circulation, borehole instability	Successfully coring, wire-line logging and cementing	Growcock et al, 2006. and 2007.
Eastern Mexico (The Tajin area)	Workover and re-completions operation (3 wells)	Oil producing depleted sands interbedded with reactive shales	Loss circulation, gas influxes	Minimal invasion, safe working environment, reduced environmental risk and cost reduction	Rea et al 2003.
Lake Maracaibo, Venezuela	Drilling low-pressure zones (9 wells)	La Rosa formation (sands, and alternating sand and shale)	Lost circulation, borehole instability, formation damage, deficient cementation	Excellent hole cleaning, inhibition and fluid invasion control	Ramirez et al. 2002. , Rea et al. 2003.
North Sea (Dutch sector)	Drilling throughout two reservoirs with different pressures	Claystone between two sand formations	Lost circulation, risk of fracturing reservoir with lower pressure, formation damage.	Successfully completed operation	White et al. 2003.
West Texas (Fusselman)	Horizontal re-entry drilling (1 well)	Fracture formation	Mechanical problems with the small tools, large fracture and lost complete returns	Excellent hole conditions, no drag, fill or instability	Brookly 1998.
North Texas	Drilling (2 wells)	Dolomitic reef zone with interconnected large vugs	Lost circulations	Successfully drilling and completion	
	Re-entry drilling (1 well)	Monterey shale (highly fractured and unstable)	Lost circulation, borehole instability	Drilling without any problems and running the slotted liner to TD, no formation damage	
	Drilling (1 well)	Sisquoc sand (unconsolidate, permeable sand)	Borehole instability and formation damage	Drilling was completed without problems, and slotted liner was successfully run	
California (near Bakersfield)	Drilling	Highly fractured sand	Mud losses in low pressure reservoir, formation damage	Minimized downhole losses and successful drilling to total depth	Ivan et al. 2001.
New Mexico, Indian Basin field	Drilling (7 wells)	Dolomite and Limestone formation containing large vugs	Lost circulation, source gas	Low corrosion, drilling without loses, no need for acid stimulation	Schaneman et al. 2003.; Kinchen et al. 2001.
Alberta	Completion and workower (1 well)	Gas producing sandstone	Sour gas, enable well completion	Successful completion and workower operations	MacPhail et al. 2008.
	Completion (1 well)	Gas producing dolomitical Limestone	Depleted reservoir, losses of kill fluid, formation damage	Successful workower operations and fluid invasion control	
Alberta	Workower (2 well)	Conglomerate sands	Fluid leakoff, high fracture treating pressure	Preventing fluid leakof under high differential pressures	

2.1.1 Components of CGA drilling fluids

Surfactants are a main constituent of colloidal gas aphron drilling fluids and are responsible for the generation of aphrons. Polymers are also used as they act as a viscosifier and an aphron stabilizer. According to Brookey (1998) there are four major components in aqueous CGA drilling fluids: fresh water, LSRV (Low Shear Rate Viscosity) Viscosifier, thermal stabilizer and an aphron generator. In subsequent years after much research and experimentation other compositions have been introduced. Table 2-2 shows the composition of an aphron based drilling system.

Table 2-2 Formulation of a typical standard aphron based drilling fluid system (Growcock et al. 2004)

Component	Function	Concentration
Fresh water/brine	Continuous phase	0.97 bbl
Soda ash	Hardness Buffer	3 lbm/bbl
Biopolymer blend	Viscosifier	5 lbm/bbl
Polymer blend	Filtration Control Agent and Thermal Stabilizer	5 lbm/bbl
Alkalinity Control Agent	pH control	0.5 lbm/bbl
Surfactant blend	Aphron Generator	2 lbm/bbl
Biocide	Biocide	0.05 gal/bbl
Polymer/Surfactant blend	Aphron Stabilizer	1 lbm/bbl
Polymer (Optional)	Mud Conditioner	1 lbm/bbl
Oligomer (Optional)	Defoamer	As needed

2.2 Structure of CGA

Sebba (1987) described the structure of as microfoams due to their very small size. Later, aphrons were termed colloidal as they display colloidal properties which allow them to flow freely. Colloidal Gas Aphrons are micro-bubbles which are generally 10-100 microns in size composed of a gaseous inner core surrounded by a thin surfactant film. Therefore, they are spherical, micron sized gas bubbles dispersed in an aqueous surfactant solution and can be seen in Figure 2-1 and 2-2. The gas containing inner core is less than 74 percent of the aphron. These micro-bubbles are encapsulated by a soapy shell layer which has an inner and outer surface and both surfaces have surfactant monolayers adsorbed on them. The inner surface is oriented such that the hydrophilic surfactant molecules point outward and the hydrophobic surfactant molecules point inward. The outer surface has the hydrophobic surfactant molecules pointing outward and hydrophilic molecules pointing inward. Between the inner and outer surfaces there is a viscous water layer. The inner surface supports the gas containing inner core while separating it from the aqueous layer. The outer surface also supports the aqueous layer.

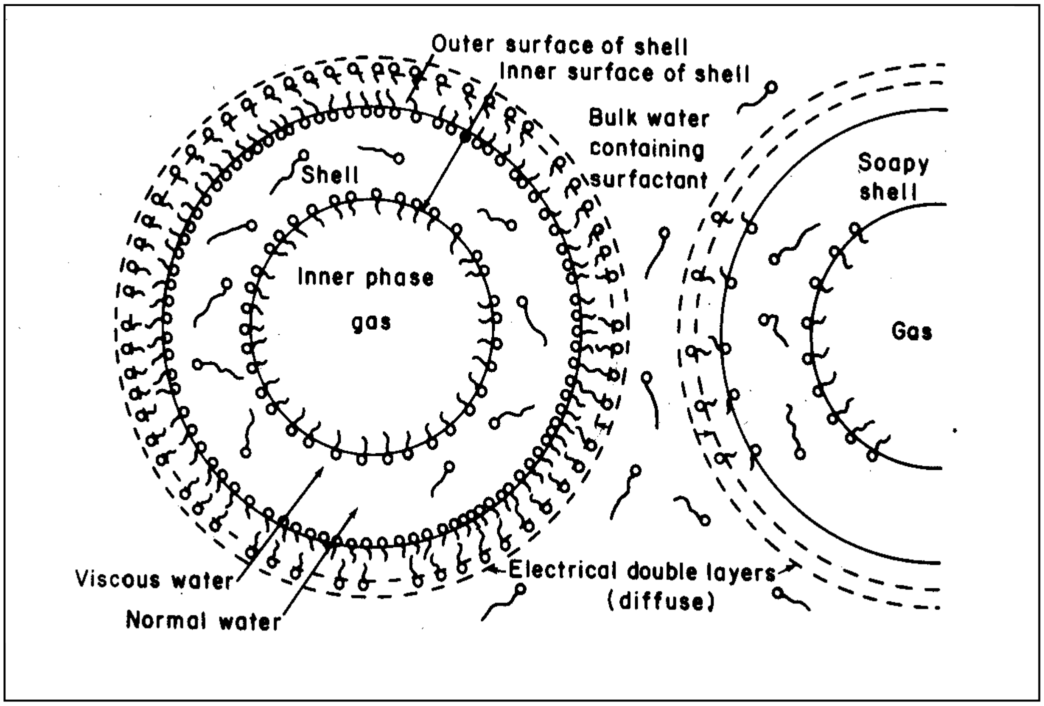

Figure 2-1 Structure of an Aphron (Sebba 1987)

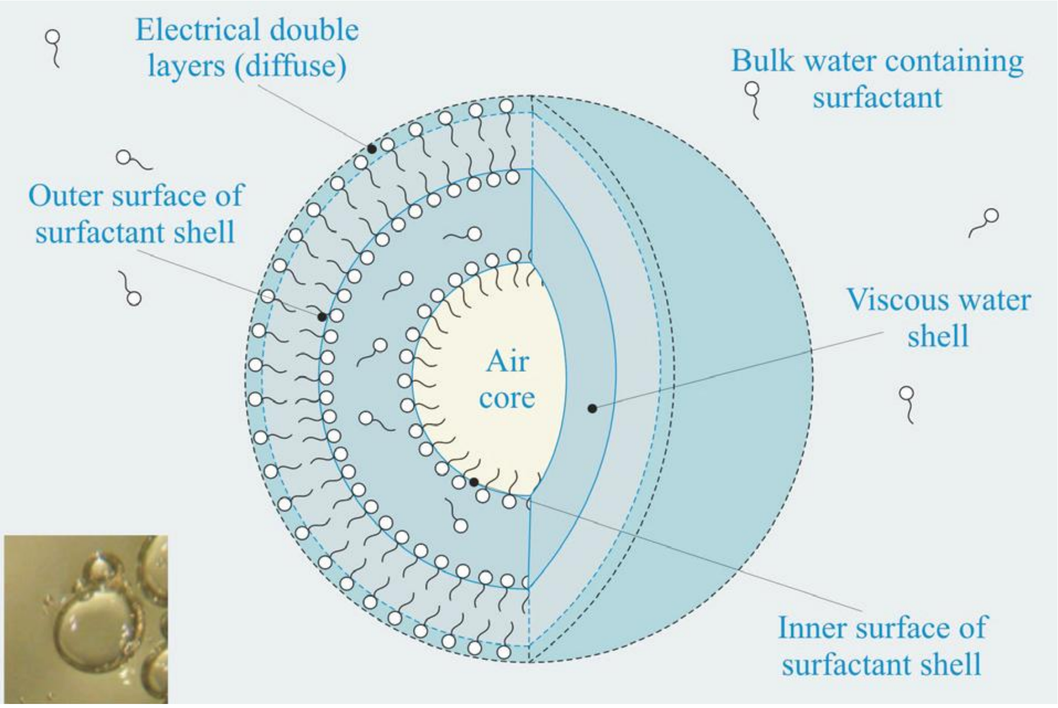

Figure 2-2 Structure of a water based aphron (Gaurina-Medimuric and Pasic, 2009)

2.3 Surfactants Used for CGA Formulation

The term surfactant is derived from “surface active agents” and is described as a chemical that reduces the surface tension of a liquid. They can also reduce the tension at the interface of two liquids or between a liquid and solid. Surfactants are used in detergents, fabric softeners, emulsions, paints, adhesives, inks and herbicides to name a few. Surfactants are classed into three main categories: anionic, cationic and non ionic. These categories are based on the nature of the charged group on the surfactant head. Anionic refers to a negatively charged group, cationic a positively charged group and non ionic to no charged group.

In aphron based drilling fluids surfactants from each category is used. Sebba (1987) mentioned Lauryl alcohol-ethylene oxide (LAEO) and Alkyl oxypolyethylene oxyethanol (Tergitol) which are both non ionic in nature. Jauregi et al (1996) also lists a number of surfactants which were used for CGA generation as shown in Table 2-3.

Table 2-3 Surfactants used for CGA generation up to 1995 (Jauregi et al. 1997)

Reference	Surfactant	Nature of Surfactant
Ciriello et al. 1982	EDHA Ethylhexadecyldimethyl ammonium bromide	Cationic
	SDBS Sodium dodecyl benzene sulfonate	Anionic
Wallis et al 1995	Arquad C-50	Cationic
Caballero et al. 1989	HTAB Hexadecyltrimethyl ammonium bromide	Cationic
Subramaniam et al. 1990	AOT Sodium bis-(2-ethyl hexyl) sulfosuccinate	Anionic
	SDBS Sodium dodecyl benzene sulfonate	Anionic
	BDHA Benzyldimethyl-n-hexadecyl ammonium chloride	Cationic
Amiri and Woodburn 1990	TTAB Tetradecyltrimethyl ammonium bromide	Cationic
Matsushita et al. 1992	HTAB Hexadecyltrimethyl ammonium bromide	Cationic
	DTAB Dodecyltrimethyl ammonium bromide	Cationic
	CPB Cetylpyridinium bromide	Cationic
	SDS Sodium dodecyl sulfate	Anionic
	SDBS Sodium dodecyl benzene	Anionic

	sulfonate	
	Tergital Polyoxyethene triglyceride alcohol	Non ionic
Roy et al. 1992	HTAB Hexadecyltrimethyl ammonium bromide	Cationic
	SDBS Sodium dodecyl benzene sulfonate	Anionic
Chapalkar et al. 1994	Tergital Polyoxyethene triglyceride alcohol	Non ionic
	SDBS Sodium dodecyl benzene sulfonate	Anionic
	HTAB Hexadecyltrimethyl ammonium bromide	Cationic
Save et al. 1993	HTAB Hexadecyltrimethyl ammonium bromide	Cationic
	SDBS Sodium dodecyl benzene sulfonate	Anionic
	LAEO Lauryl alcohol-ethylene oxide	Non ionic
Save and Pangarkar, 1993	SDBS Sodium dodecyl benzene sulfonate	Anionic
	HTAC Hexadecyltrimethy ammonium bromide	Cationic
	CPC Cetylpyridinium chloride	Cationic
	DTAC Dodecyltrimethyl ammonium chloride	Cationic
	SLS Sodium lauryl sulphase	Anionic
	DMDSAC Dimethyl distearyl ammonium chloride	Cationic
	Triton-X-100	Non ionic
	LA-EO3 Lauryl alcohol ethylene oxide	Non ionic

In the research done by Matsushita et al. (1992), the effect of surfactant, surfactant concentration, stirring speed and length of stirring time were investigated. The results showed a significant effect of mixing speed on stability when the speed was increased from 5000 to 5500 RPM with no significant effect seen in the increase from 5500 to 8500 RPM (Jauregi et al. 1997). The length of the alkyl chain in the cationic surfactants DTAB and CTAB affected the stability of the CGA produced, with the longer alkyl chain surfactant creating the most stable aphrons.

Matsushita et al (1992) also showed that stirring time affected the gas content of the aphron but not on the stability (Jauregi et al. 1997). Chapalkar et al. (1994) found that the bubbles created by non ionic surfactants were of a smaller diameter than those created by ionic surfactants. Also an increase in ionic strength was found to decrease bubble size in ionic surfactants. Increasing the surfactant concentration for Tergital, SDBS and HTAB produced smaller bubbles (Jauregi et al. 1997).

Save and Pangarkar (1993) tested cationic, anionic and non ionic surfactants. CTAC gave a higher foam height and half life while DMSDAC gave the highest foam height but the lower half life. For the anionic surfactants SDBS showed a higher half life. The non ionic surfactants were each added to a solution of CTAC and observed. There was no effect on foam height but the half-life time was improved.

Sodium bis-(2 ethyl hexyl) sulfosuccinate (AOT) was the surfactant of choice for Jauregi et al. (1997). Go Devil II was used by Belkin (2005) which is a MASI Technologies product. Bjorndalen and Kuru (2005) used hexadecyltrimethyl ammonium bromide (HTAB) and sodium dodecyl benzene sulfonate (DDBS). Spinelli et al (2010) used NOVEC FC-4432 and NOVEC FC-4430 which were commercial non ionic polymeric fluorochemical surfactants as well as poly(ethylene oxide)-poly(propylene oxide) (PEO-PPO) block copolymers called L7 and L10 with different numbers of ethylene oxide (EO) and propylene oxide (PO) units.

Feng et al (2009) did their research using JBR 425, rhamnolipid and common anionic biosurfactant with Tergitol and found that there was an increase in stability with an increase in surfactant concentration but decreased with low pH and increased salt concentrations. The anionic surfactant sodium dodecyl sulphate (SDS) was used to investigate the effects of surfactant and electrolyte concentration on bubble formation and stabilization by Xu et al. (2008). They found that the minimum bubble diameter and maximum stability occurred at concentration above the critical micelle concentration (CMC). Hashim et al. (1999) used sodium dodecyl sulphate (SDS) to investigate the mass transfer correlation in the flotation of palm oil by colloidal gas aphrons.

Sodium dodecyl sulphate was also used by Oliveira et al. (2004) to optimize micro-foam rheology for soil remediation. Flotation of microorganisms by CGAs was investigated by Hashim et al. (2000) using the cationic surfactant benzyl dimethyl hexadecyl ammonium chloride (BDHA). Zhao et al. (2009) used three different surfactants, Tween 20 - non ionic, sodium dodecyl sulphate (SDS) – anionic and cetyl trimethyl ammonium bromide (CTAB) – cationic.

2.4 Polymers used for CGA Formulation

Polymers are another important aspect of aphron drilling fluid composition. They are mostly mentioned in the literature that deals with aphrons as a drilling fluid. Other applications of colloidal gas aphrons may not need the enhanced rheological properties that polymers impart. Brookey (1998) first mentions that for aphrons to be stabilized in a drilling fluid a high yield stress, shear thinning (HYSST) polymer is used. In this case a xanthan gum biopolymer was found to effectively stabilize the aphrons and increase the low shear rate viscosity (LSRV) which encouraged good hole cleaning, cuttings suspension and invasion control.

Growcock (2005) introduced the use of a clay/polymer blend to act as a viscosifier in an alternative aphron based drilling fluid. In this alternative system polymer/surfactant blends are also added to act as aphron stabilizers. Ramirez et al (2002) also mentions the use of a biopolymer blend which is a mixture of non ionic polymers that generate high viscosities at low shear rates. There is also the addition of another polymer blend which acts as a fluid loss control agent and thermal stabilizer. However as before the specific polymer/s are not listed.

Belkin (2005) also discusses the need for the aphron base fluid to be highly shear thinning and display high LSRV with low thixotropy. Spinelli et al. (2010) prepared the base fluids for aphronization by mixing the organic phase at different concentrations of organophilic clay and viscosifiers. The viscosifiers used were Versa and Liovac 419. Bjorndalen and Kuru (2005) prepared the aphron base fluid using xanthan gum as a viscosifier and aphron stabilizer.

Electrolytes have also been added as a component of aphron drilling fluids. Xu et al. (2008) investigated the effects of surfactant and electrolyte concentration on bubble size and stability. The effect of electrolyte concentration was studied by adding sodium chloride (NaCl) at a surfactant concentration below that of the critical micelle concentration (CMC). The addition of salt decreased bubble size and improved bubble preparation to a certain extent.

2.5 CGA generation

Colloidal gas aphrons have been traditionally produced by mechanical agitation or by bubbling aphrons into the base fluid. More recently sonication has been used to produce CGAs by exposing the surfactant solution to ultrasound. Mechanical methods include the Venturi throat generator, high speed commercial blender, packed bed generator, spinning cylinder generator and the spinning disc generator.

The first method of aphron generation described by Sebba (1987) was the Venturi throat generator. To produce aphrons the surfactant solution was quickly moved through a venture throat while air was allowed through a very small opening. This method produced very small bubbles generally between 25 to 50 microns but there were disadvantages to this method as well. Micro-bubble production was very slow and the solution needed to be recycled to increase the bubble concentration. Another problem was that a very high flowrate was needed to prevent the solution from forming two distinct phases rather than entraining the bubbles, and so a powerful pump was needed.

The spinning disc generator is another method for CGA generation described by Sebba (1987) and works by bringing air into the liquid phase. This generator is made up of a horizontal disc which is placed below the surface of the surfactant solution. Two vertical baffles are attached to either side of the disc and extend above the surface of the solution. The disc is attached to a motor via a shaft and properly supported to prevent unnecessary movement. To produce CGAs the disc must rotate at speeds more than 4,000 RPM. Once this critical speed is achieved waves are formed on the surface which hit the baffles and must then re-enter the solution. An unstable thin layer of gas is trapped between the baffle and the liquid which breaks up into aphrons. The benefits of this apparatus are that it can produce large volumes of CGAs in a short time period and it is very reliable. The spinning disc generator is seen in Figure 2-3.

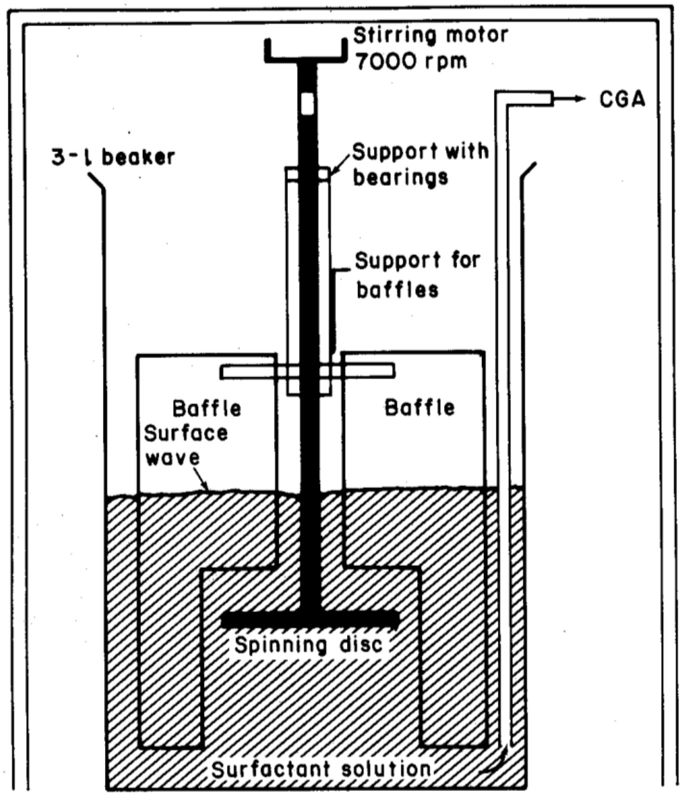

Figure 2-3 Spinning disc generator (Sebba, 1987)

Jauregi et al. (1997) used a laboratory mixer supplied by Silverson Ltd. fitted with a four blade impeller which was immersed into a baffled beaker and mixed at speeds of 5,000 to 10,000 RPM. Feng et al (2009) used a high speed stirrer at 8,000 RPM for 3 mins to produce CGAs. Xu et al (2008) preferred a homogenizer (Polytron PT-3000) produced by Kinematica Inc. Aphrons were produced by mixing at 4,000 RPM for 10 mins. Sonication was another method of aphron generation used by Xu et al. (2008) and this was carried out by a 0.5 inch ultrasound probe (Branson Sonifier 450) at a power level of 300 W for 3 mins. Hashim et al. (2000) used a spinning horizontal disc generator at a speed of 6,000 RPM in his investigation of particle bubble attachment.

Zhao (2009) used a Silverson L4RT mixer at 7,000 RPM in a baffled container. Spinelli et al. (2010) used a different method where the mixture was passed through a HPHT filter press, without a filter element under a pressure differential of 1,380 kPa. Bjorndalen and Kuru (2005) used a Brinkmann homogenizer model PT 45/80 which was modified into a four baffle system.

2.6 Yield of CGA Fluids

Creaming refers to the tendency of colloidal gas aphrons to form two layers if left undisturbed. According to Sebba (1987) if a CGA fluid is left unstirred it will separate into a foam which will float on the bulk water in about 10-15 mins. This occurs due to the density difference between aphrons and their liquid phase. Sebba (1987) also suggested that creaming could be postponed if the lateral movement conveyed to the bubbles is greater than the upward movement due to gravity. If this was carried out the creaming could be delayed by at least an hour or more. Hashim et al (1999) delayed creaming by constantly mixing the CGA fluid after generation at a speed of 1,000 RPM. Creaming can also be related to aphron yield and can indicate how much aphrons are produced. Save and Pargarkar (1993) used creaming to create a parameter called dispersion height (H_d). This was described as the height of the foam which separated from the bulk mixture, the larger the dispersion height the more CGAs were thought to be produced. To characterize CGA fluids Jauregi et al. (1997) used gas holdup which was described as the volumetric ratio between the gas volume and the final dispersion volume. If the gas volume was larger then more micro-bubbles were produced. Oliviera et al. (2004) used gas volume fraction as a means of characterizing CGA fluids and studied its effect on micro-foam rheology. Shivhare (2010) used yield as a measure of the amount of aphrons produced.

2.7 Rheology of CGA Fluids

Brookey (1998) states that to be most effective aphrons must be stabilized in a drilling fluid. To do this he determines the use of a high yield stress, shear thinning (HYSST) polymer is most appropriate. A xanthan gum biopolymer was used to viscosify the lamella separating the aphrons and the water layer in the bubble film surrounding the aphron core. This was able to strengthen the bubble film and encompassing layer to self-contain the aphrons. This feature allows them to resist expansion and compression so that they could be re-circulated. Xanthan gum increases the low shear rate viscosity (LSRV) and is an important aspect of the rheology of aphron fluids. Bjorndalen and Kuru (2005) used a Brookfield DV II Digital Cone/Plate Viscometer as well as a Fann Viscometer to conduct viscometry tests. Using a 2 lb/bbl surfactant base solution and three different concentrations of xanthan gum the LSRV was determined at 0.06-1/sec shear rate. The results are seen in Table 2-4.

Table 2-4 LSRV results using xanthan gum and a surfactant base solution (Bjorndalen and Kuru, 2005)

	Xanthan Gum Conc lb/bbl		
Properties	**1**	**3**	**5**
LSRV @ 0.6-1/sec (cP)	2767	22 067	>31 000

Schaneman et al. (2003) also used a Brookfield viscometer to measure the LSRV of the CGA drilling fluid generated using MASI Technologies products. These results are shown in Table 2-5. MacPhail et al. (2008) also recommended that the LSRV of a CGA fluid be greater than 40,000 cP or the aphrons would become unstable and break apart.

Table 2-5 Initial and final LSRV results of a CGA drilling fluid (Schaneman et al. 2003)

Properties	Initial	Final
Brookfield LSRV @ 0.3 RPM (cP)	57 088	62 400

Ivan et al. (2001) measured the LSRV of the generated aphron drilling fluid using a Brookfield viscometer as well. The LSRV was measured at 60,000 cP and he specified that this property should always be greater than 50,000 cP to ensure stability. Ramirez et al. (2002) used CGA drilling fluids in the mature reservoirs of Lake Maracaibo. A number of wells were successfully drilled and the LSRV measured. These results are seen in Table 2-6.

Table 2-6 LSRV of aphron drilling fluids used to drill the reservoirs of Lake Maracaibo (Ramirez et al. 2002)

Well Name	LSRV (cP)
VLA 1321	48 000-348 000
VLA 1325	45 000-97 000
VLA 1329,1331,1332,1334,1335	60 000-144 000

Aphron drilling fluids were also used in drilling the depleted mature fields in Mexico (Rea et al. 2003). The initial and final LSRV was reported for three different wells and can be seen in Table 2-7.

Table 2-7 LSRV of the CGA fluids used in three Mexican wells (Rea et al. 2003)

Well Name	Initial LSRV (cP)	Final LSRV (cP)
Tajin 361	95 325	75 000
Tajin 364	82 345	86 200
Tajin 321	57 088	62 400

Growcock et al. (2004) and Growcock et al. (2006) also measured the LSRV of the aphron and alternative aphron drilling fluid generated. These results are shown in Table 2-8 and 2-9.

Table 2-8 LSRV of alternative aphron based drilling fluid (Growcock et al. 2004)

System Properties	
LSRV @ 0.06 /sec (cP)	192 000

Table 2-9 LSRV of CGA fluid (Growcock et al. 2006)

System Properties	1.2% Air	17% Air
LSRV @ 0.06/sec (cP)	125 000	125 000

The LSRV is an important aspect of CGA fluids as it is strongly tied to its stability. The data presented shows different low shear rate viscosities were used in the generation and use of aphron drilling fluids. This can help establish a minimum LSRV at 40,000 cP for a stable CGA fluid. The viscosity of the CGA fluid over a range of shear rates is also of interest.

Oliveira et al. (2004) found that CGA fluids show strong shear thinning behaviour with decreasing apparent viscosity with increasing shear rate. Zhao et al. (2008) used a flow pipe viscometer to conduct rheological tests. It was found for all the surfactant concentrations tested the CGA fluids behaved in a shear thinning manner. Shivhare (2011) conducted rheological tests on an oil based aphron system. This oil based aphron drilling fluid was found to behave like a pseudo plastic type fluid with shear thinning qualities. Figure 2-4 shows the effect of surfactant concentration on the shear stress and shear rate relationship and Figure 2-5 shows the effect of surfactant concentration on the CGA fluid viscosity.

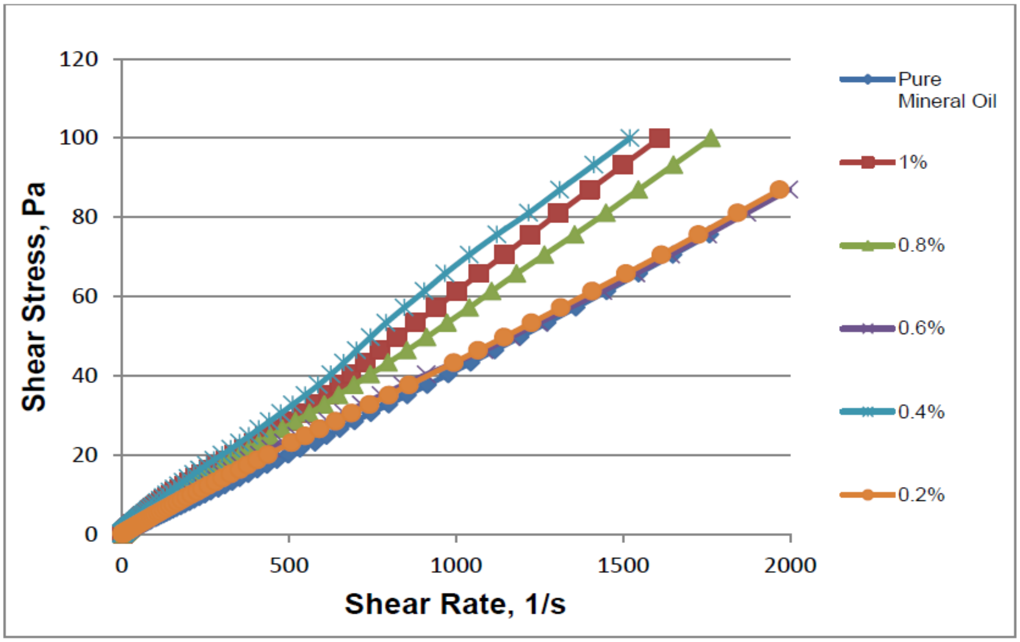

Figure 2-4 Effect of surfactant concentration on shear stress and shear rate for an oil based aphron system (Shivhare, 2010)

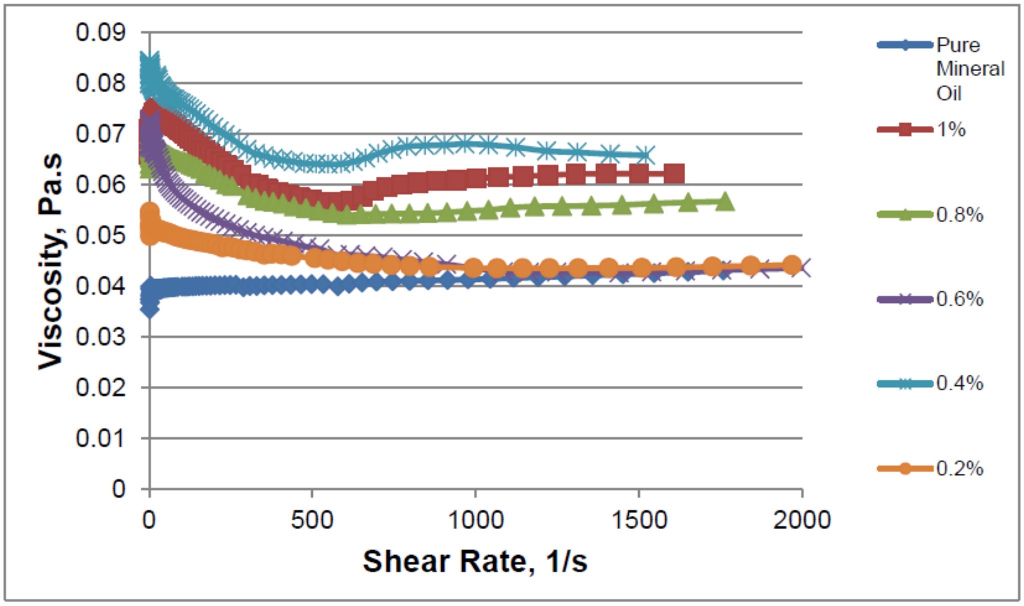

Figure 2-5 Effect of surfactant concentration on CGA fluid viscosity (Shivhare, 2011)

2.8 CGA bubble size distribution

The size of CGAs and the bubble size distribution are important parameters to stability as well as to the bridging of pores. To quantify stability as well as to determine the pore blocking ability of a CGA fluid these parameters should be known. Sebba (1987) noticed that there was a uniform size distribution immediately after aphron generation. However after a few minutes there was a distinct size distribution with the majority of the aphrons larger than 25 microns.

Feng et al. (2009) used a digital camera attached to a microscope to obtain photos of the micro-bubbles soon after preparation. The sample size was between 100-300 bubbles and mean bubble size and bubble size distribution was calculated. The initial mean bubble diameter varied between 63 and 71 microns with the majority of bubbles in the 20-140 micron diameter range. Figure 2-6 shows the results.

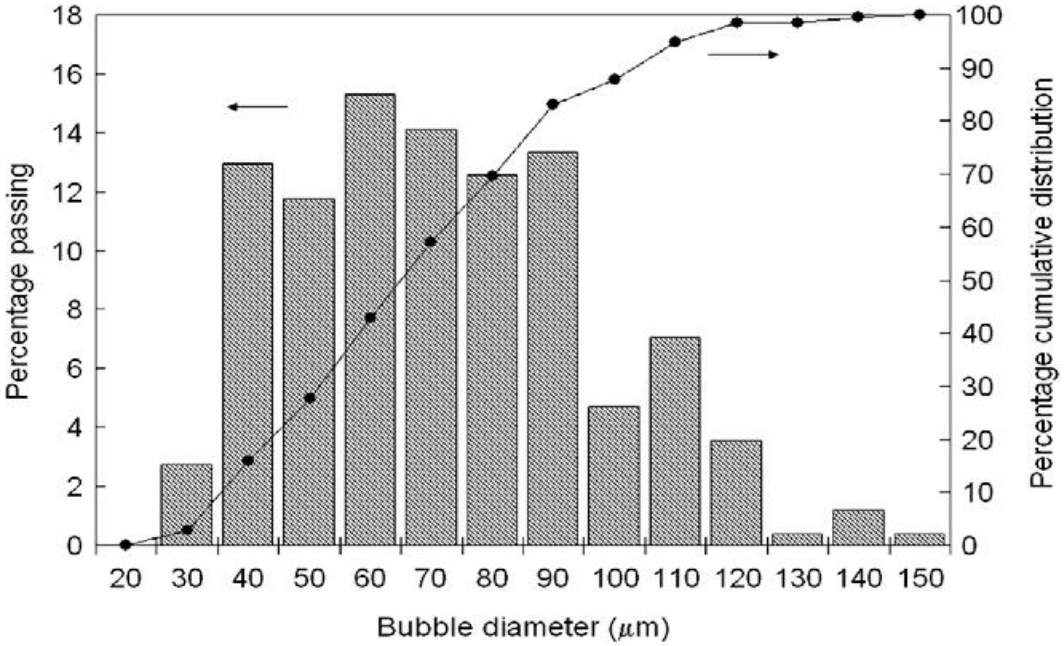

Figure 2-6 Typical bubble size distribution for a micro-bubble dispersion (Feng et al. 2009)

Xu et al (2008) measured average bubble size and bubble size distribution to calculate average bubble diameter and average size distribution. This was done to determine the effect of surfactant and electrolyte concentration. It was noted that above the critical micelle concentration (CMC) there was no change in size distribution with increasing surfactant concentration. However below the CMC the bubble size distribution was dependent on surfactant concentration.

Zhao et al. (2009) looked at the rheology of CGAs made from different surfactants. One of the parameters measured was the Sauter mean bubble radius (r_{32}). It was found that the surfactant CTAB created much smaller bubbles than those created with Tween 20 and SDS (Sodium dodecyl sulphate). The aphrons created with CTAB were in the 26.4 to 28.3 micron size range while those created with Tween 20 and SDS were 39.0 to 47.6 microns in size.

Spinelli et al (2010) used a microscope and image analysis software to measure bubble size and bubble size distribution. He also photographed each sample three times and analyzed these separately and compared them to the mean. This was done to ensure accurate bubble size distributions. Save and Pangarkar (1993) used a projection microscope to determine the bubble size distribution.

Growcock (2005) used an optical viewing system which was made up of a viewing cell, microscope and image analysis tools. Growcock et al. (2003) suggested the use of acoustic bubble spectrometry as it permits the quantitative measurements of the bubble size distribution in opaque fluids. A Laser granulometer was also used to determine bubble size distribution thorough the use of laser light scattering.

2.9 Stability of CGA Fluids

Colloidal gas aphrons are not static and will change over time. Aphron size, yield and rheological parameters will change with time as well as respond to changes in pressure and temperature. Sebba (1987) observed that aphrons are quite uniform in size immediately after generation. This uniform size distribution changes after a few minutes and aphrons of different sizes can be seen. He also noted that instability increases at temperature greater than 40˚C while the system disintegrates at temperatures above 65˚C.

Brookey (1998) suggested the use of xanthan gum to enhance stability and used an oligosaccharide as a thermal stabilizer.

Feng et al. (2009) placed the micro-bubble dispersions in 100 ml measuring cylinders and measured the liquid drainage from the dispersion. The volumes of the liquid and dispersion/foam phase were recorded over time. The final volume of the drained liquid was also recorded after the foam had collapsed entirely. The stability of the mixture was then quantified over time using the method described by Sebba (1987). This method uses the time taken for half of the liquid to drain from the dispersion (half-life) as a way to quantify stability. It was found that increasing surfactant concentration enhanced stability but increased pH and salt concentration hindered it.

Another method used to measure stability was the change in average micro-bubble diameter with time (Xu et al. 2008). A laser diffraction particle size analyzer was used to measure average size and size distribution and a surfactant concentration above the critical micelle concentration (CMC) produced the most stable aphrons. Jauregi and Varley (1996) also used the half-life method as well as gas holdup which was described as the ratio between the gas volume and the final dispersion volume.

Bjorndalen and Kuru (2006) used changes in aphron diameter over time as well as changes in yield. Factors such as time, temperature and pressure were used to investigate stability. An increase in polymer concentration was found to reduce bubble growth and stabilize yield over time. When the aphrons were exposed to a pressure change of 0 to 50 psig they decreased to about 60-70 % of their original size. Increasing temperatures induced an increase in bubble size with a larger increase noticed between 25-50˚C than between 50-75˚C.

Spinelli et al. (2010) evaluated stability by observing the change in bubble size and number over a 24 hour time period. It was seen that the addition of a second surfactant increased the number of bubbles produced as well as a reduction in bubble size. Aphrons based on pure ester was found to have slow bubble growth over time as well as only breaking after 24 hours. Save and Pangarkar (1993) used half life as well as foam height to quantify stability and found that surfactants with longer alkyl group chains were more stable than those with shorter chains. When non ionic surfactants were added there was an increase in inter-cohesive forces and enhanced lamella elasticity which in turn increased stability. Half life was also increased by raising viscosity which aided aphron stability.

2.10 CGA bridging mechanisms

An important aspect of drilling fluids is their bridging or blocking ability. Most conventional drilling fluids contain chemicals or solid additives that are responsible for this bridging/blocking ability. This is done to treat highly permeable sections of the reservoir during drilling and also production. CGA fluids can also bridge these problem reservoir areas without the use of solid particles and, therefore, without the costs associated with this use. CGA fluids use their aphrons to bridge these pores instead of using solid particles. This is of great benefit as these micro-bubbles can be easily removed when the well transitions into production.

There is still much to learn about the bridging ability of CGA fluids. However, extensive work has been conducted on the bridging/blocking ability of foams and due to their close association with aphrons; it is beneficial to look into this. The Jamin effect is described as the resistance to flow of a column of liquid which is broken up by air bubbles in a capillary tube even though there is a substantial pressure differential between the ends of the tube. This effect is though to be responsible for the bridging ability of foams. Ionel Gardescu studied this effect in detail while working on his paper “Behaviour of Gas Bubbles in Capillary spaces” (1930). He studied the resistance of a non wetting fluid to move along a water wet capillary. Colloidal Gas Aphrons can be applied to this as they act as the non wetting phase while the surrounding fluid behaves as the wetting phase. Figure 2-7 describes the Jamin effect.

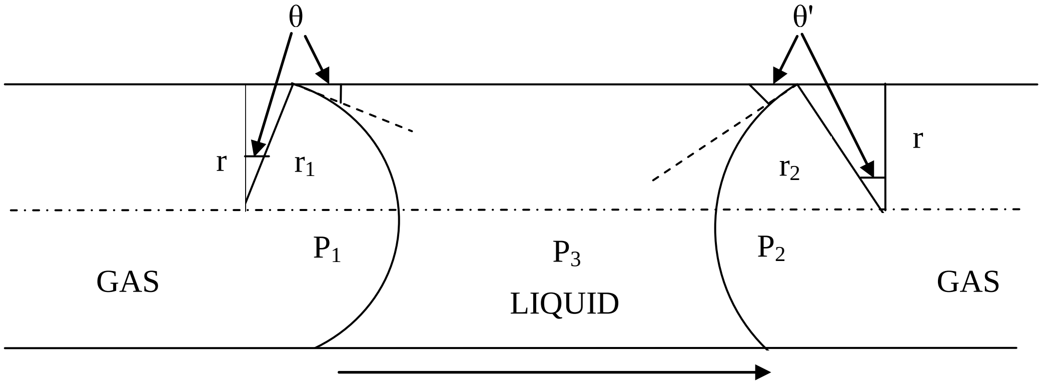

Figure 2-7 A Jamin tube with gas and liquid bubbles

Figure 2-7 shows the interaction between the two phases in the capillary tube, which is assumed to be initially dry. The liquid film of the gas bubble to the right is on a dry surface, while the liquid film of the gas bubble to the left is on a wet surface. This results in different contact angles (θ and θ') of the two bubbles where θ' is larger than θ. The radius of the gas bubble meniscuses (r_1 and r_2) will also be different based in these different contact angles. Using basic trigonometry

r_1 and r_2 can be calculated using the following equations where r is the tube radius and θ is the bubble contact angle.

$r_1 = r/\cos\theta$ (Equation 2-1) $r_2 = r/\cos\theta'$ (Equation 2-2)

To determine the pressure needed for the gas bubbles to move along the tube, the pressure at each interface must also be determined using the following equations.

$P_1 = P_3 + 2\delta/r_1$ (Equation 2-3)

$P_2 = P_3 + 2\delta/r_2$ (Equation 2-4)

P_1 refers to the pressure exerted by the gas bubble to the left while P_2 refers to the pressure exerted by the gas bubble to the right. P_3 is the pressure exerted by the liquid and δ is the interfacial tension between the gas and liquid. The difference between P_1 and P_2 will be the pressure needed to push the bubble through the capillary.

In figure 2-8a the shape of the bubble is perfectly spherical as no force is being exerted on the bubble. However as pressure is applied and the bubble is forced through the smaller capillary tube the bubble elongates and this creates two different radii seen in Figure 2-8b. If pressure is increased even more the entire bubble is forced into the capillary tube and both radii will now be equal. When this occurs there will be no resistance to movement. The maximum pressure that can be applied before the bubble radii become equal and is no longer resistant to movement is very important to bridging.

If the bubbles are replaced by CGAs and the capillary tube replaced by pore throats then this can be applied to CGAs moving through rock pores. The pressure needed to push the aphrons into the rock pores will be provided by wellbore pressure. The aphrons will then behave as the non wetting phase, enter the pore throats and display bridging behaviour.

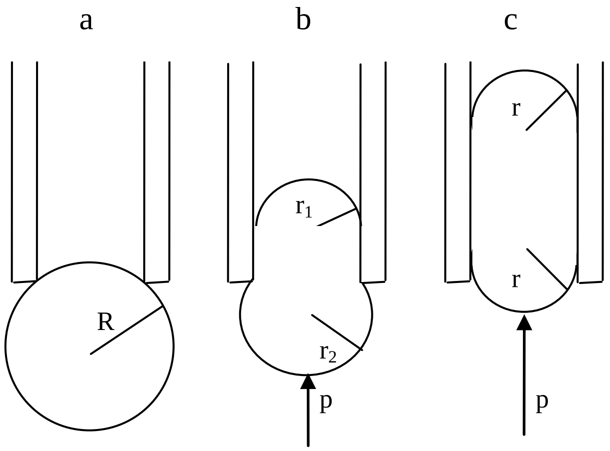

Figure 2-8 Change in bubble shape when moving through a reduced opening (Gardescu 1930)

Growcock (2006) states that aphrons exhibit little affinity for each other or for rock surfaces and so resist coalescence and aggregation. They prefer to remain as discrete micro-bubbles. It was thought that aggregates of CGAs would also show the same bridging behaviour as single aphrons and be able to enter larger formation fractures and faults. In this way the aphron aggregates would build a solids free bridge which could later be removed by pressure change. However, this would require aphrons to coalesce which does not occur. It can be said that aphrons are able to bridge only at the pore level and they will need to be sized to fit the pore size distribution.

2.10.1 Core flooding

Core flooding tests are carried out by pumping the fluid under investigation through a packed core or porous media. This is done to determine rock permeability as well to see how well different fluids will flow through it. Core flooding tests are also done to evaluate the bridging ability of a fluid across a core sample.

Growcock et al. (2005) conducted return permeability tests in Berea sandstone at 65˚C using an inlet pressure of 2,500 psi and an outlet pressure of 200 psi. These tests were done to determine the formation damage potential of CGA fluids. The formation damage produced by aphrons was very low as the return permeability was as much as 80%. This was analogous to a well made reservoir drilling fluid. CGAs were also found to have no affinity to limestone and silica surfaces which would make them easier to remove. This would minimize formation damage as well. Growcock et al. (2007) looked at the flow of aphron fluids through porous media. Aphrons quickly move to concentrate at the fluid front when the CGA fluid enters the porous media. This is called bubbly flow and is thought to create a special microenvironment that separates the bulk fluid from the porous media. This limits fluid invasion. Bjorndalen et al. (2007) conducted tests using a micro-model to visually understand the blocking mechanism. Stable foam was created and injected into the micro-model where a pressure rise was noted. This indicated that the porous media was blocked by this foam and shows that aphron fluids can reduce formation damage. The foam was also easily removed by water to indicate that this effect was reversible. Bjorndalen et al. (2010) used a radial cell to conduct formation damage tests. The cell was packed with sand and saturated with a specific fluid. The CGA fluid was then injected and the pressure monitored. An increasing pressure drop was observed between the injection and production ports which indicated a buildup of aphrons. After this the saturating fluid was re-injected to determine the return permeability and level of formation damage. Shivhare (2011) conducted core flooding tests using a radial cell and an oil based CGA fluid. An increasing resistance to the flow of the oil based CGA fluid through the radial cell was noticed. This indicated the aphron buildup across the pore structure of the radial cell created an effective seal for controlling the invading fluid into the formation.

2.11 EOR Techniques and Review

Chemical enhanced oil recovery processes include polymer, surfactant, alkaline and micellar/emulsion floods as well as combinations of these. Miscible methods include high pressure miscible drives, using a hydrocarbon gas, nitrogen or carbon dioxide, as well as displacement by liquid hydrocarbons (Ali and Thomas, 1996). Polymer flooding uses a small amount of a high molecular weight water-soluble polymer which is added to a waterflood type operation. The choice of polymer and concentration are very important factors to this process. Polymer flooding increases the oil recovery by improving the sweep efficiency but there are many other factors to consider. This process may face problems such as polymer degradation due to very saline interstitial water, temperature, polymer ageing, and polymer gel formation (Ali and Thomas, 1996). Polymer floods have been seen to be more effective for moderately viscous oils in the range of 5-200 mPa.s and are better suited to reservoir permeabilities higher than 20 mD. The reservoir temperature should also not be higher than 80˚C and the presence of a gascap or bottom water zone would encourage polymer channelling (Ali and Thomas, 1996). Sandstone reservoirs are also preferred (Alkafeef and Zaid, 2007). Therefore this chemical EOR technique requires quite specific conditions to be suitable for use.

Surfactant flooding is used in EOR as they can lower the interfacial tensions and change wetting properties. The addition of the surfactant decreases the interfacial tension between oil and formation water, lowers the capillary forces and facilitates oil mobilization (Samanta et al. 2011). One of the main problems with this method is the loss of surfactant to the rock matrix through mechanisms like adsorption, precipitation and changes in phase behaviour (Ali and Thomas, 1996). Surfactants are also costly chemicals. Puerto et al. 2010 indicated that reservoirs with temperatures greater than 70˚C and salinities up to 200,000 mg/L may not be suitable for surfactant flooding due to precipitation of the surfactant or phase separation.

Alkaline flooding consists of injecting solutions of sodium hydroxide, sodium carbonate, sodium silicate or potassium hydroxide into the reservoir. The alkaline solution alters the wettability of the rock as well as reacts with the acids in the oil to create a surfactant in situ which will reduce the interfacial tension (Alkafeef and Zaid, 2007). For this technique oil viscosity of less than 35 cP with a reservoir permeability of greater than 20 mD is recommended. Sandstone reservoirs are also preferred (Alkafeef and Zaid, 2007).

Micellar or microemulsion flooding is a recovery process generally used for light oils. This process consists of the injection of a micellar solution slug, followed by a polymer solution slug, which is driven by waterflood (Ali and Thomas, 1996). The micellar solution is usually made up of water, hydrocarbons, 10-15% surfactants, alcohol and small amounts of salt. This technique requires much background work into the flood design to tailor it to the reservoir. It is also restricted to light oil with viscosities less than 20 mPa.s, low salinity reservoirs and low to medium temperatures. Another major problem with micellar flooding is that it requires small well spacing which increases the operating cost of this technique (Ali and Thomas, 1996).

The use of CGA fluids as a chemical enhanced recovery process would be beneficial. It has been established that colloidal gas aphrons are not attracted to each other or to mineral surfaces (Growcock et. al. 2004). This means that they will not cling to pore walls and would move freely through reservoir pores which would be advantageous for a recovery fluid. Another benefit is that CGA fluids could be used on different lithologies, and not limited to sandstone reservoirs. Aphron drilling fluids were used successfully in dolomitic limestone and sandstone reservoirs in completion and workover applications (MacPhail et al. 2008). Aphrons could also be used on lower permeable reservoirs if the micro-bubbles are suitably sized. Colloidal gas aphrons have also been found to withstand compression to at least 4,000 psig and so could be used in reservoirs up to this pressure limit (Belkin et al. 2005).

3. EXPERIMENTAL SET-UP, MATERIALS AND PROCEDURES

The equipment, materials and procedures used in this study are detailed in the following sections.

3.1 Materials used in CGA production

3.1.1 Aqueous Fluid

In this study the target was to produce aqueous colloidal gas aphrons and deionized water was used as the aqueous phase. Deionized water was produced using the Elga Purelab Ultra shown in Figure 3-1.

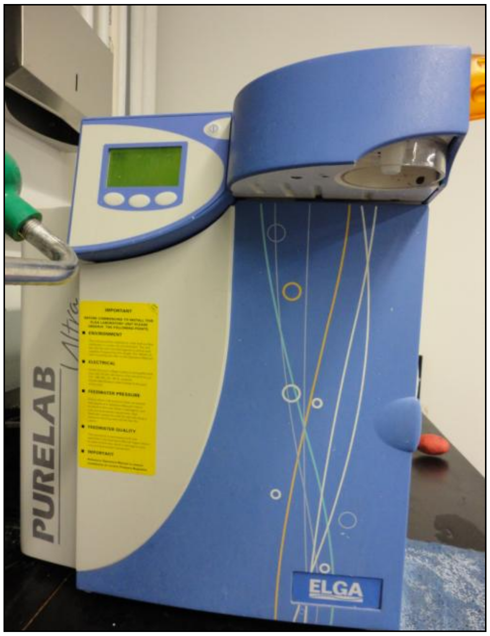

Figure 3-1: Elga Purelab Ultra used to produce deionized water

3.1.2 Polymer

The addition of polymer to the base fluid improves the rheological characteristics such as shear viscosity and low shear rate viscosity (LSRV). This results in much more stable micro-bubbles as the size increase over time is reduced. Different polymers were used in the initial screening to determine the best polymer suited to the generation of stable aqueous colloidal gas aphrons.

Barazan D (Xanthan gum)

This is a biopolymer that provides viscosity and suspension without the need for clays. It disperses rapidly, provides thixotropic properties and Non-Newtonian flow characteristics at low concentrations over a wide range of salinities. This polymer was supplied by Baroid Industrial Drilling Products.

Table 3-1 Physical Properties of Barazan D (Baroid® Products Data Sheet)

Property	**Description**
Appearance	Yellow to white powder
pH (1% aqueous solution)	6.3
Specific gravity	1.6

CMC – Carboxymethyl cellulose

This polymer is a cellulose derivative and is synthesized by the alkali catalyzed reaction of cellulose and chloroacetic acid. The polar carboxyl groups render the cellulose soluble and chemically reactive. It is used as a drilling mud additive where it acts as a viscosifier and water retention agent. It is an off white to light beige powder in appearance. This was sourced from the undergraduate drilling lab.

Liqui-Vis EP (HEC)

This is a high purity HEC (hydroxyethyl cellulose) polymer which is dispersed in a water soluble carrier. It is designed to viscosify fresh water and low weight brines for drill-in fluid applications. This product was obtained as a sample from Baroid Industrial Drilling Products.

Table 3-2 Physical Properties of Liqui-Vis (Baroid® Products Data Sheet)

Property	**Description**
Appearance	Off white suspension
Flash Point	200˚F (93˚C)
Pour Point	50˚F (10˚C)
Specific Gravity @ 75˚F (23.9˚C)	1.08

N-Vis (Xanthan Gum)

This product is a high quality xanthan gum polymer. It is used in reservoir drill-in fluids to provide solid suspension and hole cleaning capabilities. It is designed to minimize reservoir formation damage. This was also obtained as a sample from Baroid Industrial Drilling Products.

Table 3-3 Physical Properties of N-Vis (Baroid® Products Data Sheet)

Property	**Description**
Appearance	Dispersible beige powder
Bulk density	45 lb/ft^3, 721 kg/m^3
Mesh Size (% through 40 mesh)	95

Quik-trol

This is a modified natural cellulose polymer which can provide filtration control in small quantities in most water based drilling fluid systems. Quik-trol was also sourced from the undergraduate drilling lab.

Table 3-4 Physical Properties of Quik-Trol (Halliburton® Products Data Sheet)

Property	**Description**
Appearance	White powder
pH (1% aqueous solution)	8.0

3.1.3 Surfactants

Surfactants are chemicals which can lower the surface tension of a liquid, the interfacial tension between liquids or between a liquid and a solid. They are usually organic solvents which are comprised of a hydrophilic head and a hydrophobic tail and as such are amphiphilic in nature. Surfactants are used to encourage bubble stability and are divided into three main groups: cationic, anionic and non ionic. This classification is based on the presence and nature of the charged group on the surfactant head. If there is a net positive charge on the head of the surfactant then it is considered cationic, if there is a net negative charge then it is anionic. Surfactants which contain no charged groups are considered non ionic.

For this study a surfactant from each group was chosen: CTAB (Cetyltrimethyl Ammonium Bromide) – cationic, DDBS (Sodium Dodecyl Benzene Sulfonate) – anionic and Tergitol (15-S-12) – non ionic.

Table 3-5 Physical Properties of CTAB (bioWORLD® Product Data Sheet)

Property	**Description**
Chemical Formula	$C_{19}H_{42}BrN$
Appearance	White powder
Odour	Slight ammoniacal
Molecular Weight	364.48 g/mol
pH (1% solution/water)	5-7.5
Melting Point	250˚C (482˚F)
Solubility in water	10%
HLB Number	10

Table 3-6 Physical Properties of DDBS (Sigma-Aldrich® Product Data Sheet)

Property	**Description**
Chemical Formula	$C_{18}H_{29}NaO_3S$
Appearance	Off white powder
Molecular Weight	348.49 g/mol
Boiling Point	Decomposes
Melting Point	144.5˚C (292.1˚F)
HLB Number	11.7

Table 3-7 Physical Properties of Tergitol (Sigma-Aldrich® Product Data Sheet)

Property	**Description**
Chemical Description	C_{11}-C_{15} secondary ethyloxalated alcohol
Appearance	Colourless liquid
Density	0.993 g/cm^3
Flash Point	186˚C (367˚F) – closed cup
HLB Number	14.5

3.2 Other Lab Materials

3.2.1 Mineral Oil

Dyed Mineral Oil was used in both the Visual Cell and Radial Core flooding experiments. Mineral Oil is light paraffin oil composed mainly of paraffins and cyclic paraffins.

Table 3-8 Physical Properties of Mineral Oil (Fisher Scientific® Product Data Sheet)

Property	**Description**
Physical state	Liquid
Appearance	Water-white
Odour	None
Vapour Pressure	<0.1 mm Hg
Viscosity	<33.5 centistokes @ 40˚C
Boiling Point	260-426˚C
Solubility	Insoluble in water
Specific Gravity/Density	0.83@15.6˚C
Molecular Composition	Paraffin mixture
API Gravity	39˚API

3.2.2 Glass Beads

Two sizes of glass of glass beads were used. For the radial cell Spheriglass A-Glass 3000 solid glass spheres were used and were supplied by Potter's Industries Inc. The particle size distribution was 30-50 microns and specific gravity was equal to 2.5. For the visual cell solid glass spheres of a 50-80 mesh size with a particle size distribution of 177-297 microns was used and obtained through Sil Industrial Minerals.

3.3 Equipment

3.3.1 Homogenizer

To generate Colloidal Gas Aphrons the Polytron PT 6100 digital homogenizer was used. This piece of equipment is a product of Kinematica Inc and can rotate at speeds up to 26,000 RPM.

Figure 3-2 Polytron PT 6100 digital homogenizer

3.3.2 Digital Scale

The precision balance Ohaus EP 2102 Explorer Pro was used as a digital scale.

Figure 3-3 Ohaus EP 2012 Explorer Pro

3.3.3 Microscope

Measurements of micro-bubbles over time and bubble size distributions were done using the Leica DM 6000M microscope. There was a camera attached at the top of the device for taking images.

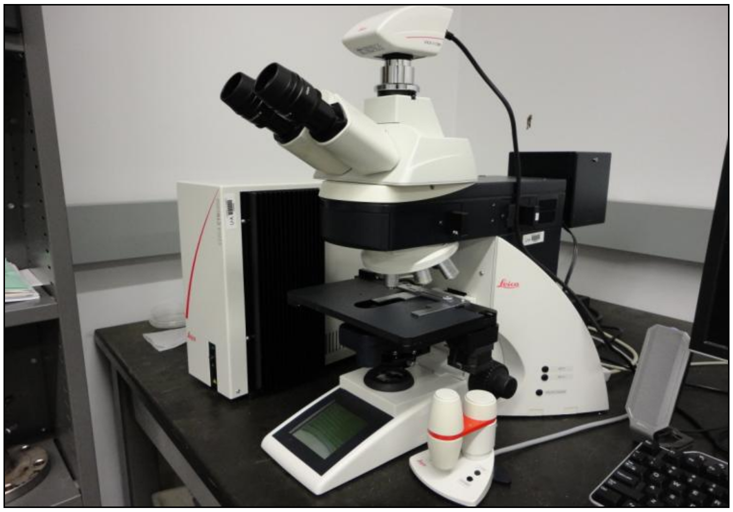

Figure 3-4 Leica DM 6000M microscope

3.3.4 Rheometer

The rheometer used is the Bohlin CVOR which is manufactured by Malvern Instruments. This device has a shear range of 0.0001 to 10 000 s^{-1}. There were two available cell types to conduct rheological tests: the CVOR 150 Peltier cell and the High Pressure cell. For this study the CVOR 150 Peltier cell was used which is a cone and plate measuring system. The sample was placed in the 0.15 mm gap between the rotating upper cone of an inclination of 4° and a diameter of 40 mm. The fixed lower plate had a diameter of 60 mm.

Figure 3-5 Bohlin CVOR Rheometer

3.3.5 Syringe Pumps

Two different syringe pumps were used due to their capacities and pressure limits. For the visual cell experiments the Chemyx Nexus 250 ml syringe pump was used and is seen in Figure 3-6. For the larger volume core experiments the ISCO D 500 syringe pump was used. The capacity of this pump was 500 ml with an operating limit of 3750 psi and is shown in Figure 3-7.

Figure 3-6 Chemyx Nexus 250 ml syringe pump

Figure 3-7 ISCO D 500 syringe pump

3.3.6 Visual Cell

The visual cell experiments were conducted using an acrylic model to enable time lapse photos to be taken and real time monitoring. This model was 0.225 m in length, 0.07 m in width and 0.014 m in height. This apparatus contained one injection port and one production port located at either end of the model which encouraged a linear flow pattern. These ports were spanned the width of the model. The pressure transducer is seen connected to the injection port for pressure monitoring and is seen in Figure 3-8.

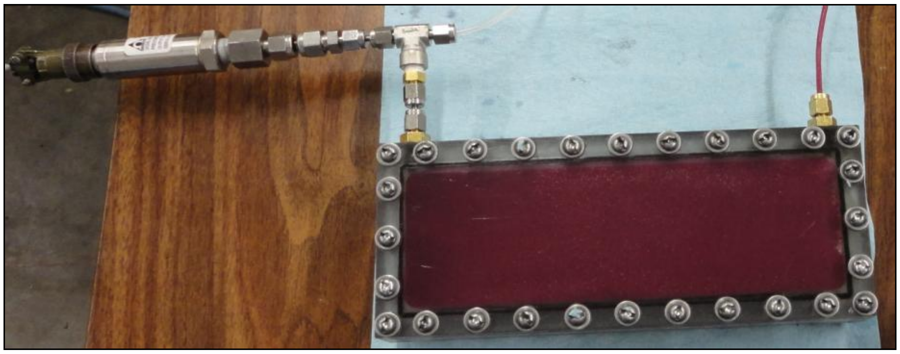

Figure 3-8 Visual cell

3.3.7 Radial Cell

The core flooding experiments was conducted using a radial cell set-up. This set-up was specially designed to withstand high pressures as well as simulate radial flow. This was desirable as radial flow is more pertinent to field conditions and applications. The radial cell allowed glass beads to be tightly packed in and function as a core in these experiments.

The radial cell is comprised of one inlet for injection seen at the centre of the apparatus and two outlets for production seen on the outer edges. This mimics the field set-up of an injection well and two production wells.

The radial cell has an internal diameter of 98 mm and a height of 191 mm. The radius of the injection line was 7 mm with both production lines having a radius of 3.6 mm. The perforation height was 145 mm and both the injector and producers were surrounded by a screen mesh of about 10 microns. The inner portion of the radial cell was also surrounded by a screen mesh to encourage radial flow to the producer ports. Both ends of the radial cell are removable and one end was utilized to pack the glass beads. The radial cell apparatus is shown in Figure 3-9.

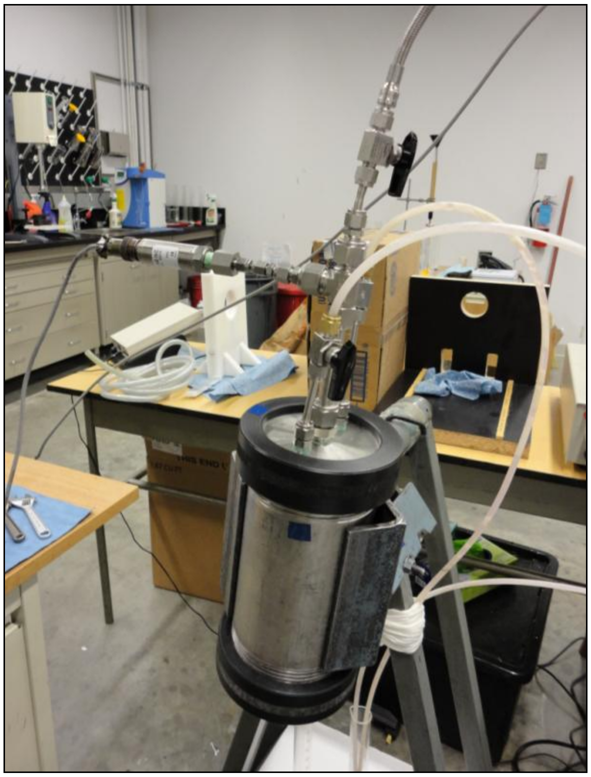

Figure 3-9 Radial cell

3.3.8 Data Acquisition

The data acquisition system used was made up of two pressure transducers connected to the data logging system. These two pressure transducers have different pressure ranges of 0-100 psi and 0-500 psi and were both made by Omegadyne. A National Instruments data acquisition system (NI USB-9219) was used which transferred the pressure readings to the computer. These pressure readings were then interpreted and recorded using the Labview Signal Express software, also supplied by National Instruments.

3.4 Experimental Set-Up and Procedures

This section details the experimental setup and procedures involved in this study. The procedures involved in the generation and characterization of aqueous colloidal gas aphrons is described as well as the experimental set-up of the visual cell and radial cell.

3.4.1 Experimental Procedure for the Production of Aqueous CGA Fluid

Preparation of the Base Fluid

To prepare aqueous colloidal gas aphrons, the base fluid must first be formulated and is comprised of deionized water and polymer. In previous work, the desired amount of polymer was slowly added to 400 ml of water over a 16 minute period (Bjorndalen and Kuru, 2005). This was done to prevent clumping and to ensure an even distribution of the polymer. This base fluid was then allowed to cool to room temperature. In this study 350 ml of water was placed in a measuring jar to which the required amount of polymer was added. The jar was then closed and shaken vigorously for 1 minute until the polymer was evenly dispersed. This method prevented clumping as well as the time needed to allow the base fluid to cool to room temperature.

Preparation of the Aqueous CGA Fluid

Using the base fluid from above, the required amount of surfactant is added. This mixture is then agitated using the Polytron DT6100 for a specific time. This homogenizer is designed to encourage air entrapment through its dispersing aggregate. The mixture was agitated for 1 minute at a speed of 8000 RPM. To ensure the uniformity of micro-bubbles as well as the standardization of the procedure, the shearing speed and shearing time was kept constant. Following the mixing, the aqueous CGA fluid was used for characterization without any time delay.

3.4.2 Experimental Procedure for the Characterization of Aqueous CGA Fluid

Measurement of micro-bubble diameter

To measure micro-bubble diameter the Leica DM 6000M microscope was used. This is an optical microscope with a camera attached at the top of the device. The microscope is also connected to a computer for viewing and storing the images taken. Figure 3-10 shows a picture of aphrons taken using the microscope. Immediately after aphronization the sample is poured into three different petri dishes with care taken to ensure a thin layer of sample. If the sample layer is too thick then not enough light will be able to penetrate and will affect the quality of the images. Multiple photos are then taken of each petri dish using the camera and the Leica Materials Workstation software. The images are then saved and opened using the Leica Measurements Workstation software. In this program by using the mouse, the bubble diameter is drawn and these measurements are saved into a table using the manual measurements option and can be seen in Figure 3-11. No scaling factor is needed as the program adjusts to accommodate changes in image size. This data can then be exported to Microsoft Excel and manipulated.

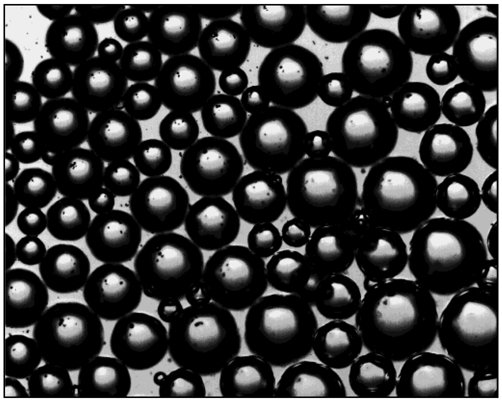

Figure 3-10 Picture of aphrons under microscope

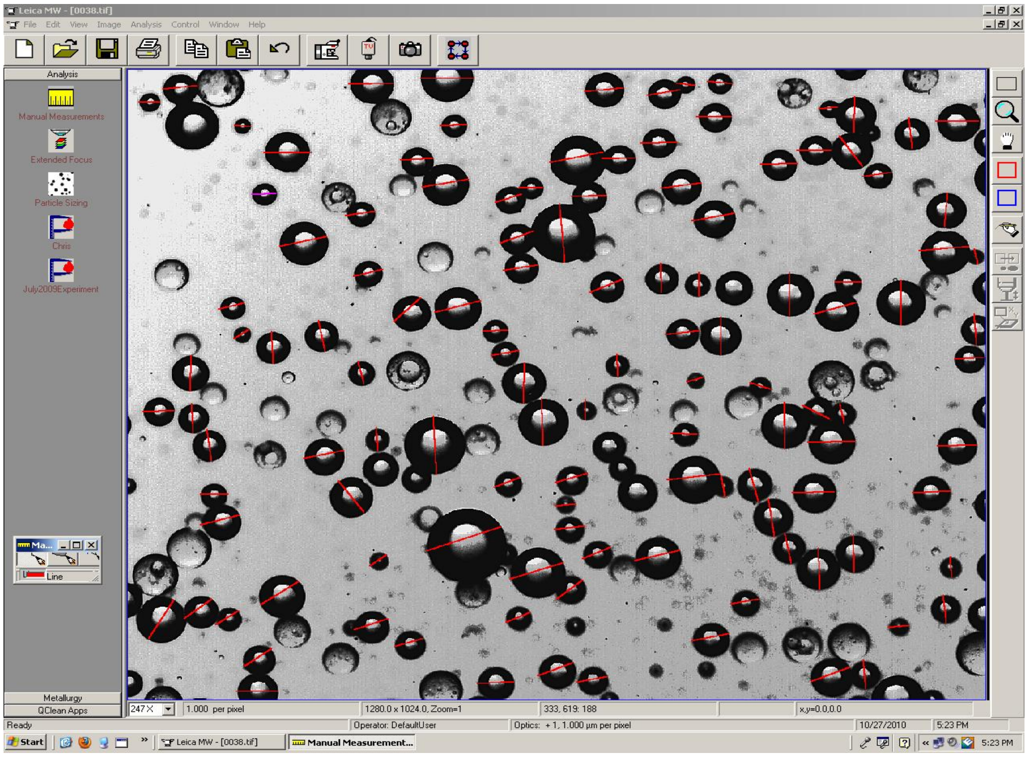

247 X | 1.000 per pixel | 1280.0 x 1024.0, Zoom=1 | 333, 619: 188 | x,y=0.0,0.0

Ready | Operator: DefaultUser | Optics: + 1, 1.000 µm per pixel | 10/27/2010 | 5:23 PM

Figure 3-11 Screenshot of measurement of micro-bubble diameter

Micro-bubble diameter analysis

Many micro-bubble diameter measurements were made using the above procedure. The number of measurements taken per aqueous CGA fluid sample was more than 300 and less than 1,000. This ensured that the data was not skewed by a small sample size and an accurate representation of the data was depicted. The data in Microsoft Excel was then sorted according to micro-bubble size and their frequency. Using this, a cumulative micro-bubble size distribution curve was produced (similar to a particle distribution curve). An example of a particle size distribution plot is shown in Figure 3-12 and from this graph the median d_{50} was determined. This refers to the diameter at which 50% of the micro-bubbles are larger and the other 50% are smaller. This d_{50} diameter was plotted against time to give an indication of the change in micro-bubble size over time. This is particularly important to stability as the smaller micro-bubbles will be more stable and display a smaller change in size over time. Another method of micro-bubble diameter analysis utilizes bubble size distribution. This was done by counting the number of micro-bubbles which fell into the following categories: 0-20, 20-40, 40-60, 60-80, 80-100, 100-120, 120-140, 140-160, 160-180, 180-200 and >200 microns. This number was then expressed as a percentage of the entire sample and was done using the same time intervals as the d_{50} measurements. The most suitable surfactant was determined using these methods of micro-bubble diameter analysis.

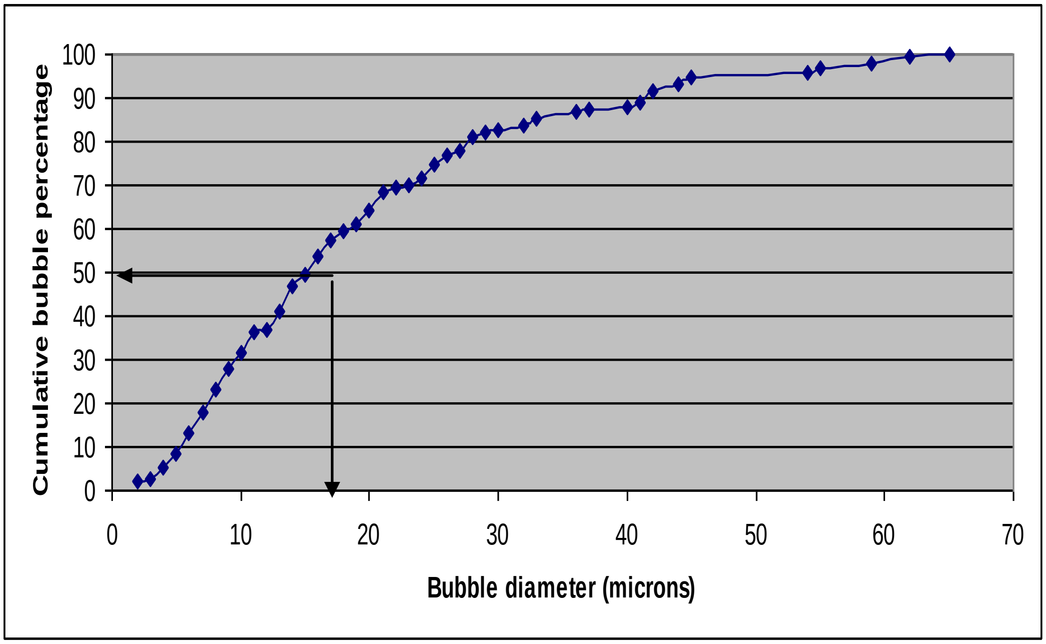

Figure 3-12 Sample cumulative bubble size distribution

Yield Tests

If a CGA fluid is left undisturbed after mixing it will tend to cream. This occurs due to the density difference between the two phases. This characteristic has been used to determine yield and quantify stability. To determine yield, a sample is poured into a 100 ml measuring cylinder after aphronization. The total height of the sample is recorded along with the height of the drained liquid over the time. Yield is then calculated using the Equation 3-1.

$$\text{Yield} = [(\text{total height} - \text{height of drained liquid}) \div \text{total height}] \times 100 \qquad \text{Equation 3-1}$$

Yield is used to determine how well a surfactant or polymer influences stability. The more stable micro-bubbles will not collapse and so the drained liquid sector will be very small and grow slowly over time. The most stable formulations will have a high yield which will decrease very slowly with time.

3.4.3 Visual Cell Set-Up

After the ideal formulation for aqueous colloidal gas aphrons was chosen it was tested on both the visual and radial cells. To prepare the visual cell for flooding experiments requires a number of steps. Firstly, it is cleaned and dried. Then the (50-80 mesh) glass beads are evenly poured into the apparatus using a beaker. The Visual Cell is then covered and the glass beads shaken to one end. This is done to ensure tight packing with no air spaces in the sand pack. More glass beads are added and shaken until the apparatus is completely full and a tight sand pack is created. Then the O-ring on the lid of the visual cell is greased using Dow Corning Molykote 55. Dow Corning High Vacuum Grease is then applied to the area outside the O-ring on both parts of the apparatus. These two products are used to ensure an airtight seal and quality pressure data. The visual cell is then closed by fitting and tightening the screws. This model is then connected to the Chemyx Nexus syringe pump which has been filled with dyed mineral oil. The glass beads are then saturated using the dyed mineral oil which is pumped at a rate of 1 ml/min. When the mineral oil is barely seen coming out of the production port, pumping is stopped. The amount of oil pumped is then recorded as this corresponds to the amount of oil contained in the model. After this, the syringe pump is cleaned and then filled with the flooding fluid. The pressure transducer is then connected to the visual cell and pump. A measuring cylinder is placed at the production port to collect the mineral oil that will be produced. A schematic of this set-up can be seen in figure 3-13. The flooding experiment is started at a pumping rate of 0.3 ml/min. This pumping rate was chosen because at higher rates the pressure would cause the apparatus to leak. Time lapse images are taken at intervals throughout the experiment using a digital camera mounted on a tripod. The experiment is stopped when nearly all the mineral oil is produced or the amount of mineral oil produced is very little. Breakthrough time is noted and the amount of oil produced is recorded in 10 minute intervals.

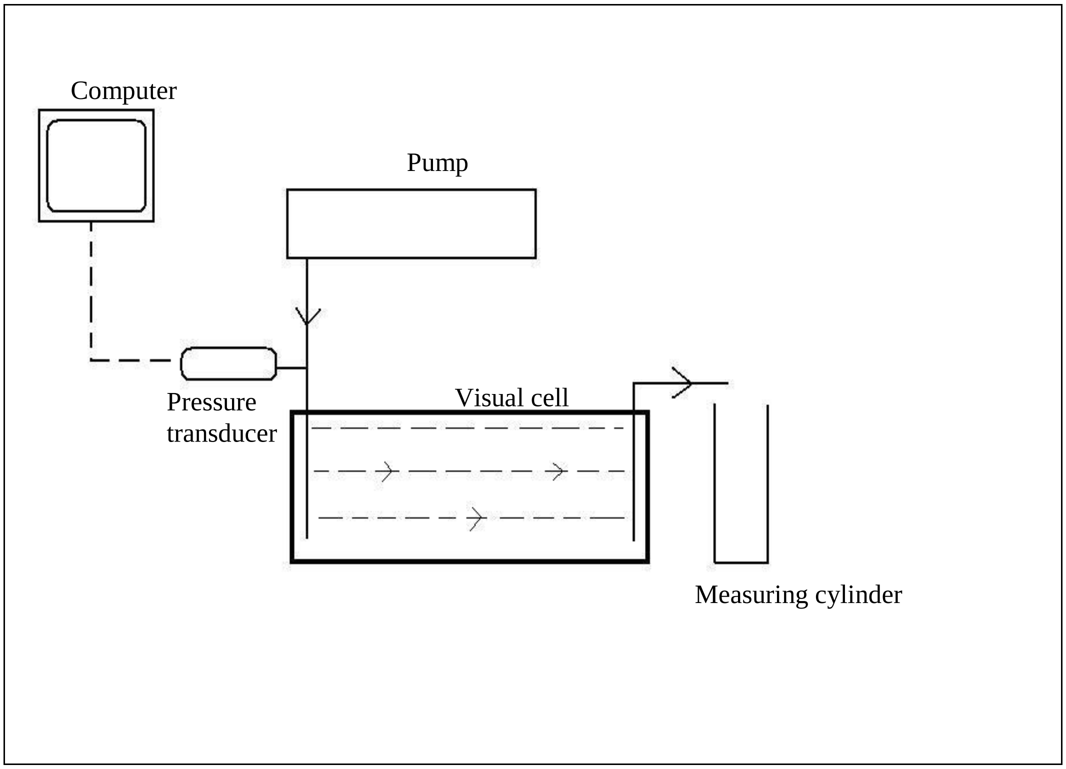

Figure 3-13 Visual cell set-up

3.4.4 Radial Cell Set-Up

The radial cell is cleaned and dried before it is secured into place. The top part of the apparatus containing the ports is fitted and fixed into place by using a rubber mallet. The outer ring is then secured to make an airtight seal. The radial cell is then turned upside down. From this open end, the required amount of glass beads is added in small quantities. The rubber mallet is then used intermittently to vibrate the cylinder to ensure tight packing. The capacity of this vessel is 2,000 g of the Spheriglass A-Glass 3000. The circular mesh is then positioned before securing the bottom end using the rubber mallet. Again, another outer ring is used to ensure an airtight seal. The apparatus is then turned upright and the pressure transducer connected. The ISCO D5000 syringe pump is then filled with 500 ml of dyed mineral oil. The pump is connected to the Radial Cell and the production ports on the apparatus are closed. The injection port is opened and the pump is started at a rate of 1 ml/min. After saturation, the radial cell is left to rest overnight. The following morning, the pump is cleaned and filled with the flooding fluid. The production ports are opened and the production lines are placed into a measuring cylinder. The experiment is then started at a rate of 4 ml/min and the amount of produced oil is recorded in 10 minute intervals. Breakthrough time and the amount of recovered oil are noted. As before, the experiment is stopped when oil recovery is very low.

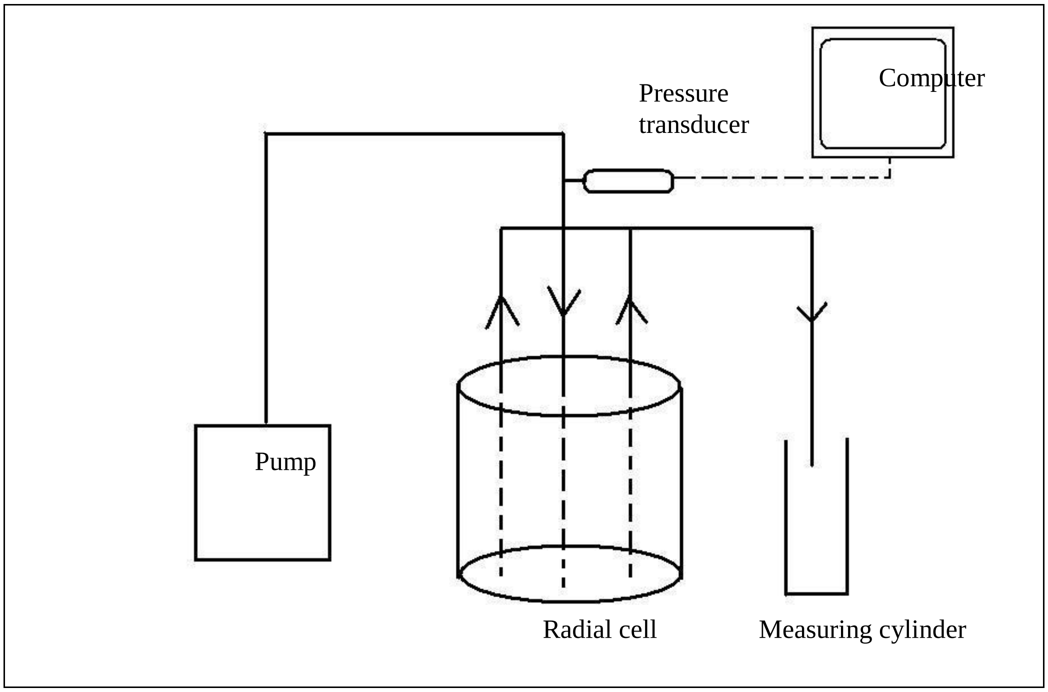

Figure 3-14 Radial cell set-up

4. RHEOLOGICAL CHARACTERIZATION OF AQUEOUS APHRON FLUIDS

This chapter will detail the reasoning and data behind the choice of each component of the resulting colloidal gas aphron fluid. Rheological tests, bubble sizing and bubble size distribution will help determine the right chemical component to add to the CGA formulation. The aqueous CGA fluid is made up of de-ionized water, polymer and surfactant. Using the tests mentioned above the optimum concentration of each must be determined to create the most stable aqueous colloidal gas aphron fluid.

4.1 Polymer

The use of a polymer is to improve the rheological properties such as shear viscosity and low shear rate viscosity (LSRV). These two properties are related to the stability of the aqueous micro-bubble fluid. The viscous water shell in aphrons must have a minimum viscosity to remain stable according to Ivan et al. 2002. Water molecules have a tendency to diffuse out of this viscous water film and into the bulk water which results in the destabilization of the aphron. The rate of transfer of these water molecules is also described as inversely proportional to viscosity (Ivan et al. 2002). Therefore higher LSRV values will result in more stable aphrons as this transfer of water molecules is prevented. Brookey (1998) used a biopolymer to viscosify the lamella separating aphrons and the water layer in the bubble film surrounding the aphron core. This resulted in more stable aphrons which were better able to resist expansion and compression. Five different polymers were tested to determine the one most suitable. These five polymers were: Xanthan gum (Barazan D), Carboxymethylcellulose (CMC), Hydroxyethylcellulose (Liqui-Vis EP), Xanthan gum (N-Vis) and another cellulose based polymer (Quik-Trol). These polymers were tested by making solutions of these products with de-ionized water.

4.1.1 Xanthan gum (Barazan D)

This polymer provides viscosity and suspension without the need for clays. This product was chosen as it is actively used as a component in drilling and reservoir fluids. Brookey (1998) and (Bjorndalen and Kuru, 2005) used this product to enhance the stability of the CGA fluid. Table 4-1 shows the effect of increasing concentration of xanthan gum on the LSRV. The LSRV is seen to quickly increase with rising polymer concentration. The highest LSRV is 143,000 cP at 4.0 lb/bbl xanthan gum concentration.

Table 4-1 LSRV data for various concentrations of xanthan gum

Conc (lb/bbl)	LSRV @ 0.1/sec (cP)	LSRV @ 0.1/sec (Pa.s)
0.5	3 130	3.13
1.0	18 940	18.94
2.0	51 520	51.52
3.0	104 000	104.00
4.0	143 000	143.00

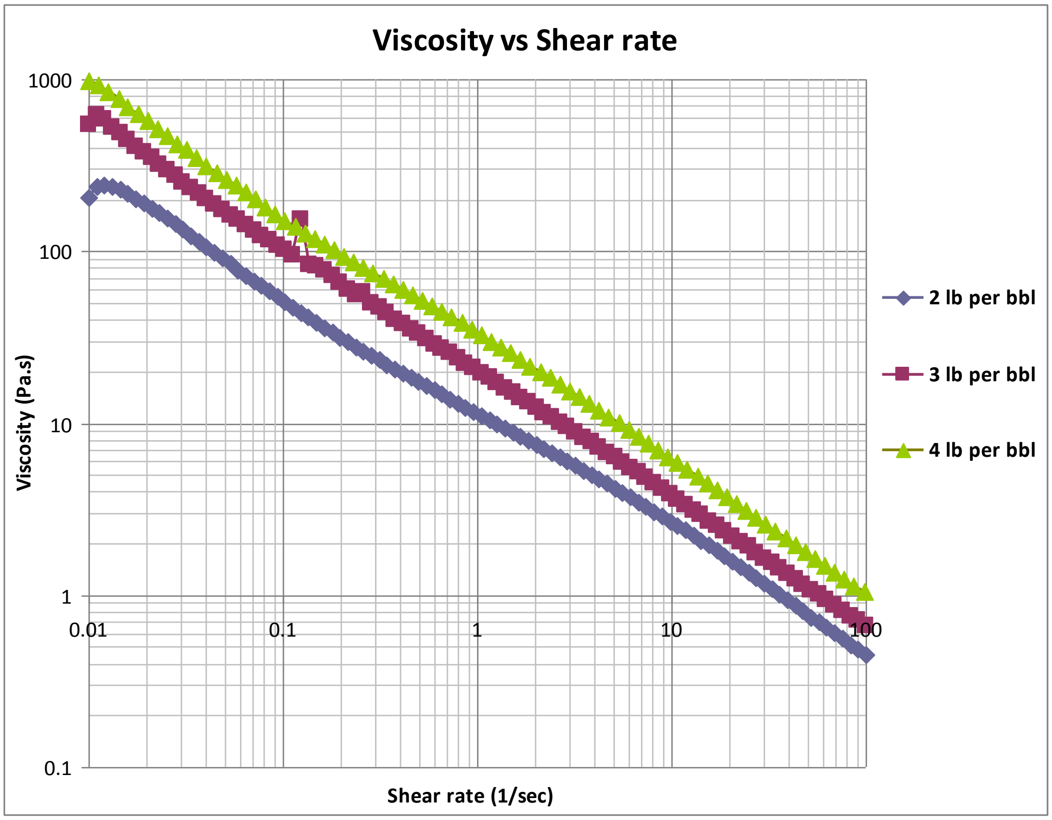

Figure 4-1 Viscosity vs. shear rate for different xanthan gum concentrations

Shear thinning or pseudoplastic behaviour is seen in Figure 4-1 as with increasing shear rate there is a corresponding decrease in viscosity. This type of behaviour is expected in polymer solutions.

4.1.2 Carboxymethylcellulose (CMC)

This polymer is a cellulose derivative and is synthesized by the alkali catalyzed reaction of cellulose with chloroacetic acid. It is used as a drilling mud additive where it acts as a viscosifier and water retention agent. Table 4-2 shows that an increase in CMC concentration from 0.5 to 1.0 lb/bbl does not impact the LSRV, however a further increase in concentration to 2.0 lb/bbl gives a small increase from 110 to 115 cP. At 3.0 lb/bbl the highest LSRV is observed at 130 cP.

Table 4-2 LSRV results for various concentrations of CMC

Conc (lb/bbl)	LSRV @ 0.1/sec (cP)	LSRV @ 0.1/sec (Pa.s)
0.5	110	0.11
1.0	110	0.11
2.0	115	0.09
3.0	130	0.13

4.1.3 Hydroxyethyl cellulose (Liqui-Vis EP)

This is high purity hydroxyethylcellulose (HEC) polymer which is dispersed in a soluble carrier. It is used to increase the viscosity of fresh water and low weight brines in the drilling industry. Table 4-3 shows a very small increase in the LSRV with larger concentrations of polymer. The lowest LSRV was 40 cP at 0.5 lb/bbl with the highest LSRV being 100 cP at 3.0 lb/bbl.

Table 4-3 LSRV results for various concentrations of HEC

Conc (lb/bbl)	LSRV @ 0.1/sec (cP)	LSRV @ 0.1/sec (Pa.s)
0.5	40	0.04
1.0	80	0.08
2.0	90	0.09
3.0	100	0.1

4.1.4 Xanthan gum (N-Vis)

This is also a high quality xanthan gum polymer. It is used to provide good solid suspension and hole cleaning to reservoir drill in fluids. Table 4-4 shows the increase in LSRV with a corresponding increase in polymer concentration. The largest rise in LSRV is seen between the 1.0 to 2.0 lb/bbl concentrations with the smallest increase occurring between the 2.0 and 3.0 lb/bbl concentrations. The highest LSRV achieved was 31,000 cP at 3.0 lb/bbl.

Table 4-4 LSRV results for various concentrations of xanthan gum

Conc (lb/bbl)	LSRV @ 0.1/sec (cP)	LSRV @ 0.1/sec (Pa.s)
0.5	8 000	8
1.0	14 000	14
2.0	30 000	30
3.0	31 000	31

4.1.5 Cellulose polymer (Quik-Trol)

This polymer is also a cellulose polymer and is used to provide filtrate control in water based drilling fluids. Table 4-5 shows small increases in LSRV with increasing polymer concentration. The largest increase in the LSRV occurred between 2.0 and 3.0 lb/bbl polymer concentration.

Table 4-5 LSRV results for various concentrations of cellulose polymer

Conc (lb/bbl)	LSRV @ 0.1/sec (cP)	LSRV @ 0.1/sec (Pa.s)
0.5	120	0.12
1.0	260	0.26
2.0	1 200	1.20
3.0	2 600	2.60

Examining the data in Tables 4-1 to 4-5 it can be seen that different polymers produced different LSRV results for similar concentrations. These results are shown in Figure 4-2. It is apparent that xanthan gum (Barazan D) provides the highest LSRV of all the polymers and showed the largest rise in LSRV with increasing concentration. This led to the decision to use xanthan gum (Barazan D) as the polymer for this study's CGA formulation. To determine the optimum concentration of xanthan gum research was done into the LSRV used in proven aphron drilling fluids. MacPhail et al. (2008) specified that the LSRV should be greater than 40,000 cP in a CGA fluid to prevent aphrons from becoming unstable and breaking apart. At a xanthan gum (Barazan D) concentration of 2.0 lb/bbl the LSRV was 51,520 cP which was clearly above 40,000 cP. Therefore the polymer concentrations of 2 lb/bbl and 3 lb/bbl would both be suitable. This was later narrowed to one concentration after testing of the surfactants.

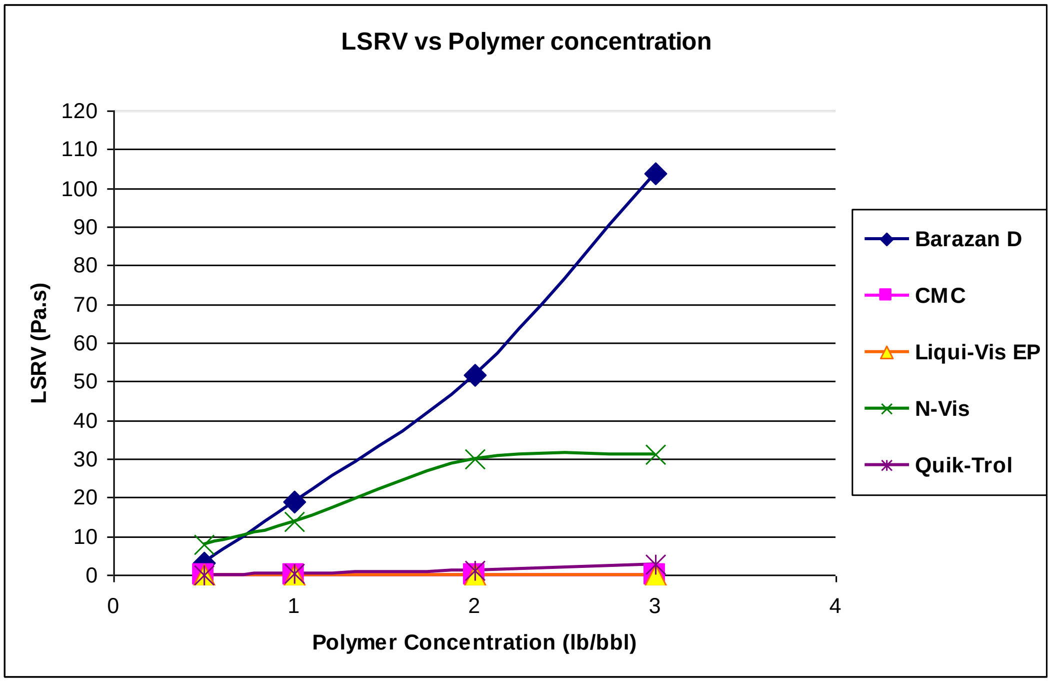

Figure 4-2 LSRV for various concentrations of each polymer

4.2 Surfactant

Surfactants are a major chemical constituent in CGA fluids and are used primarily as aphron generators. Their main function is to reduce the surface tension between two liquids. For this study three surfactants were used: CTAB (Cetyltrimethyl Ammonium Bromide) – cationic in nature, Tergitol (15-S-12) – non ionic and DDBS (Sodium Dodecyl Benzene Sulfonate) which was anionic. The surfactants are classified according to the nature of the charged group present on the surfactant head. Cationic refers to a positively charged group, anionic refers to a negatively charged group and non ionic refers to neither positively nor negatively charged group. To determine the most suitable surfactant d_{50} bubble sizing and bubble size distribution tests were conducted. These methods have been explained fully in the previous chapter. These tests were carried out using a base solution of de-ionized water with 2 lb/bbl xanthan gum polymer. Increasing surfactant concentrations were then tested using this base solution.

Effect of Mixing Procedure

In the generation of CGA fluids the base fluid (comprised of water and polymer) is usually prepared first with the surfactant added later. Figure 4-3 compares the effect of immediate mixing of all chemicals with that of using a prepared base fluid. In the immediate mixing sample no preparation of the base fluid occurred prior to adding the surfactant. The measured polymer and surfactant amounts were added to de-ionized water and immediately mixed. This test was conducted using 2 lb/bbl xanthan gum (Barazan D), a CTAB concentration of 0.2% and de-ionized water. Figure 4-3 shows that using a prepared base fluid creates much smaller aphrons than those created using immediate mixing throughout the 0-360 mins time frame. This supports the use of a prepared base fluid in the mixing procedure rather than mixing all components at once.

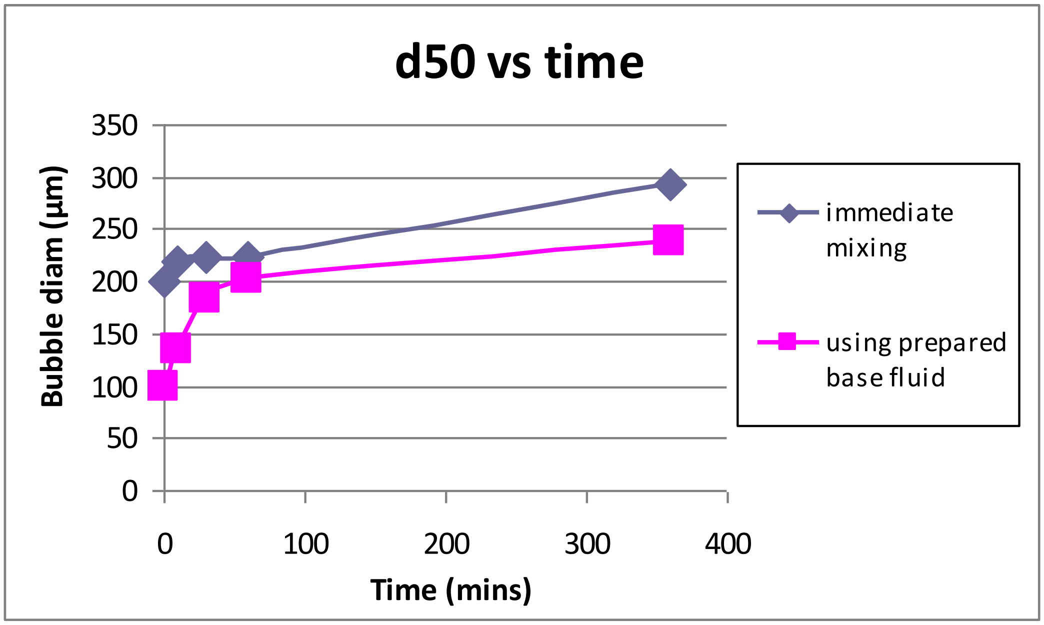

Figure 4-3 d_{50} results over time comparing mixing procedures

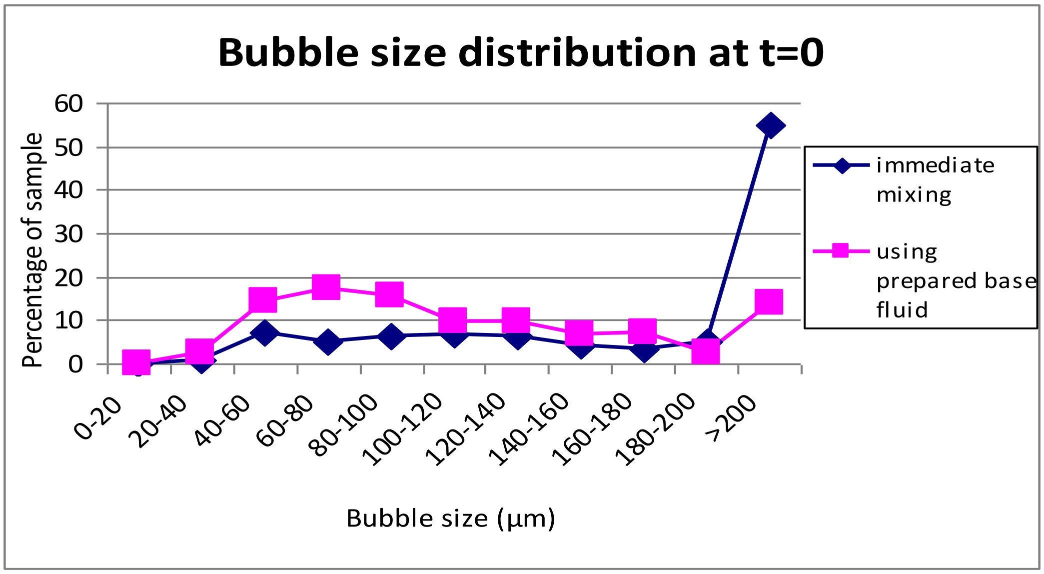

Figure 4-4 Bubble size distribution at 0 mins for different mixing procedures

Figure 4-4 shows much difference in the bubble size distribution using two different mixing procedures. The procedure using the prepared base fluid created a larger percentage of aphrons that were less than 180 microns in size that the procedure using immediate mixing. The sample prepared using immediate mixing was mostly comprised of aphrons greater than 200 microns in size (approximately 55%) while only 14% of the aphrons from the sample using the prepared base fluid fell into this category.

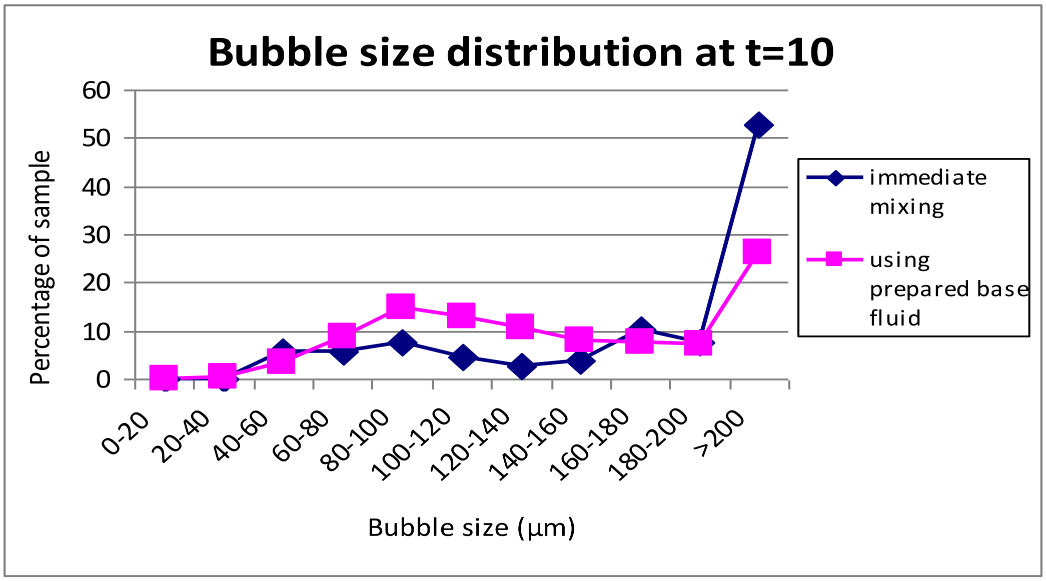

Figure 4-5 Bubble size distribution at 10 mins for different mixing procedures

At 10 mins Figure 4-5 shows that using a prepared base fluid creates a larger percentage of aphrons less than 160 microns in size as compared to immediate mixing. The sample prepared using immediate mixing has a larger percentage of aphrons greater than 200 micron in size than that using the prepared base fluid.

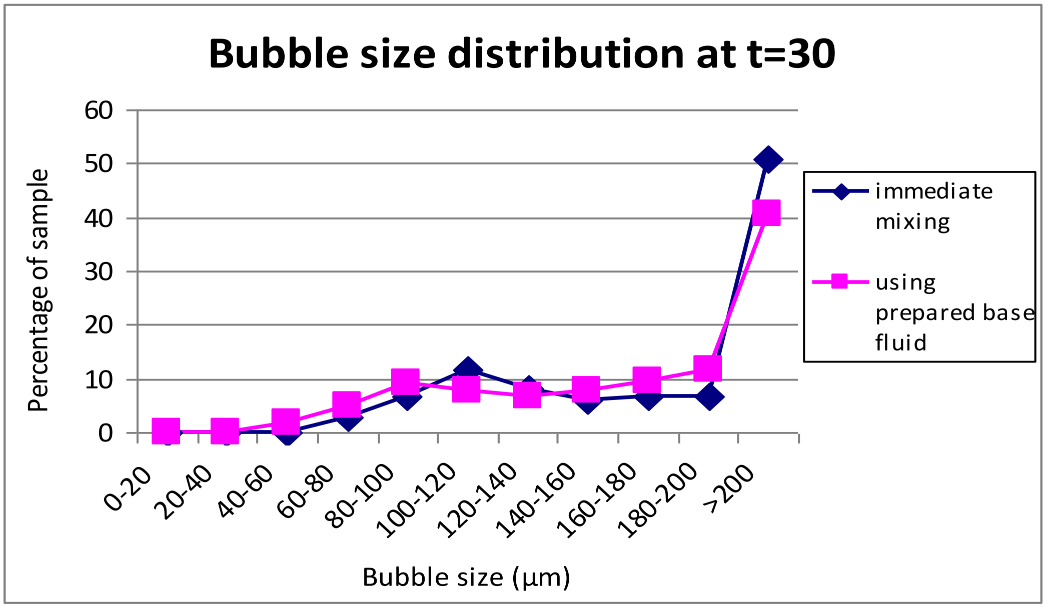

Figure 4-6 Bubble size distribution at 30 mins for different mixing procedures

Figure 4-6 shows that using the prepared base fluid produces a larger percentage of aphrons in the 0-100 and 120-200 micron size range. The sample using immediate mixing had more aphrons larger than 200 microns than the sample using the prepared base fluid.

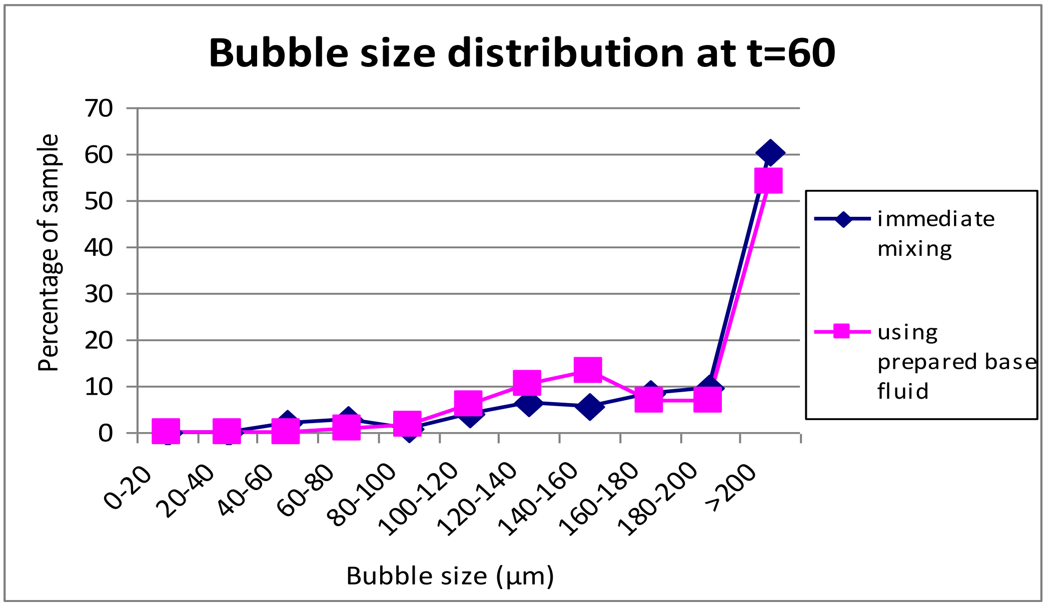

Figure 4-7 Bubble size distribution at 1 hour for different mixing procedures

Figure 4-7 shows much more aphrons were in the 80-160 micron range for the sample prepared using the base fluid than that of the sample prepared by immediate mixing. The sample using immediate mixing also had more aphrons which were larger than 160 microns than the prepared base fluid sample.

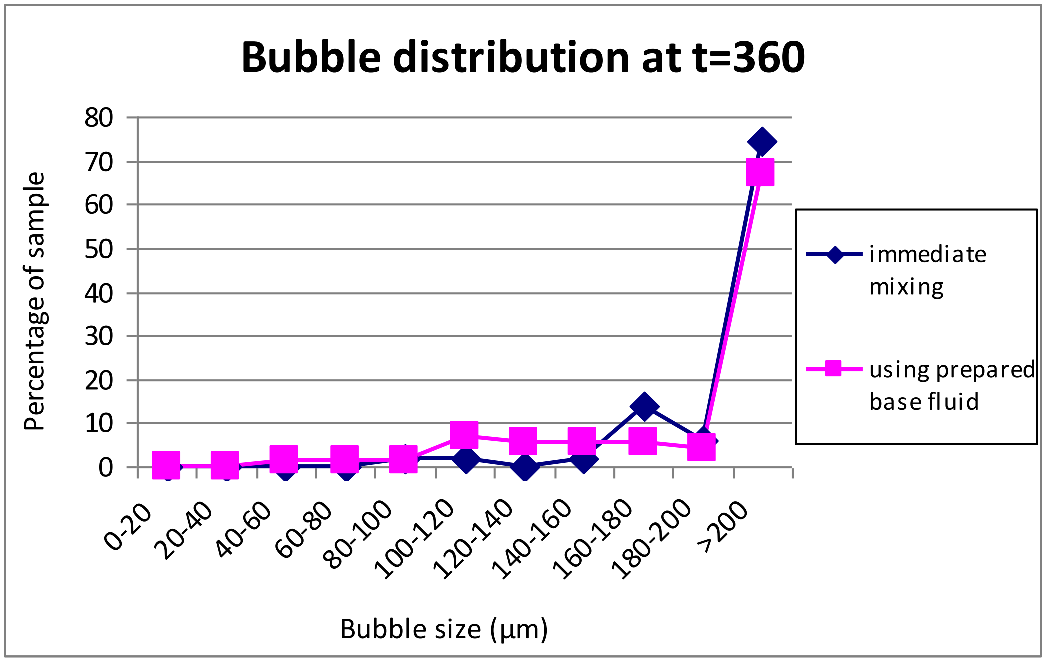

Figure 4-8 Bubble size distribution at 6 hours for different mixing procedures

At 6 hours about 75% of the sample prepared using immediate mixing was made up of aphrons larger than 200 microns seen in Figure 4-8. In the sample using the prepared base fluid aphrons which were less than 80 microns in size are still present unlike the sample using immediate mixing. There were also more aphrons in the 100-160 size range in the sample using the prepared base fluid than in the sample using immediate mixing. Figures 4-3 to 4-8 all support the use of a prepared base fluid rather than immediate mixing as this creates smaller sized aphrons in larger quantities.

4.2.1 CTAB (Cetyltrimethyl Ammonium Bromide)

This surfactant was tested as Zhao et al. (2009) found that very small bubbles were created generally in the 26.4 to 28.3 micron range. As mentioned above a 2 lb/bbl solution of xanthan gum (Barazan D) and deionized water was used as a base solution. Table 4-6 shows that the 0.5% concentration having the smallest d_{50} diameter of 76.75 microns at 0 mins as compared to the other concentrations. This trend continued until 6 hours where the 0.5% concentration has the largest diameter of all the tested concentrations which suggests that during the 1-6 hour period this concentration was the least stable. The 0.2% mixture is seen as most suitable as there is a slow gradual increase in d_{50} diameter with time even though the d_{50} diameter at 0 mins is larger than that of the 0.5% concentration.

Table 4-6 d_{50} measurements vs. time for various CTAB concentrations

CTAB conc	**0.20%**	**0.50%**	**1.00%**
Time (mins)	**d 50 (µm)**	**d 50 (µm)**	**d 50 (µm)**
0	98.5	76.75	112.25
10	135.5	131.5	186.25
30	182.5	170	203.25
60	202.17	191.5	205
360	239	396	285

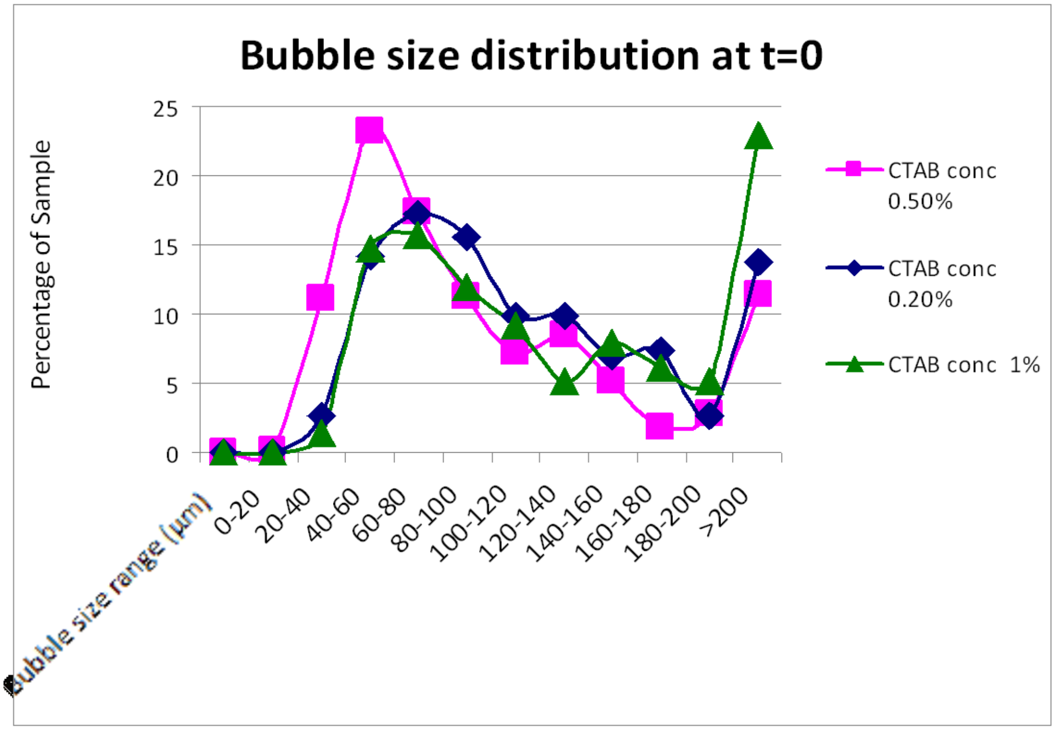

Figure 4-9 Bubble size distribution at 0 mins for various CTAB concentrations

Figure 4-9 shows that at 0 mins the bubble size distribution varied for each tested concentration. The CTAB concentration of 0.5% had most bubbles in the 20-80 micron range than the 0.2% and 1.0% mixtures. In the 80-200 range all concentrations followed the same trend as there was a general decrease in the number of bubbles as the bubble size increased. However, there was an increase in the number of bubbles greater than 200 microns for all CTAB concentrations with the 1% mixture having the most bubbles in this category.

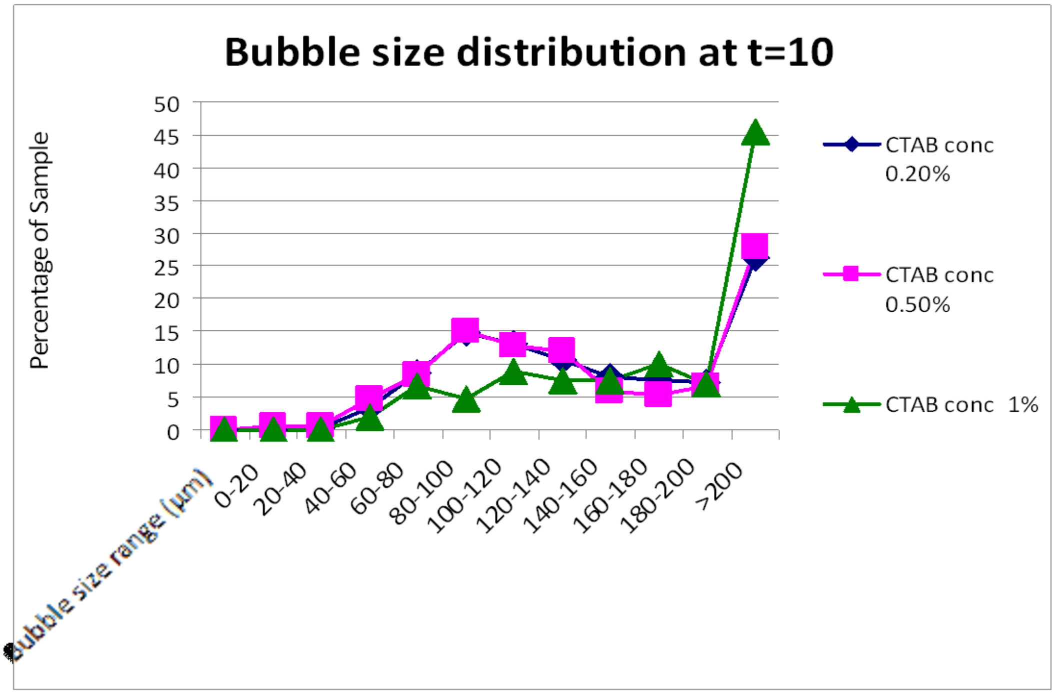

Figure 4-10 Bubble size distribution at 10 mins for various CTAB concentrations

At 10 mins Figure 4-10 shows the bubble size distribution was quite similar for the 0.2% and 0.5% CTAB concentrations as their line graphs almost overlaps. The 1% CTAB concentration was also similar to the 0.2% and 0.5% mixtures in the 0-200 micron range but almost 45% of its sample was comprised of bubbles greater than 200 microns in size.

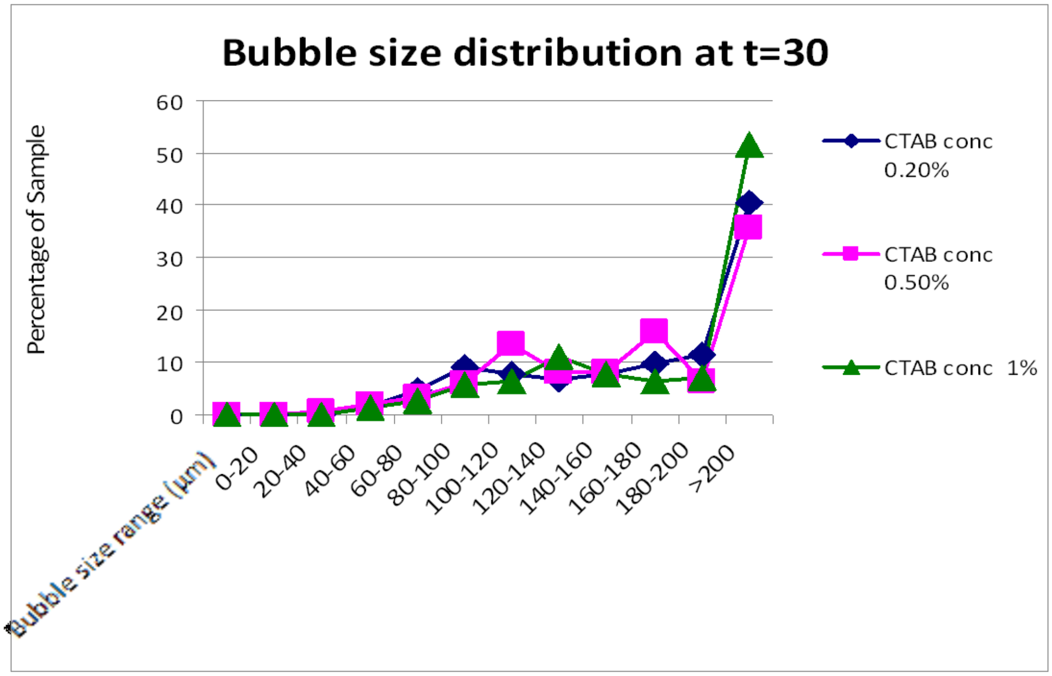

Figure 4-11 Bubble size distribution at 30 mins for various CTAB concentrations

At 30 mins Figure 4-11 shows the bubble size distribution for all concentrations which looks quite similar. The line graph is now skewing to the right as the bubbles are becoming larger in size. All concentrations show a larger number of bubbles that are greater than 200 microns in size. The 0.2% mixture has similar numbers of bubbles in the 80-200 micron range while the 0.5% mixture shows small fluctuations. The 1% CTAB concentration has most of its bubbles larger than 200 microns.

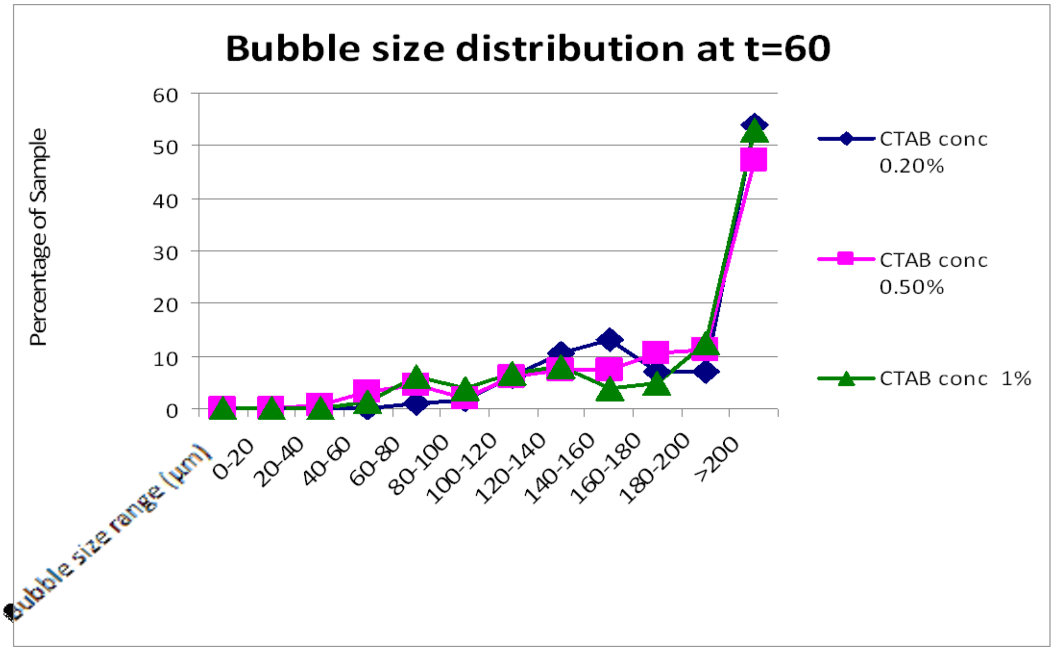

Figure 4-12 Bubble size distribution at 1 hour for various CTAB concentrations

Figure 4-12 shows a bubble size distribution which is quite similar to Figure 4-6. The number of bubbles larger than 200 microns has increased for all concentrations.

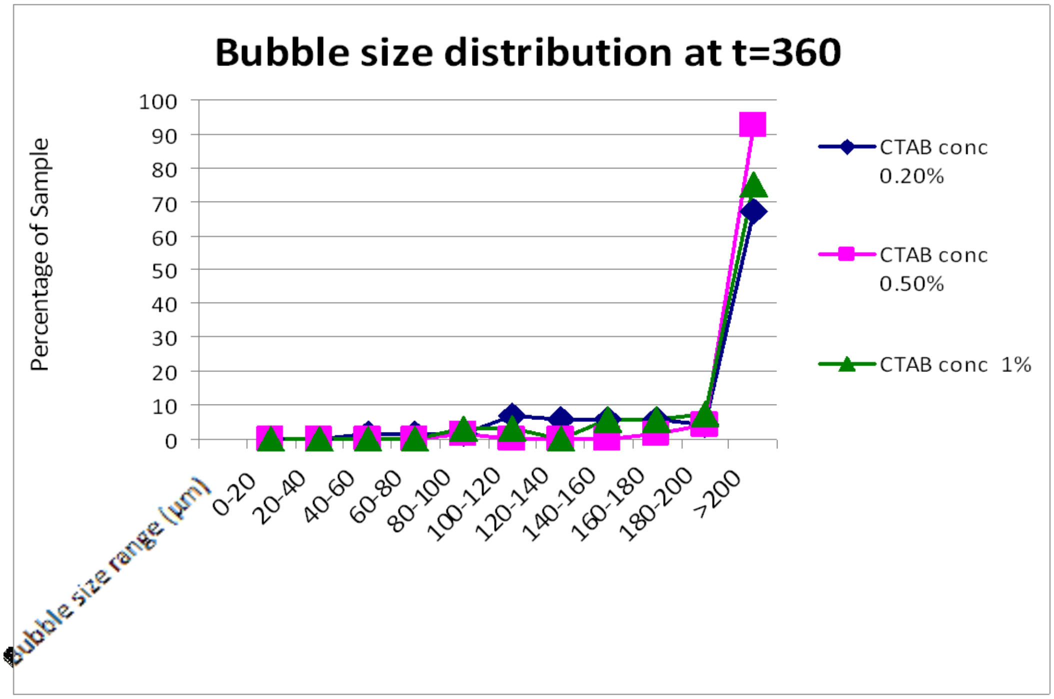

Figure 4-13 Bubble size distribution at 6 hours for various CTAB concentrations

Figure 4-13 shows that the 0.2% CTAB mixture has the more bubbles less than 200 microns than the 0.5% and 1.0% mixtures. The 0.5% CTAB concentration has more than 90% of its sample comprised of bubbles greater than 200 microns. This is followed by the 1.0% CTAB concentration at 75% with the 0.2% concentration having the least number of bubbles in this size range.

Using Figures 4-9 to 4-13 the 0.2% and 0.5% CTAB mixtures showed similar bubble size distributions while the 1% concentration was consistently made up of larger bubbles. Figure 4-13 shows more than 90% of the 0.5% CTAB concentration made up of bubbles bigger than 200 microns while the 0.2% mixture had less than 70% from this category. These observations support the d_{50}

diameter data in Table 4-6 and from this the 0.2% CTAB concentration was chosen as the most stable.

Yield experiments were conducted using the CTAB concentrations as above. In these tests no polymer was used as in these mixtures no clear interface between the aphrons and the drained liquid could be seen. Therefore a mixture of only CTAB and de-ionized water was used to determine yield.

Table 4-7 Yield results over time for various CTAB concentrations

Time (mins)	**Yield (%)**		
	CTAB concentration (%)		
	0.20	**0.50**	**1.00**
0	100	100	100
10	82	68	70
20	69	66	64
30	62	64	64
40	62	64	64
50	62	63	62
60	61	62	62
90	59	60	61
120	58	56	59
150	55	53	58
180	54	50	58
210	54	49	57
240	53	48	56

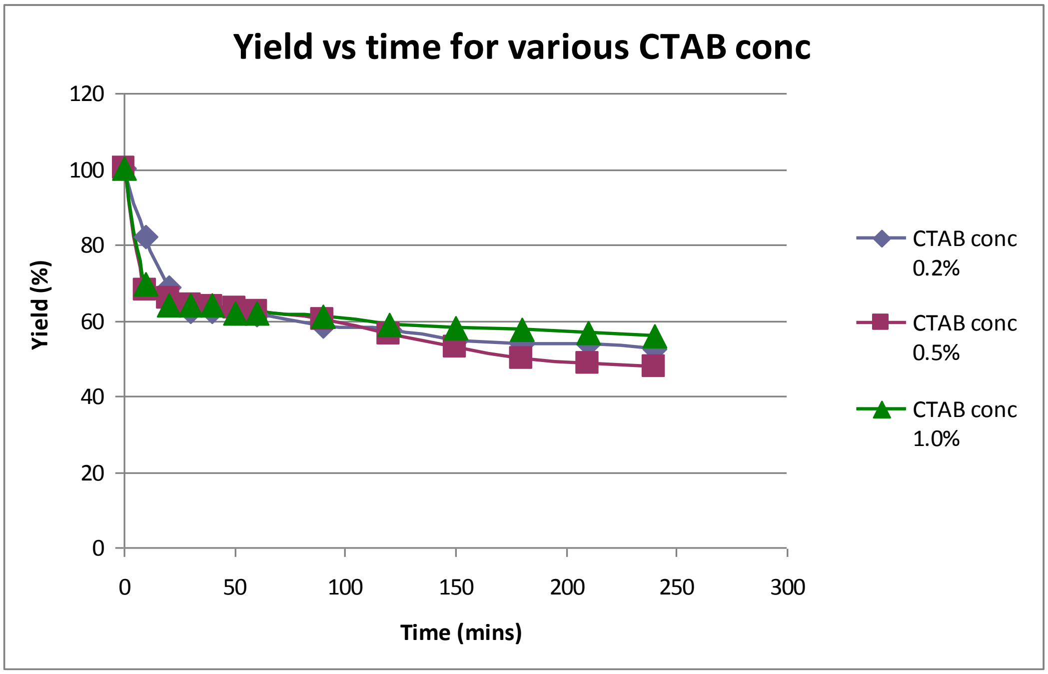

Figure 4-14 Yield results over time for various CTAB concentrations

Table 4-7 and Figure 4-14 show the yield results over time for the three tested concentrations of CTAB. Figure 4-14 shows similar yield results for all three concentrations and Table 4-7 gives more detailed data. Table 4-7 shows that the 0.5% concentration of CTAB had the fastest decrease in yield of all the concentrations. The 0.2% mixture had the slowest decrease in yield from 0-60 mins. From 60-240 mins the yield for both the 0.2% and 1.0% mixtures decreased slowly with the 1% mixture having a slightly slower decrease. At 240 mins the 1% mixture had the highest yield of 56%, followed by the 0.2% mixture at 53% with the 0.5% mixture having the least yield at 48%. Using the yield data, d_{50} diameter measurements and bubble size distributions for 0.2%, 0.5% and 1.0% CTAB mixtures the 0.2% concentration is chosen as the most stable.

4.2.2 Tergitol

This surfactant was first suggested for aphron generation by Sebba (1987) and is a secondary ethyloxylated alcohol. Tergitol was tested using the same base solution described above, 2 lb/bbl xanthan gum (Barazan D) mixed in deionized water. The Tergitol concentrations tested were 0.2%, 0.5% and 1.0% to allow accurate comparison with the data discussed for CTAB. Table 4-8 shows quite similar d_{50} measurements for 0.2% and 0.5%. The 1% concentration has the largest diameter throughout the 6 hour period as compared to the other concentrations. The 0.5% Tergitol concentration starts out as the smallest d_{50} diameter at 54 microns with the 0.2% concentration having a diameter of 62 microns. The 0.2% concentration then shows a smaller increase in diameter from 62 to 89 microns than the 0.5% concentration which grows from 54 to 101 microns. The opposite occurs at 30 mins with the 0.5% concentration having a smaller increase in diameter from 101 to 114 microns than the 0.2% mixture which grows from 89 to 130 microns. At 1 hour and 6 hours the d_{50} diameter is extremely similar for the 0.2% and 0.5% Tergitol concentrations.

Table 4-8 d_{50} measurements vs. time for various Tergitol concentrations

Tergitol conc	**0.20%**	**0.50%**	**1.00%**
Time (mins)	**d 50 (µm)**	**d 50 (µm)**	**d 50 (µm)**
0	62	54	72
10	89	101	103
30	130	114	134
60	150	151	179

360	313	312	332

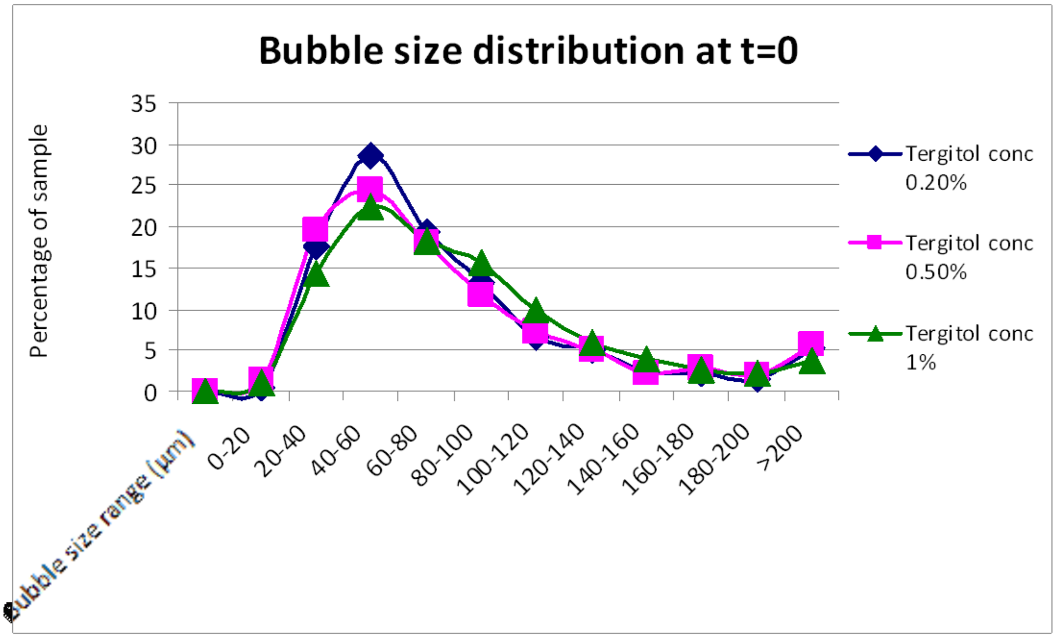

Figure 4-15 Bubble size distribution at 0 mins for various concentrations of Tergitol

At 0 mins the majority of aphrons are within the 0-120 microns in size for all concentrations of Tergitol. The 0.2% mixture has about 30% of its aphrons in the 40-60 micron category with the 0.5% mixture having about 24%. The 1% Tergitol concentration had slightly more aphrons that are between 80 and 180 micron in size than the other two concentrations.

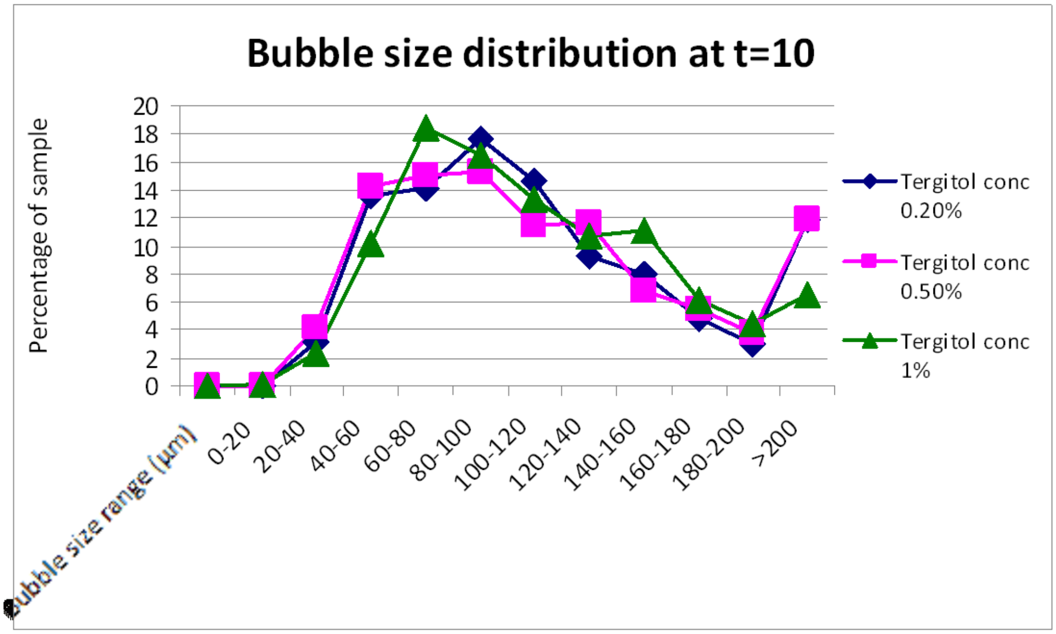

Figure 4-16 Bubble size distribution at 10 mins for various concentrations of Tergitol

At 10 mins the bubble size distribution for all concentrations is quite similar and is seen in Figure 4-16. The 1% Tergitol mixture has the most bubbles within the 60-80 micron category while both the 0.2% and 0.5% mixtures have the most aphrons in the 80-100 micron category. The 1% mixture also has the most bubbles in the 120-200 micron range as compared to the other two concentrations. However only 6% of the 1% Tergitol mixture were made up of bubbles greater than 200 microns as compared to 12% for both the 0.2% and 0.5% mixtures.

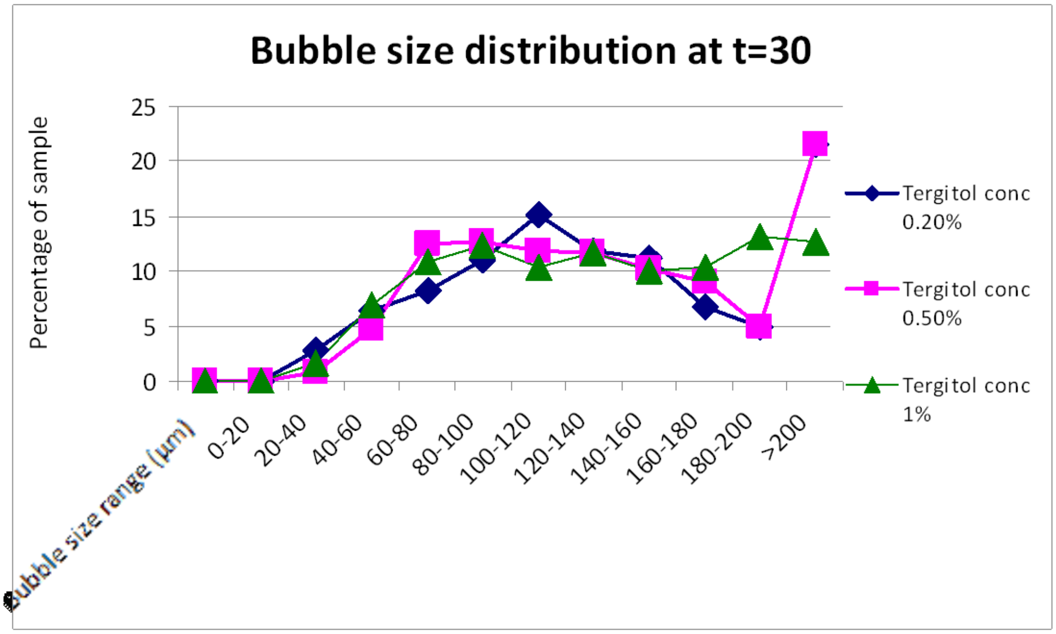

Figure 4-17 Bubble size distribution at 30 mins for various concentrations of Tergitol

At 30 mins for all concentrations the majority of the aphrons in the sample falls into the 40-180 micron range seen in Figure 4-17. The 1 % Tergitol concentration has the least number of aphrons which are greater than 200 microns in size. The 0.2% and 0.5% concentrations are both have about 22% of their samples comprised of aphrons greater than 200 microns.

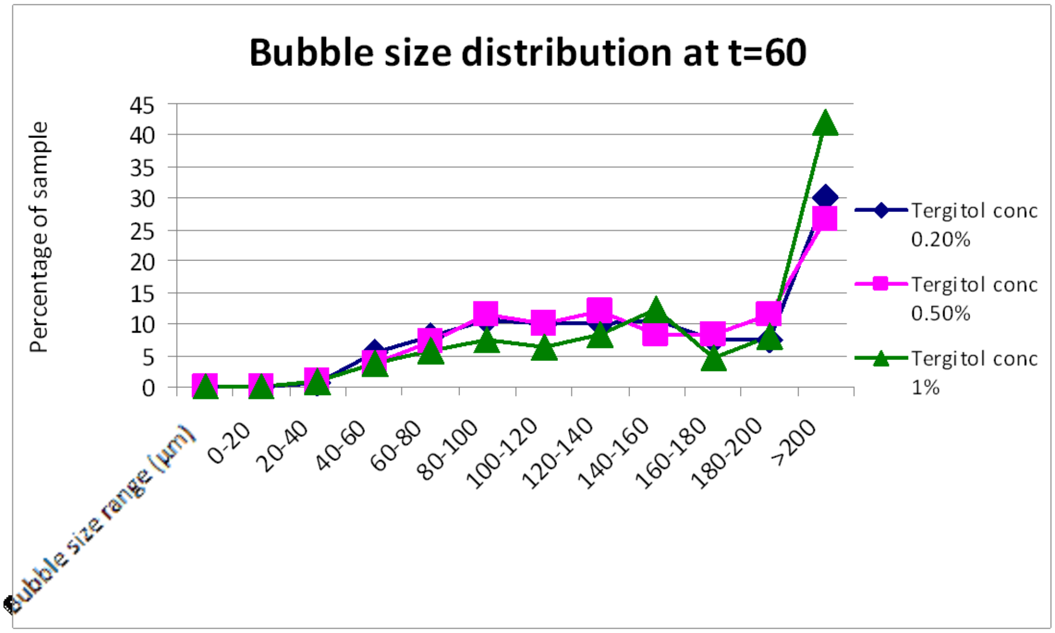

Figure 4-18 Bubble size distribution at 1 hour for various concentrations of Tergitol

In Figure 4-18 the Tergitol concentration of 1% has the least number of aphrons which are less than 140 microns in size. The 0.2% and 0.5% mixtures have similar numbers of bubbles in the 0-140 size range. The 1% mixture has 45% of its aphrons greater than 200 microns in size which is a sustantial change from 13% at 30 mins. The 0.2% and 0.5% has 25-30% of its aphrons larger than 200 microns.

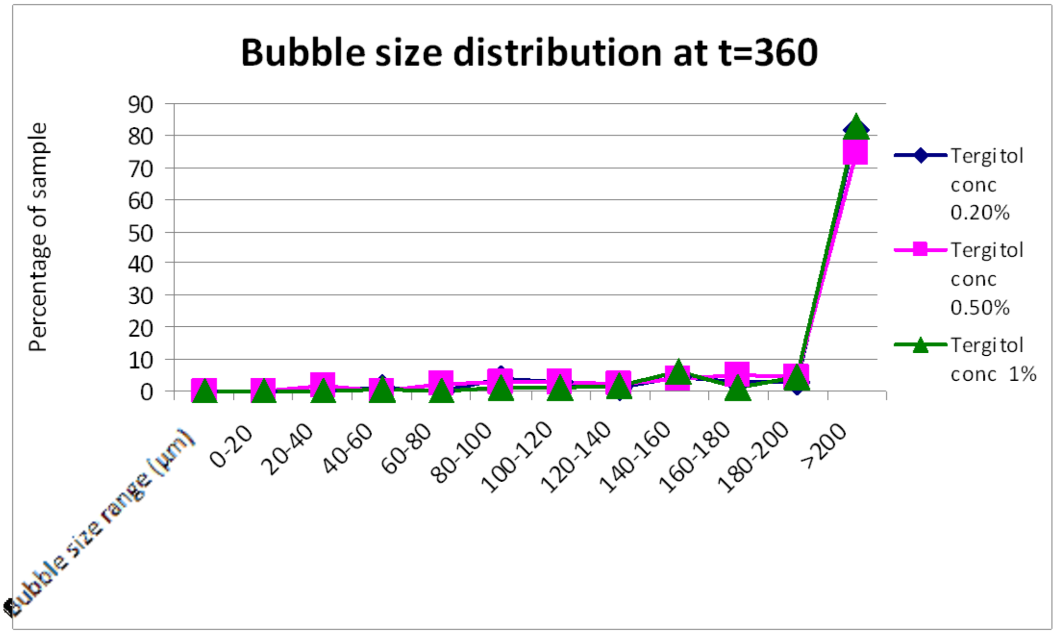

Figure 4-19 Bubble size distribution at 6 hours for various concentrations of Tergitol

At 6 hours the bubble size distribution of the 0.2% and 0.5% Tergitol mixtures are almost identical. The 1% concentration has the least number of aphrons less than 200 microns in size. As with the d_{50} measurement the bubble size distributions of the Tergitol concentrations of 0.2% and 0.5% are quite similar. To determine the optimum Tergitol concentration the yield for each concentration needs to be examined.

Yield experiments were also conducted using the similar concentrations as before with Tergitol and can be seen in Table 4-9 and Figure 4-16.

Table 4-9 Yield tests over time for various Tergitol concentrations

Time (mins)	Yield (%)		
	Tergitol concentration (%)		
	0.20	**0.50**	**1.00**
0	100	100	100
10	68	79	70
20	58	65	40
30	52	61	28
40	46	50	21
50	35	40	17
60	33	33	14
90	28	25	9
120	19	21	3
150	13	14	3
180	11	12	0
210	7	12	0
240	5	6	0

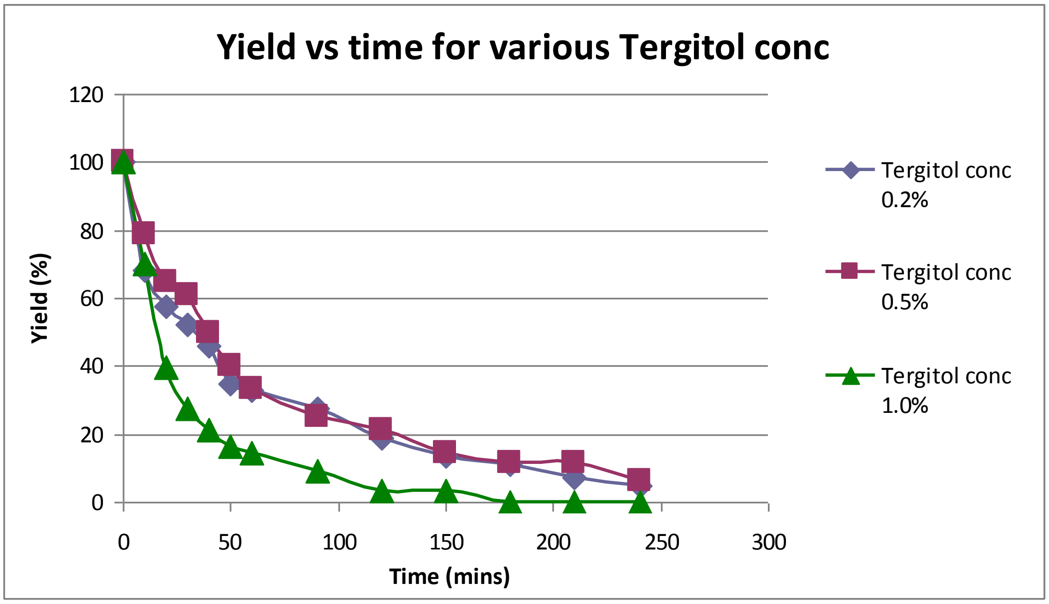

Figure 4-20 Yield tests over time for various Tergitol concentrations

Figure 4-20 shows that the 1% Tergitol mixture collapsed the quickest and had the lowest yield after 4 hours as compared to the 0.2% and 0.5% mixtures. Table 4-9 shows that the 0.5% mixture gave a slightly better yield for all time intervals except at 90 mins. This data supports the 0.5% Tergitol concentration as slightly more stable than the 0.2%. In comparing Figures 4-14 and 4-20 CTAB performed much better on yield experiments than Tergitol and may be a better surfactant choice than Tergitol.

4.2.3 DDBS (Sodium Dodecyl Benzene Sulfonate)

Bjorndalen and Kuru (2006) used the surfactant DDBS in their study of the stability of micro-bubble based solutions under downhole conditions. Figure 4-21 shows the measured bubble diameter for 0.035, 0.35 and 1 lb/bbl concentrations of DDBS over a three hour time period. The 1 lb/bbl concentration is easily identified as the most stable as it has the smallest bubble diameter throughout the experiment and is above the critical micelle concentration. Bjorndalen (2010) stated that at a surfactant concentration below the critical micelle concentration (CMC) the average CGA diameter is larger than at a surfactant concentration above the CMC. This CMC was found to be 0.35 lb/bbl for 2 lb/bbl and 3 lb/bbl xanthan gum solutions using surface tension measurements. At 0 mins the 1 lb/bbl DDBS concentration has an average diameter of about 50 microns while the other two concentrations have an average diameter greater than 100 microns. The 0.035 lb/bbl concentration is the least stable as at 3 hours the average bubble diameter is close to 400 microns and is much larger than the other two mixtures as it is below the CMC. As this data showed the concentration of 1 lb/bbl DDBS to be very stable this surfactant and concentration was further tested.

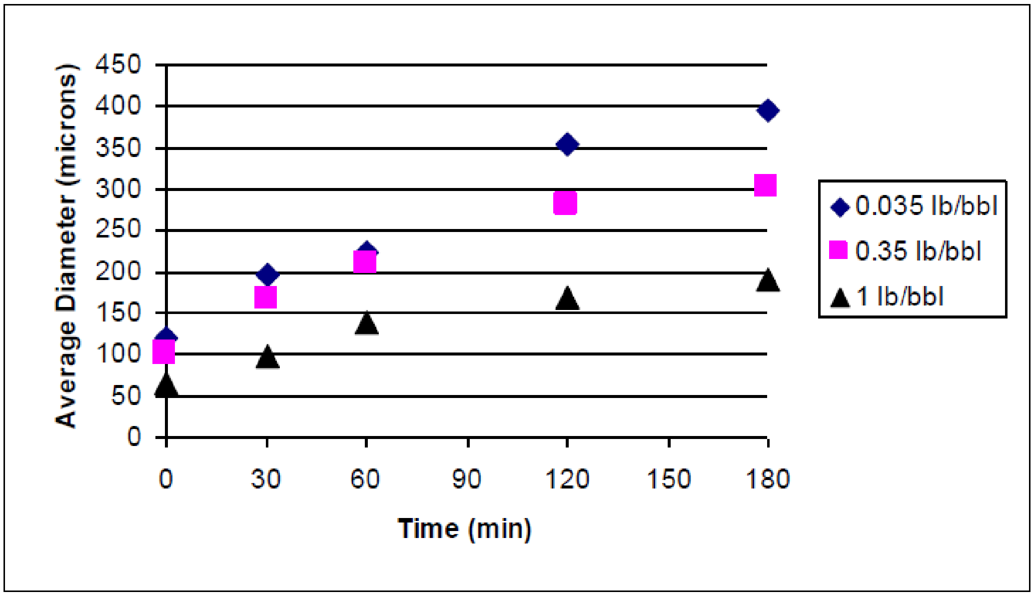

Figure 4-21 Effect of time and DDBS concentration on average bubble diameter with 2 lb/bbl xanthan gum (Bjorndalen and Kuru, 2006)

DDBS was then tested using concentrations of 0.2%, 0.5% and 1% as previously with CTAB and Tergitol. These tests were conducted using a 2 lb/bbl and 3 lb/bbl xanthan gum base solution with 1 lb/bbl DDBS. Both bubble size distributions and measured d_{50} diameters were examined at 0, 10, 60, and 360 mins as done with the previous two surfactants. This was done to determine the optimum polymer concentration for the CGA fluid formulation as both 2 lb/bbl and 3 lb/bbl xanthan gum concentrations were above the critical viscosity of 40 000 cP indicated by MacPhail et al. 2008 to ensure aphron stability.

Table 4-10 d_{50} measurements vs time for 2 lb/bbl and 3 lb/bbl xanthan gum

	1 lb/bbl DDBS	
Xanthan gum conc	**2 lb/bbl**	**3 lb/bbl**
Time (mins)	**d 50 (µm)**	**d 50 (µm)**
0	53	53
10	86	112
30	141	134
60	154	164
360	248	264

At 0 mins the d_{50} diameters for both xanthan gum concentrations is identical at 53 microns as shown in Table 4-10. At 10 mins there is a smaller increase in diameter from 53 to 86 microns for the 2 lb/bbl concentration as compared to the 3 lb/bbl concentration. At 30 mins the bubble diameter for the lesser xanthan gum concentration is slightly larger than that of the 3 lb/bbl concentration. However at

60 and 360 mins the d_{50} diameter for the 2 lb/bbl is smaller than that of the 3 lb/bbl concentration. These measurements indicate that the 2 lb/bbl concentration of xanthan gum performs better in aphron stabilization than the 3 lb/bbl concentration.

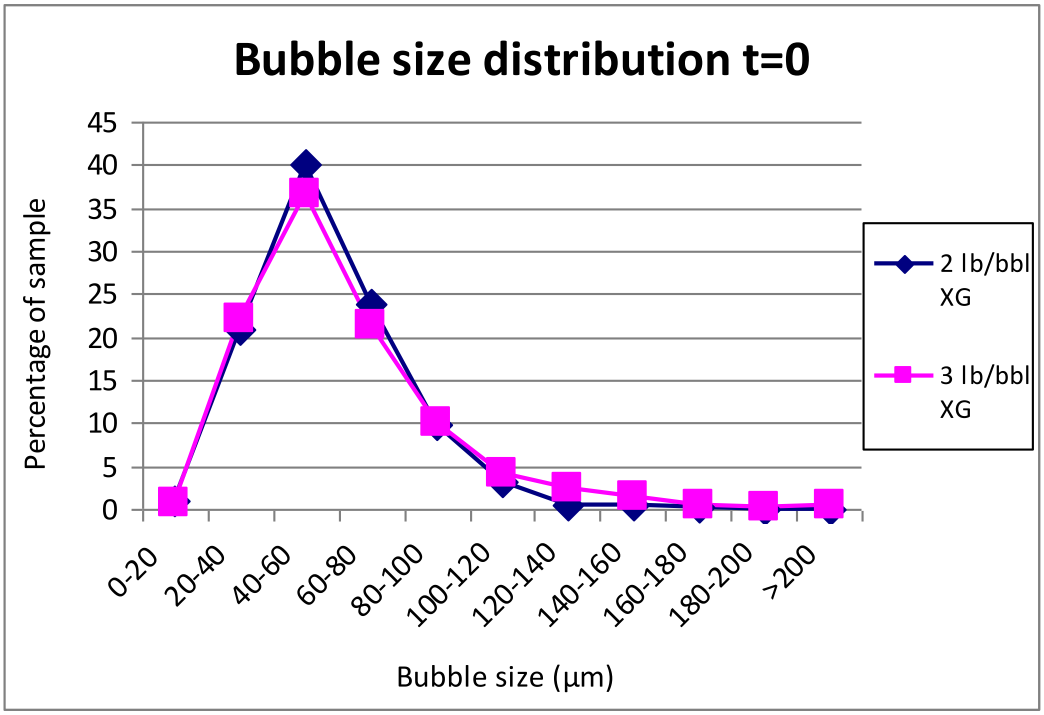

Figure 4-22 Bubble size distribution at 0 mins for different XG concentrations

Figure 4-22 shows very similar bubble size distributions for both concentrations of xanthan gum. The 2 lb/bbl concentration has slightly more aphrons in the 40-80 micron categories than the 3 lb/bbl. In the 100-180 micron size range the 3 lb/bbl had more aphrons of this size than the 2 lb/bbl concentration.

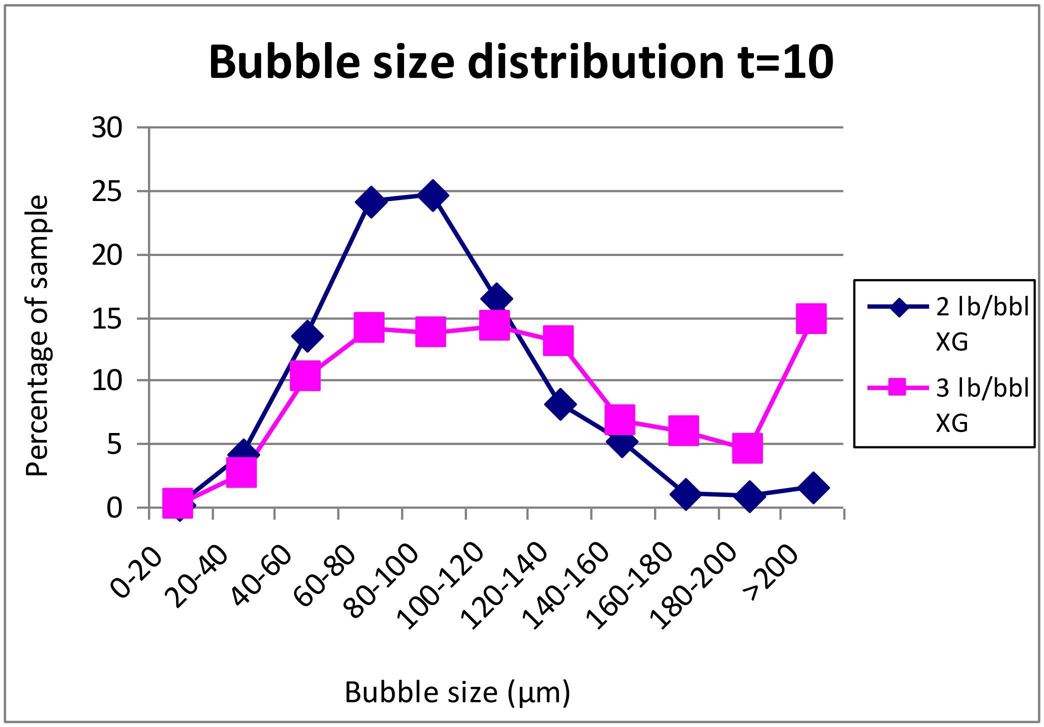

Figure 4-23 Bubble size distribution at 10 mins for different XG concentrations

At 10 mins there is a big difference in the bubble size distribution for both concentrations of xanthan gum as seen in Figure 4-23. The 2 lb/bbl concentration has a much larger number of aphrons which are less than 120 microns in size while the 3 lb/bbl mixture has more aphrons larger than120 microns. Therefore the 2 lb/bbl concentration is made up of more aphrons less than 120 microns in size than the 3 lb/bbl concentration.

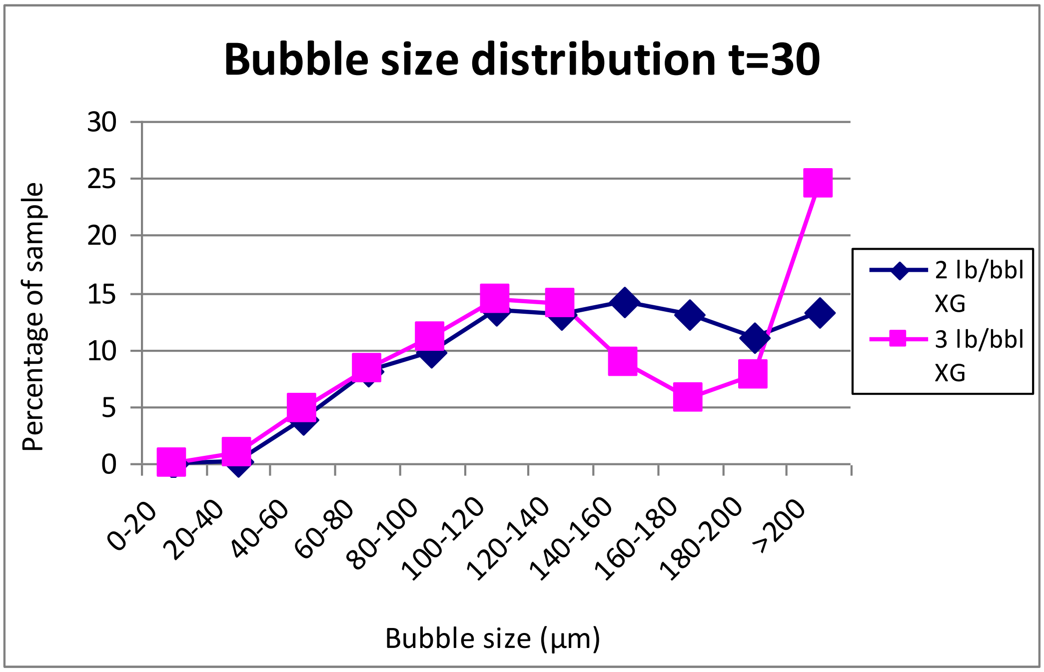

Figure 4-24 Bubble size distribution at 30 mins for different XG concentrations

In Figure 4-24 the bubble size distribution for both concentrations are similar up to 140 microns in size. After this the 2 lb/bbl concentration shows a generally even bubble size distribution from 140 to greater than 200 microns. However the 3 lb/bbl concentration shows a marked increase in the number of aphrons greater than 200 microns in size (almost 25% of the sample).

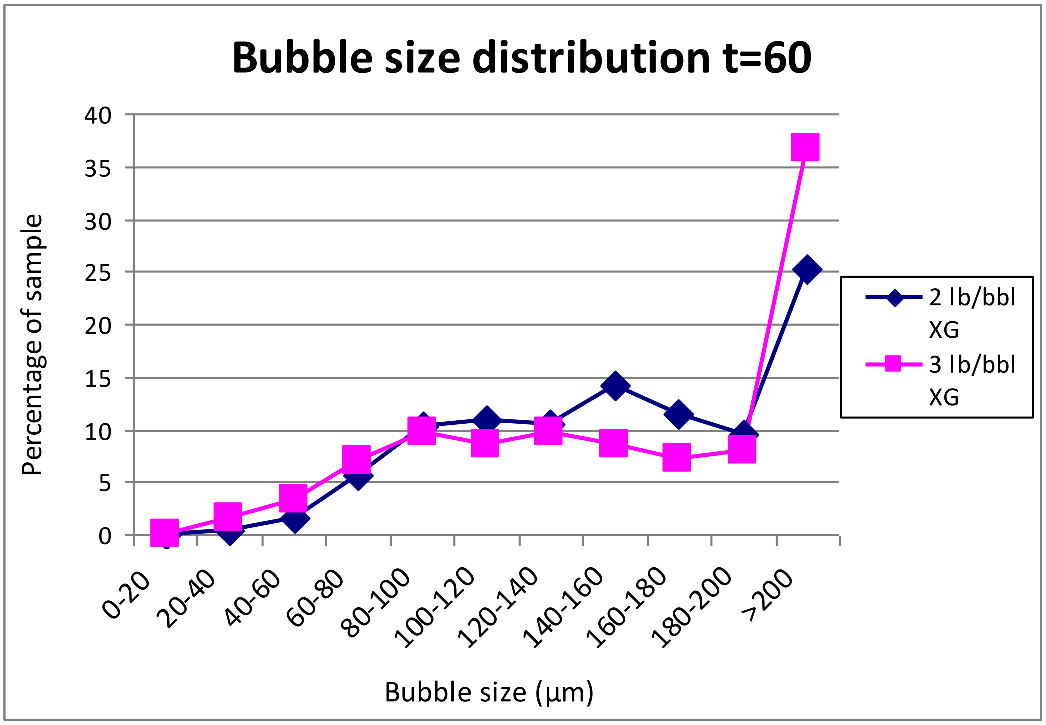

Figure 4-25 Bubble size distribution at 1 hour for different XG concentrations

After 1 hour the sample percentage of aphrons greater than 200 microns for 3 lb/bbl is more than 35% as compared to 25% for the 2 lb/bbl concentration. Both concentrations have similar bubble size distribution from 0 to 100 microns but this then changes in the 100 to 200 micron categories. The 2 lb/bbl concentration has more bubbles of this size than the 3 lb/bbl concentration.

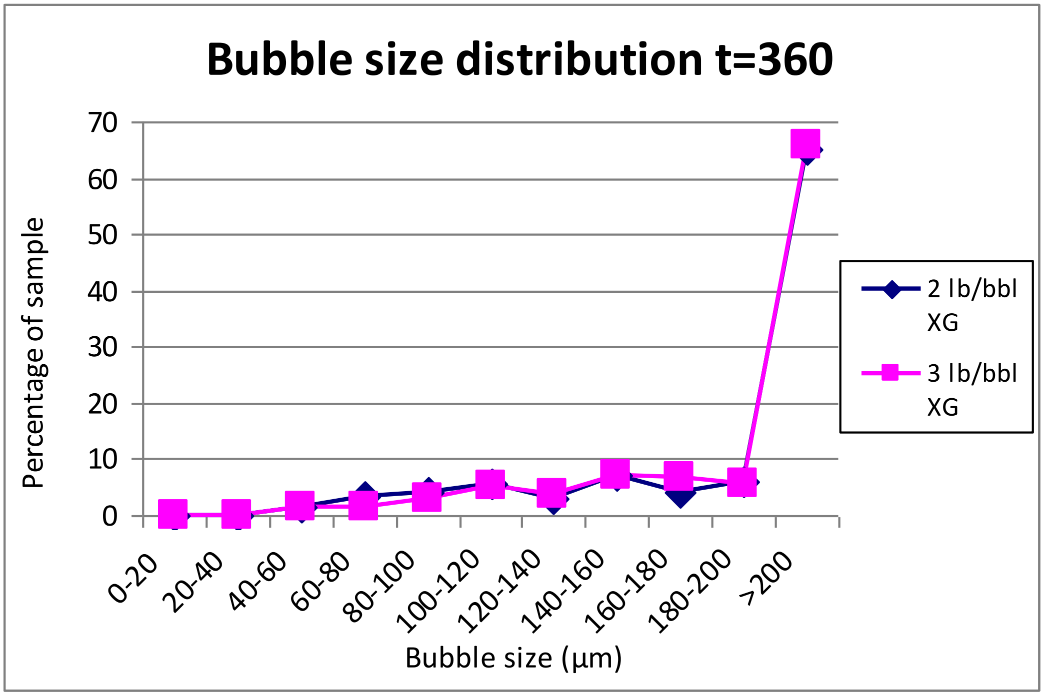

Figure 4-26 Bubble size distribution at 6 hrs for different XG concentrations

After 6 hours the bubble size distribution of both concentrations look very alike as seen in Figure 2-26. However the 2 lb/bbl concentration has slightly more aphrons which are 60 to 100 microns in size. Using the d_{50} measurements in Table 4-10 and the bubble size distributions in Figures 4-22 to 4-26 the 2 lb/bbl xanthan gum (Barazan D) concentration proved to be slightly better at stabilizing aphrons than the 3 lb/bbl concentration.

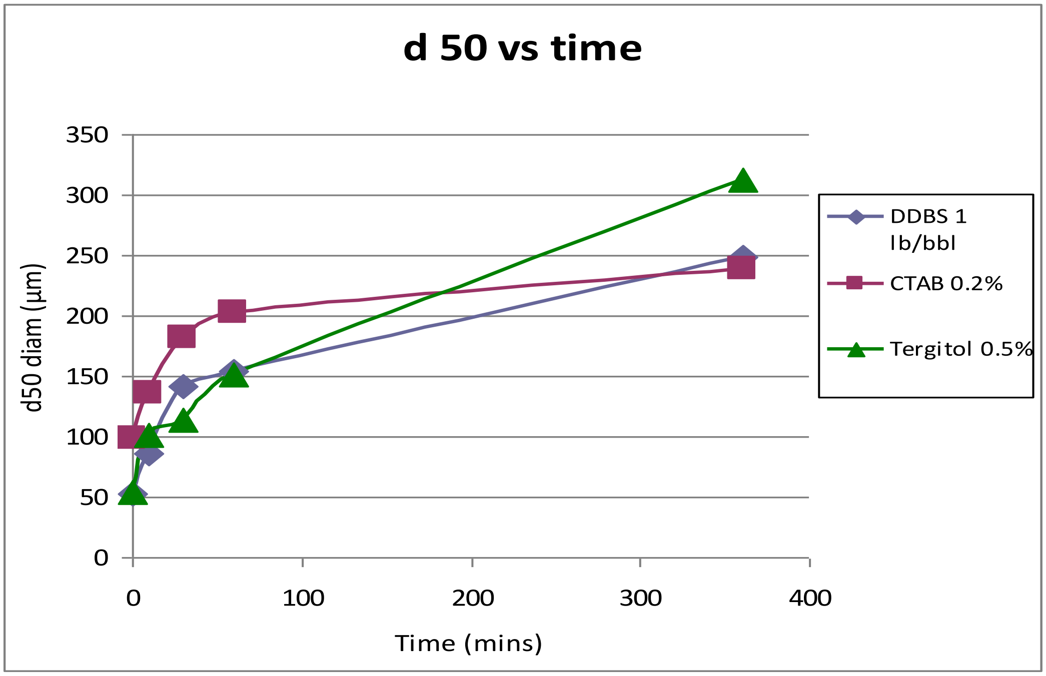

Figure 4-27 d_{50} results over time for different concentrations of surfactants

Figure 4-27 compares the most stable concentrations for each of the three surfactants. Tergitol and DDBS both have diameters of approximately 50 microns at 0 mins which slowly changes up to 60 mins. At 360 mins Tergitol has the largest diameter as compared to the other two surfactants. CTAB has a fairly large diameter of about 100 microns at 0 mins. This grows to about 200 microns at 60 mins and at 360 mins the diameters for CTAB and DDBS are very similar. This data suggests that DDBS is the best surfactant choice. To verify this, Figures 4-28 to 4-32 will compare the bubble size distributions for these surfactants.

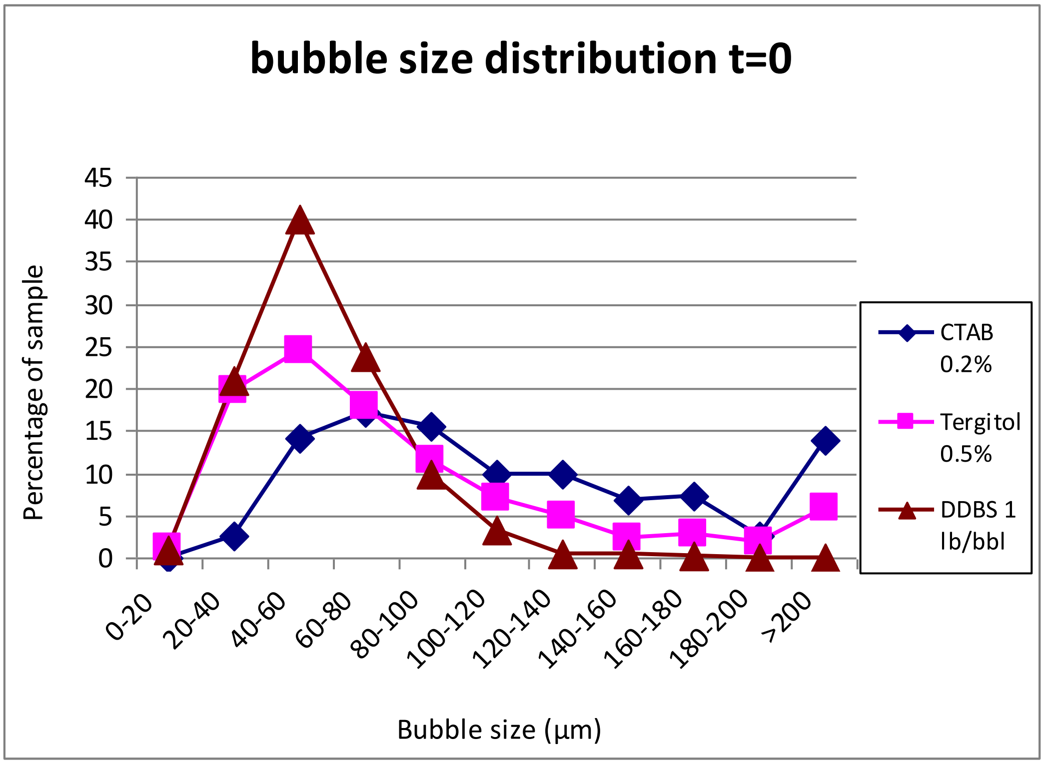

Figure 4-28 bubble size distribution at 0 mins for CTAB, Tergitol and DDBS

At 0 mins DDBS had the most aphrons between 20 to 80 microns in size as compared to the other surfactants which is seen in Figure 4-28. DDBS also had little of no aphrons greater than 120 microns while CTAB and Tergitol had significant amounts in this size category. CTAB also created the most aphrons greater than 200 microns in size which was then followed by Tergitol while DDBS had no aphrons greater than 200 microns.

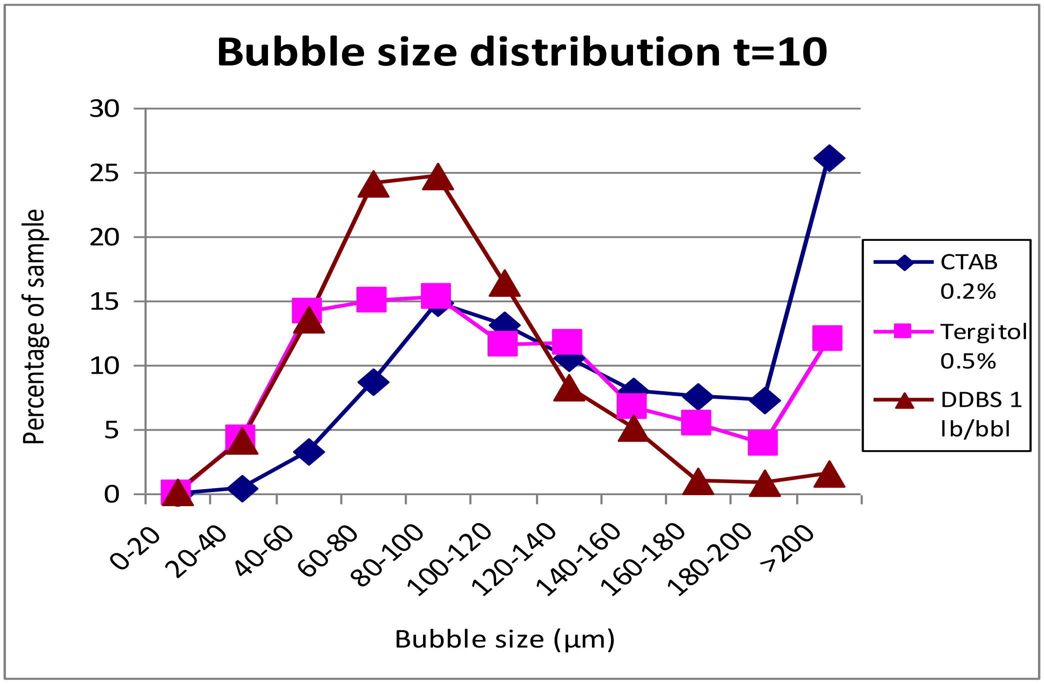

Figure 4-29 Bubble size distribution at 10 mins for CTAB, Tergitol and DDBS

Figure 4-29 shows the bubble size distribution for each of the three surfactants at 10 mins. The majority of the DDBS sample was made up of aphrons between 40 and 120 microns with almost 50% falling into the 60-100 micron category. CTAB had the least aphrons that were less than 120 microns in size while more than 25% of its sample was made up of aphrons larger than 200 microns. Tergitol had more aphrons that CTAB that were less than 120 microns in size but much less when compared to DDBS. DDBS also had the least number of aphrons larger than 120 microns when compared to the other surfactants.

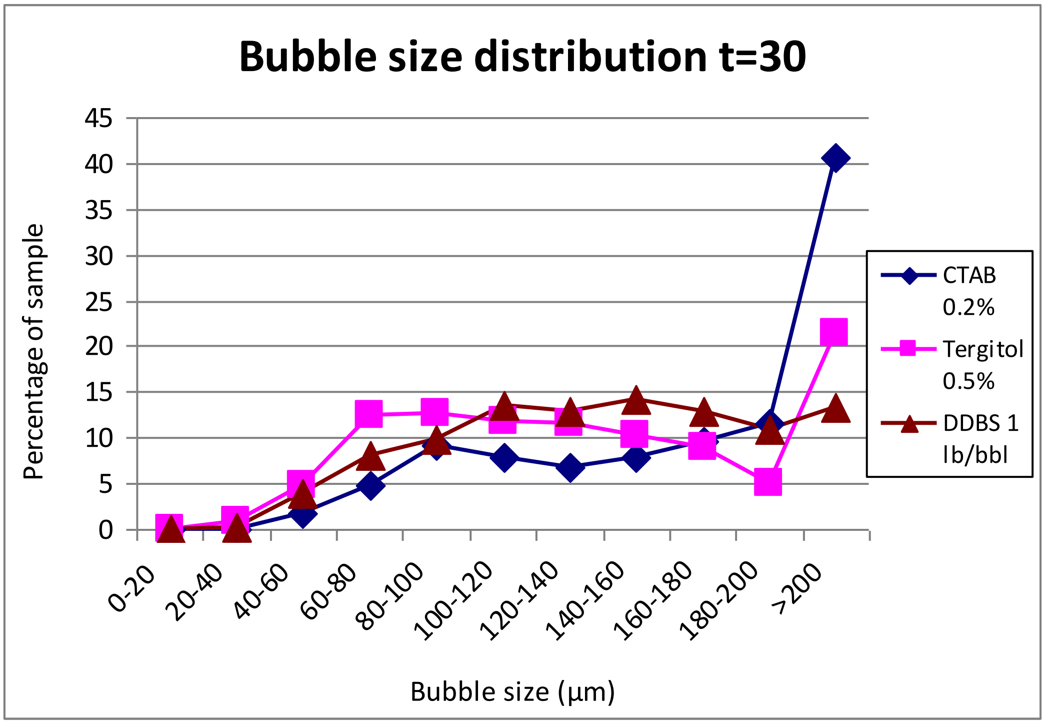

Figure 4-30 Bubble size distribution at 30 mins for CTAB, Tergitol and DDBS

At 30 mins Tergitol and DDBS have similar bubble size distributions as shown in Figure 4-30. CTAB had the lowest number of aphrons less than 160 microns in size as compared to the Tergitol and DDBS. CTAB also had about 42% of its sample comprised of aphrons greater than 200 microns as compared to 23% with Tergitol. DDBS had the least number of aphrons in greater than 200 microns.

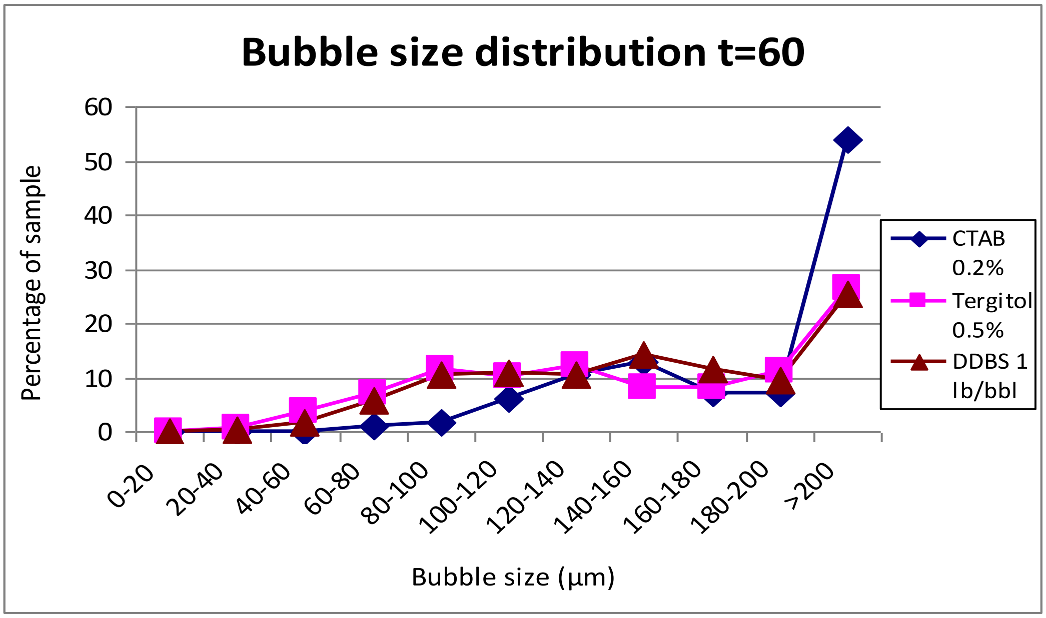

Figure 4-31 Bubble size distribution at 1 hour for CTAB, Tergitol and DDBS

At 1 hour the bubble size distributions of CTAB and Tergitol are quite similar, seen in Figure 4-31. As in Figure 4-28 to 4-31 CTAB had the most aphrons greater than 200 microns as compared to the other surfactants. Tergitol had slightly more aphrons in this category when compared to DDBS.

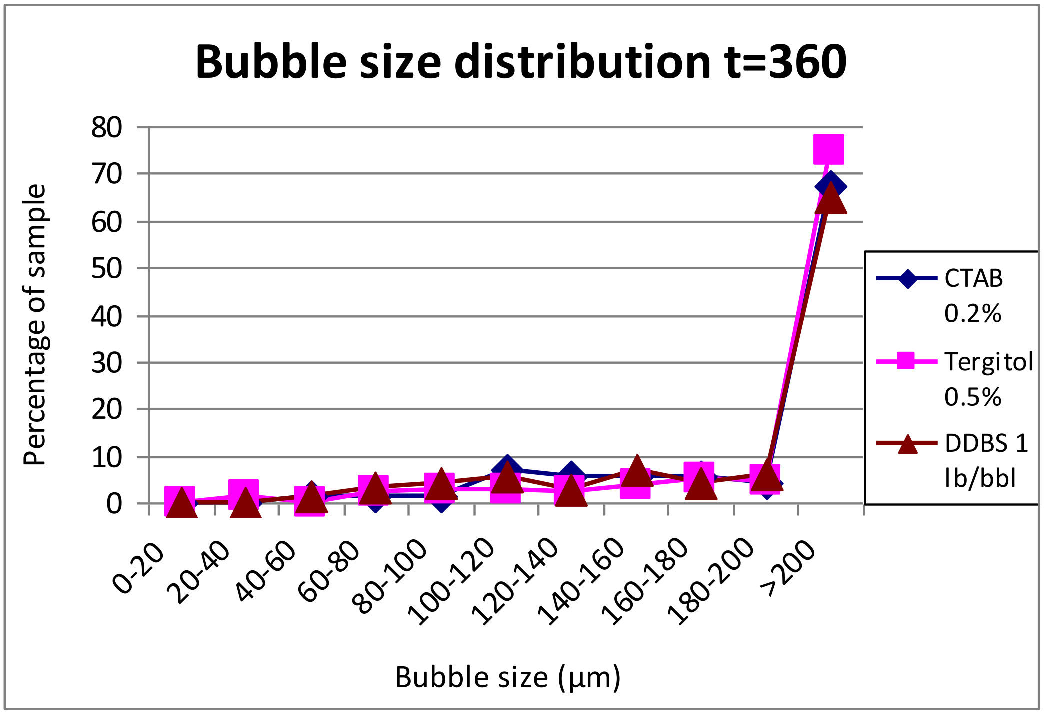

Figure 4-32 Bubble size distribution at 6 hrs for CTAB, Tergitol and DDBS

After 6 hours all surfactants showed similar bubble size distributions seen in Figure 4-32. However, Tergitol had the most aphrons which were larger than 200 microns followed by CTAB. DDBS had the least number of aphrons greater than 200 microns in size. Using Figures 4-27 to 4-32 1 lb/bbl DDBS is the best surfactant choice and is the most stable when compared to CTAB and Tergitol. Another important observation was after 6 hours CTAB precipitated out of the mixture which led to further aphron instability.

4.3 Formulation of Optimum Aqueous CGA fluid

The chosen formulation for the generation of the colloidal gas aphron fluid was a base fluid of de-ionized water and 2 lb/bbl xanthan gum (Barazan D) polymer with 1 lb/bbl DDBS as the surfactant. Figures 4-33 and 4-34 show the rheological characterization of the CGA fluid. The LSRV of the CGA fluid at 0.1 sec^{-1} was determined to be 42,000 cP (42 Pa.s) which was above the critical LSRV of 40,000 indicated by MacPhail et al. 2008 to prevent aphron breakup.

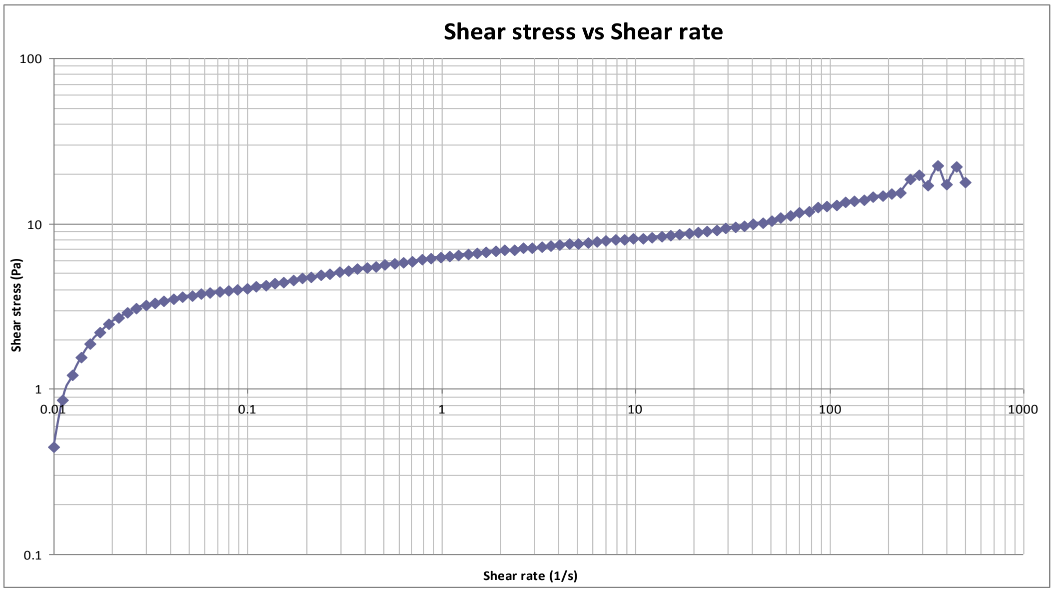

Figure 4-33 Shear stress vs. shear rate for CGA fluid

Figure 4-33 shows the effect of increasing shear rate on shear stress for the CGA fluid. The CGA fluid behaves in a pseudo plastic manner with shear thinning behaviour. Figure 4-34 shows the effect of shear rate on viscosity for the CGA fluid and the shear thinning behaviour of the CGA fluid is apparent with high viscosities at low shear rates and low viscosities at high shear rates.

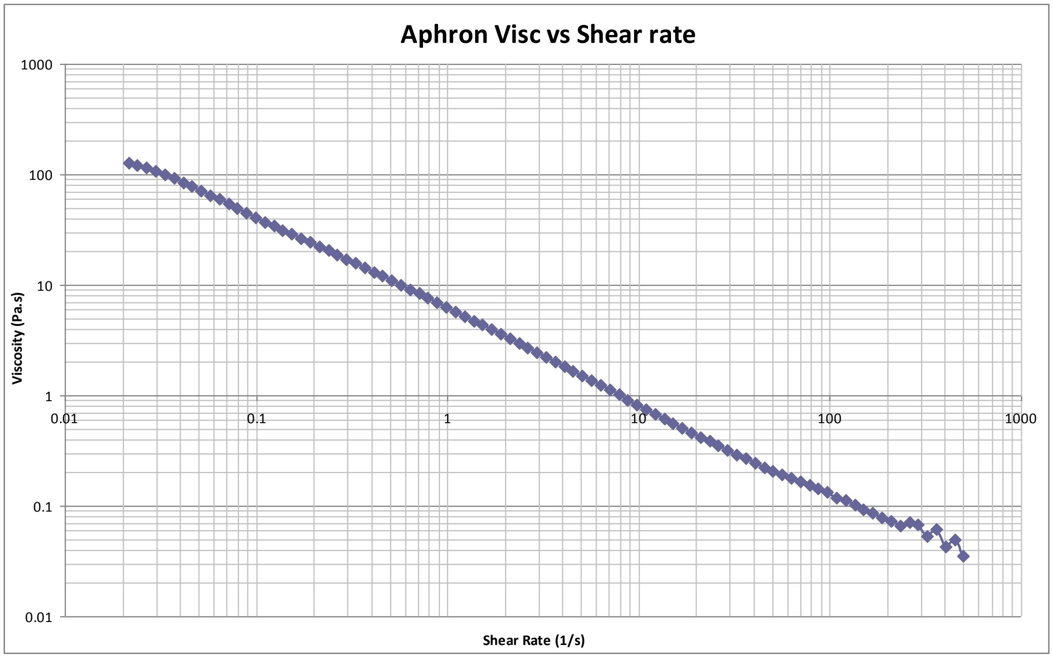

Figure 4-34 Viscosity vs. Shear rate for CGA fluid

5. VISUAL CELL

In the previous chapter the colloidal gas aphron formulation was chosen. This was determined as the most stable and was comprised of a base solution of de-ionized water and 2 lb/bbl xanthan gum (Barazan D) polymer with 1 lb/bbl DDBS (Sodium Dodecyl Benzene Sulfonate) surfactant. Colloidal gas aphrons were then generated using this formulation using the procedure described in 3.4.1.

The performance of this CGA fluid as a recovery fluid was tested in visual cell experiments. This apparatus was tightly packed with glass beads and saturated with a known amount of dyed mineral oil. The CGA fluid was then injected at a rate of 0.3 ml/min and total oil recovery, breakthrough and fluid retention time was recorded. This procedure is fully detailed in Chapter 3. This rate was decided upon after much experimentation. Initially the visual cell was packed with glass beads which had a permeability of 1.3 D. The first injection rate used was 1.0 ml/min which did not work as the apparatus leaked profusely before the experiment was completed due to high pressure. Lower rates were then tested from 0.9 to 0.4 ml/min to determine if a lower injection rate would solve the leakage problem by reducing the pressure drop across the porous media. This did not work so another approach was used. The porous media was formed by using the larger 50-80 mesh size glass beads and several injection rates were again tested. The rate that worked was 0.3 ml/min which did not generate pressure losses greater than the limit of the visual cell. The porosity of the visual cell varied from 37 to 39% due to the packing of the glass beads.

The pressure drop due to the flow of the CGA fluid across the visual cell was recorded. The behaviour of the CGA fluid was also monitored through the use of time lapse photos showing frontal displacement patterns.

In addition to the micro-bubble based fluid other type of fluids were investigated to compare their performance as a recovery fluid. The recovery experiments were conducted by using: a) micro-bubble based fluid, b) aqueous polymer solutions, c) aqueous surfactant-polymer solutions mixed at low shear rates d) water, e) water followed by micro-bubble based fluid and f) water followed by aqueous polymer solutions. Each experiment was conducted twice to check the repeatability of results. The results of the recovery experiments are presented in the following sections.

5.1 CGA Fluid

These experiments were conducted by using the CGA fluid prepared by mixing of de-ionized water, 2 lb/bbl xanthan gum (Barazan D) polymer, and 1 lb/bbl DDBS (Sodium Dodecyl Benzene Sulfonate) surfactant. The injection rate of the CGA fluid was 0.3 ml/min throughout the experiment. The pore volume of the glass beads packed in the visual cell was measured as 87 ml for both experiments. The results from each experiment are seen in Table 5-1 and 5-2. The injection pressure profile observed for these experiments are showed in Figure 5-1.

Table 5-1 Oil recovery using CGA fluid - experiment run 1

Time	Vol. of Fluid Injected	Vol. of Oil Produced	Cumulative Oil Produced	Vol. of CGA Fluid Produced
0	0	0	0	0
10	3	0	0	0
20	6	1	1	0
30	9	1	2	0
40	12	1	3	0
50	15	1	4	0
60	18	1	5	0
70	21	2	7	0
80	24	1	8	0
90	27	2	10	0
100	30	1	11	0
110	33	1	12	0
120	36	2	14	0
130	39	1	15	0
140	42	2	17	0
150	45	2	19	0
160	48	2	21	0
170	51	2	23	0
180	54	2	25	0
190	57	2	27	0
200	60	2	29	0
210	63	2	31	0
220	66	3	34	0
230	69	2	36	0
240	72	2	38	0
250	75	2	40	0
260	78	2	42	0
270	81	2	44	0
280	84	2	46	0
290	87	3	49	0
300	90	3	52	0
310	93	2	54	0
320	96	3	57	0
330	99	2	59	0
340	102	2	61	0
350	105	3	64	0
360	108	2	66	0
370	111	2	68	0
380	114	3	71	0
390	117	2	73	0
400	120	3	76	0
410	123	1	77	2
420	126	0	77	3

Breakthrough Time = 406 mins	**Pore Volume = 87 ml**
Injected Fluid Retention Time = 420 mins	**Total Oil Recovery = 89%**

Table 5-2 Oil recovery using CGA fluid - experiment run

Time	Vol. of Fluid Injected	Vol. of Oil Produced	Cumulative Oil Produced	Vol. of CGA Fluid Produced
0	0	0	0	0
10	3	0	0	0
20	6	2	2	0
30	9	1	3	0
40	12	1	4	0
50	15	1	5	0
60	18	1	6	0
70	21	2	8	0
80	24	2	10	0
90	27	1	11	0
100	30	1	12	0
110	33	2	14	0
120	36	1	15	0
130	39	2	17	0
140	42	1	18	0
150	45	2	20	0
160	48	2	22	0
170	51	2	24	0
180	54	2	26	0
190	57	2	28	0
200	60	2	30	0
210	63	2	32	0
220	66	2	34	0
230	69	2	36	0
240	72	2	38	0
250	75	2	40	0
260	78	2	42	0
270	81	3	45	0
280	84	2	47	0
290	87	2	49	0
300	90	3	52	0
310	93	2	54	0
320	96	2	56	0
330	99	3	59	0
340	102	2	61	0
350	105	3	64	0
360	108	2	66	0
370	111	2	68	0
380	114	3	71	0

390	117	2	73	0
400	120	2	75	0
410	123	2	77	2
420	126	1	78	3
Breakthrough Time = 402 mins			**Pore Volume = 87 ml**	
Injected Fluid Retention Time = 420 mins			**Total Oil Recovery = 90%**	

Table 5-1 and 5-2 show quite similar breakthrough times of 402 and 406 mins, with total oil recovery of 89% and 90% respectively.

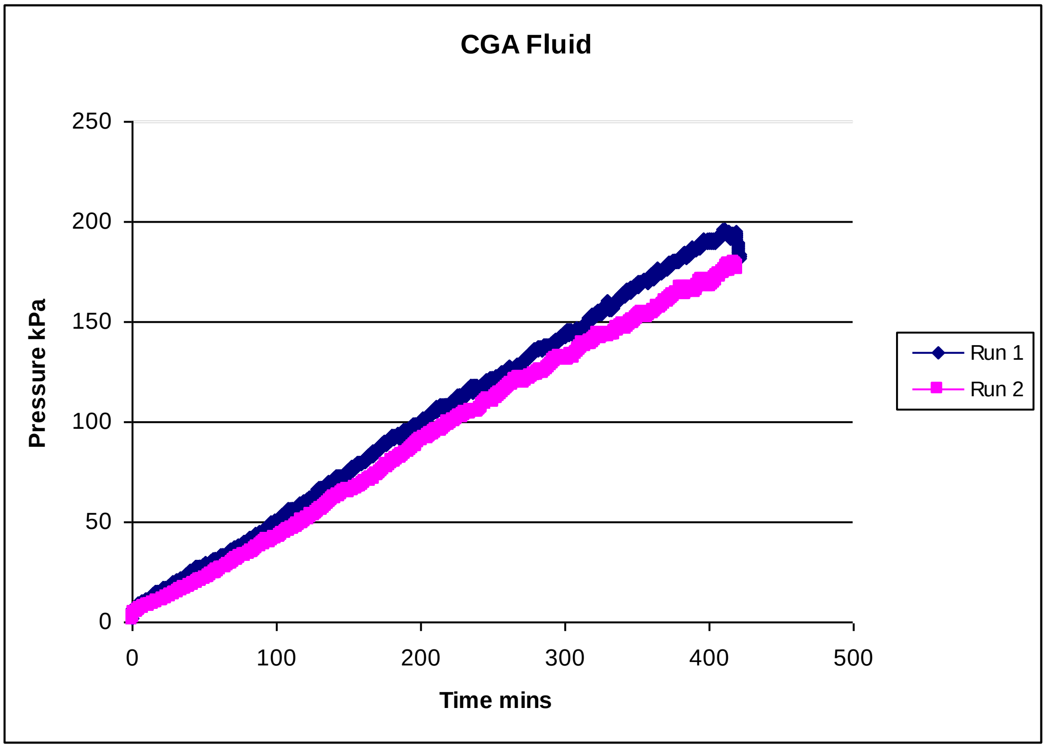

Figure 5-1 Visual cell pressure data for CGA fluid experiment run 1 & 2

Figure 5-1 shows a smooth linear increase in pressure for the CGA fluid. This is due to the blocking or bridging ability of the colloidal gas aphrons. At the beginning of the experiment the pore spaces between the glass beads are filled with the dyed mineral oil. As the CGA fluid is injected aphrons enter these filled pore spaces and displace the oil. A slow buildup of aphrons occurs as more aphrons move into the pore spaces which results in a corresponding increase in pressure. This pressure increase continues as aphrons continually fill pore spaces. The maximum pressure drop was 200 kPa.

0 mins 30 mins 60 mins

90 mins 120 mins 150 mins

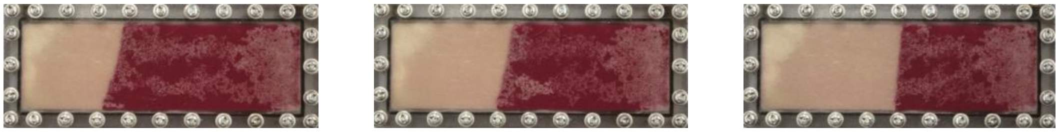

180 mins 210 mins 240 mins

270 mins 300 mins 330 mins

360 mins 390 mins 420 mins

Figure 5-2 Time lapse photos of CGA fluid flood

Figure 5-2 shows the movement of the fluid front as the CGA fluid is injected. From 0 to 90 mins the CGA fluid front moves slowly as it attempts to become linear. This is reflected by the cumulative recovery results in Tables 5-1 and 5-2 in for same time period which are the lowest when compared to the rest of the experiment. From 90 to 210 mins the fluid front continues to straighten and the recovery data in Tables 5-1 and 5-2 reflects this. The oil recovery improves even more from 210 mins onward as the fluid front straightens up even more until it is almost perpendicular to the length of the visual cell at 270 mins. The fluid front continues to progress in a linear manner until breakthrough occurs.

5.2 Aqueous Polymer Solution

The polymer solution used in these flooding experiments comprised of de-ionized water and 2 lb/bbl xanthan gum (Barazan D). This was also the base fluid used in the generation of the CGA fluid and was prepared using the same procedure. Table 5-3 and 5-4 and Figure 5-2 show the results from the polymer flood.

Table 5-3 Oil recovery using polymer - experiment run 1

Time	Vol. of Fluid Injected	Vol. of Oil Produced	Cumulative Oil Produced	Vol. of Polymer Produced
0	0	0	0	0
10	3	0	0	0
20	6	1	1	0
30	9	1	2	0
40	12	2	4	0
50	15	1	5	0
60	18	2	7	0
70	21	2	9	0
80	24	2	11	0
90	27	2	13	0
100	30	2	15	0

110	33	3	18	0
120	36	2	20	0
130	39	3	23	0
140	42	3	26	0
150	45	2	28	0
160	48	3	31	0
170	51	3	34	0
180	54	2	36	0
190	57	2	38	0
200	60	3	41	0
210	63	2	43	0
220	66	3	46	0
230	69	3	49	0
240	72	3	52	0
250	75	2	54	0
260	78	3	57	0
270	81	3	60	0
280	84	3	63	0
290	87	3	66	0
300	90	3	69	0
310	93	2	71	0
320	96	2	73	0
330	99	2	75	1
340	102	2	77	2
350	105	0	77	2
360	108	0	77	4
Breakthrough Time = 327 mins			**Pore Volume = 82 ml**	
Injected Fluid Retention Time = 360 mins			**Total Oil Recovery = 94%**	

Table 5-4 Oil recovery using polymer - experiment run 2

Time	**Vol. of Fluid Injected**	**Vol. of Oil Produced**	**Cumulative Oil Produced**	**Vol. of Polymer Produced**
0	0	0	0	0
10	3	1	1	0
20	6	2	3	0
30	9	2	5	0
40	12	3	8	0
50	15	2	10	0
60	18	2	12	0
70	21	3	15	0
80	24	2	17	0
90	27	2	19	0
100	30	2	21	0
110	33	3	24	0
120	36	3	27	0

130	39	3	30	0
140	42	3	33	0
150	45	3	36	0
160	48	3	39	0
170	51	3	42	0
180	54	3	45	0
190	57	3	48	0
200	60	3	51	0
210	63	3	54	0
220	66	3	57	0
230	69	3	60	0
240	72	2	62	0
250	75	3	65	0
260	78	3	68	0
270	81	3	71	0
280	84	3	74	0
290	87	3	77	1
300	90	0	77	3
310	93	0	77	4
Breakthrough Time = 284 mins			**Pore Volume = 82 ml**	
Injected Fluid Retention Time = 310 mins			**Total Oil Recovery = 94%**	

Table 5-3 and 5-4 show different breakthrough times with Table 5-3 at 327 mins and Table 5-4 at 284 mins. This difference in breakthrough times occurred due to the formation and behaviour of the polymer fluid front. Experiment run 2 had the shorter breakthrough time as the fluid formed a linear front much faster and so progressed quicker than Experiment run 2. This is supported by the recovery data in Table 5-3 and 5-4 with Table 5-4 showing that more oil was produced earlier in the experiment than Table 5-3. However, the total oil recovered was the same at 94% with the pore volumes also the same at 82 ml.

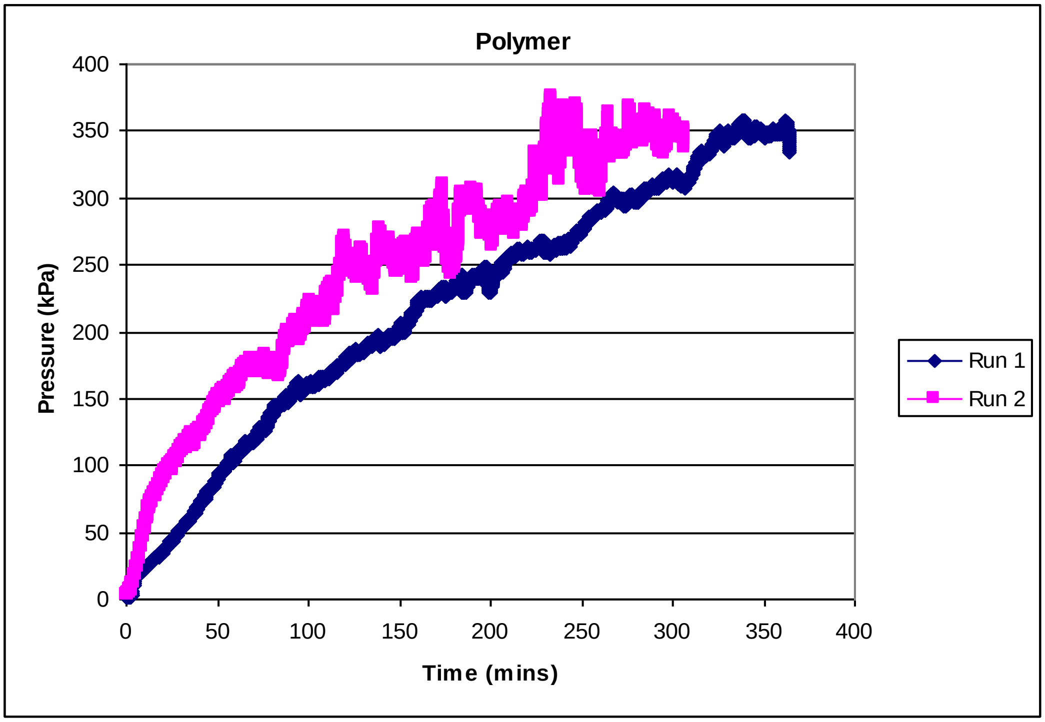

Figure 5-3 Visual cell pressure data for polymer run 1 & 2

Figure 5-3 shows the pressure data recorded for experiment runs 1 and 2 using the aqueous polymer solutions. There is fairly steep increase in the pressure as the polymer solution enters the pore spaces and adsorption occurs. Towards the end of each experiment the pressure data is seen to slightly level off which coincides with breakthrough. After breakthrough some of the mineral oil is still being produced. The maximum pressure drop seen was 360 kPa.

0 mins

30 mins

60 mins

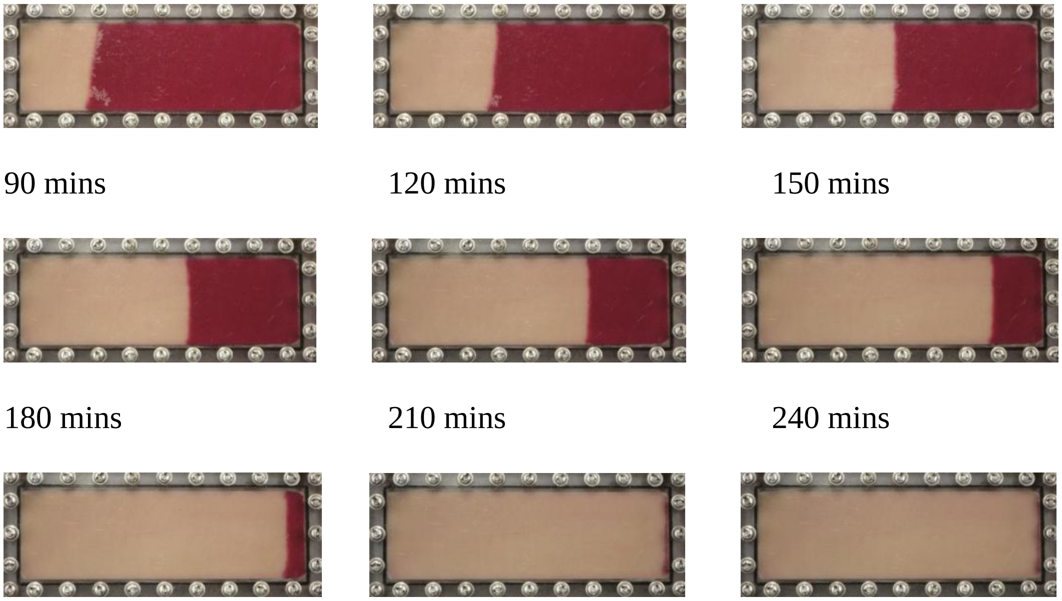

90 mins 120 mins 150 mins

180 mins 210 mins 240 mins

270 mins 300 mins 310 mins

Figure 5-4 Time lapse photos of polymer flood

Figure 5-4 shows the movement of the aqueous polymer solution across the visual cell. The fluid front moves quite quickly and at 30 mins it is almost linear. After 60 mins the linear fluid front continues to move rapidly across the visual cell. This is supported by the recovery data in table 5-4. At 310 mins the experiment is stopped as the polymer solution is the only produced fluid.

5.3 Aqueous Polymer and Surfactant Solution (mixed at low shear rates)

This fluid was made up of the base fluid (de-ionized water and 2 lb/bbl xanthan gum polymer) with 1 lb/bbl surfactant added. This was then mixed at a low shear rate of 500 RPM for 1 minute. No colloidal gas aphrons were created due to the low mixing rate. This fluid was then injected into the visual cell.

Table 5-5 Oil recovery using polymer/surfactant experiment run 1

Time	Vol. of Fluid Injected	Vol. of Oil Produced	Cumulative Oil Produced	Vol. of Injected Fluid Produced
0	0	0	0	0
10	3	0	0	0
20	6	0	0	0
30	9	2	2	0
40	12	2	4	0
50	15	3	7	0
60	18	2	9	0
70	21	2	11	0
80	24	2	13	0
90	27	3	16	0
100	30	3	19	0
110	33	3	22	0
120	36	3	25	0
130	39	3	28	0
140	42	2	30	0
150	45	3	33	0
160	48	3	36	0
170	51	3	39	0
180	54	3	42	0
190	57	3	45	0
200	60	3	48	0
210	63	3	51	0
220	66	3	54	0
230	69	3	57	0
240	72	3	60	0
250	75	3	63	0
260	78	2	65	0
270	81	3	68	0
280	84	1	69	0
290	87	2	71	0
300	90	1	72	0
310	93	2	74	1
320	96	0	74	2
Breakthrough Time = 302 mins			**Pore Volume = 81 ml**	
Injected Fluid Retention Time = 320 mins			**Total Oil Recovery = 91%**	

Table 5-6 Oil recovery using polymer/surfactant experiment run 2

Time	Vol. of Fluid Injected	Vol. of Oil Produced	Cumulative Oil Produced	Vol. of Injected Fluid Produced
0	0	0	0	0
10	3	0	0	0
20	6	0	0	0
30	9	2	2	0
40	12	2	4	0
50	15	2	6	0
60	18	3	9	0
70	21	2	11	0
80	24	3	14	0
90	27	3	17	0
100	30	3	20	0
110	33	3	23	0
120	36	3	26	0
130	39	3	29	0
140	42	3	32	0
150	45	2	34	0
160	48	3	37	0
170	51	3	40	0
180	54	3	43	0
190	57	3	46	0
200	60	3	49	0
210	63	2	51	0
220	66	3	54	0
230	69	3	57	0
240	72	2	59	0
250	75	3	62	0
260	78	2	64	0
270	81	3	67	0
280	84	2	69	0
290	87	2	71	0
300	90	2	73	0
310	93	2	75	0
320	96	1	76	1
330	99	0	76	2
Breakthrough Time = 317 mins			**Pore Volume = 81 ml**	
Injected Fluid Retention Time = 330 mins			**Total Oil Recovery = 94%**	

Table 5-5 and 5-6 show similar breakthrough times of 302 and 317 mins with both experiments having a pore volume of 81 ml. The total oil recovered was 91% in Table 5-5 and 94% in Table 5-6.

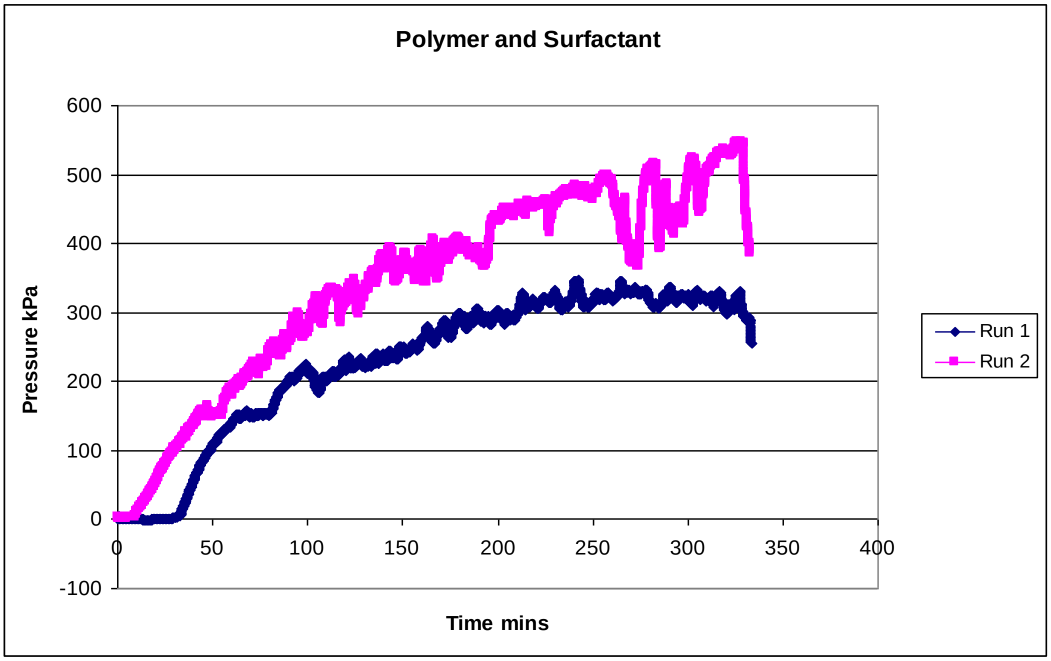

Figure 5-5 Visual cell pressure data for polymer/surfactant run 1 & 2

Figure 5-5 shows the pressure data for recorded for experiments using the aqueous polymer/surfactant solution. The higher pressure curve corresponds to the total oil recovery of 94%. The difference in the pressure curves may be a result of increased polymer adsorption to the pore walls. The maximum pressure drop was 547 kPa.

0 mins

30 mins

60 mins

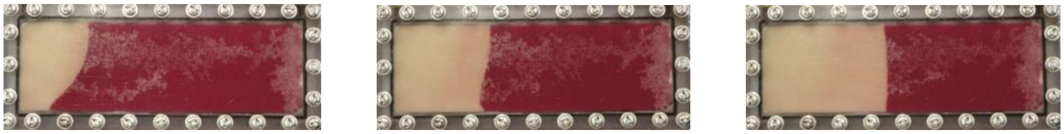

90 mins 120 mins 150 mins

180 mins 210 mins 240 mins

270 mins 300 mins 330 mins

Figure 5-6 Time lapse photos of polymer/surfactant flood

Figure 5-6 shows quick movement of the polymer/surfactant solution front across the visual cell. At 60 mins the front has extended the width of the visual cell and continues to straighten up. At 150 mins the fluid front is fully linear and moves forward in this manner until the end of the experiment.

5.4 Water

Water flooding is commonly used in the field as a secondary recovery mechanism after the natural reservoir drive energy is diminished. De-ionized water was used for these experiments. Tables 5-7 and 5-8 show the oil recovery results while Figure 5-4 shows the pressure profile.

Table 5-7 Oil recovery using water – experiment run 1

Time	Vol. of Water Injected	Vol. of Oil Produced	Cumulative Oil Produced	Vol. of Water Produced
0	0	0	0	0
10	3	3	3	0
20	6	3	6	0
30	9	3	9	0
40	12	3	12	0
50	15	3	15	0
60	18	3	18	0
70	21	3	21	0
80	24	2	23	1
90	27	2	25	1
100	30	1	26	1
110	33	1	27	1
120	36	2	29	1
130	39	2	31	2
140	42	1	32	2
150	45	1	33	2
Breakthrough Time = 77 mins			**Pore Volume = 83 ml**	
Injected Fluid Retention Time = 150 mins			**Total Oil Recovery = 40%**	

Table 5-8 Oil recovery using water – experiment run 2

Time	Vol. of Water Injected	Vol. of Oil Produced	Cumulative Oil Produced	Vol. of Water Produced
0	0	0	0	0
10	3	3	3	0
20	6	3	6	0
30	9	3	9	0
40	12	3	12	0
50	15	3	15	0
60	18	3	18	0
70	21	3	21	0
80	24	2	23	1
90	27	2	25	1
100	30	1	26	1
110	33	2	28	1
120	36	1	29	2
130	39	1	30	2
140	42	1	31	2
150	45	1	32	3
Breakthrough Time = 75 mins			**Pore Volume = 82 ml**	
Injected Fluid Retention Time = 150 mins			**Total Oil Recovery = 39%**	

Tables 5-7 and 5-8 both show low breakthrough times of 75 and 77 mins with similar pore volumes of 83 and 82 ml. The total oil recovered is also quite similar at 40% and 39% respectively.

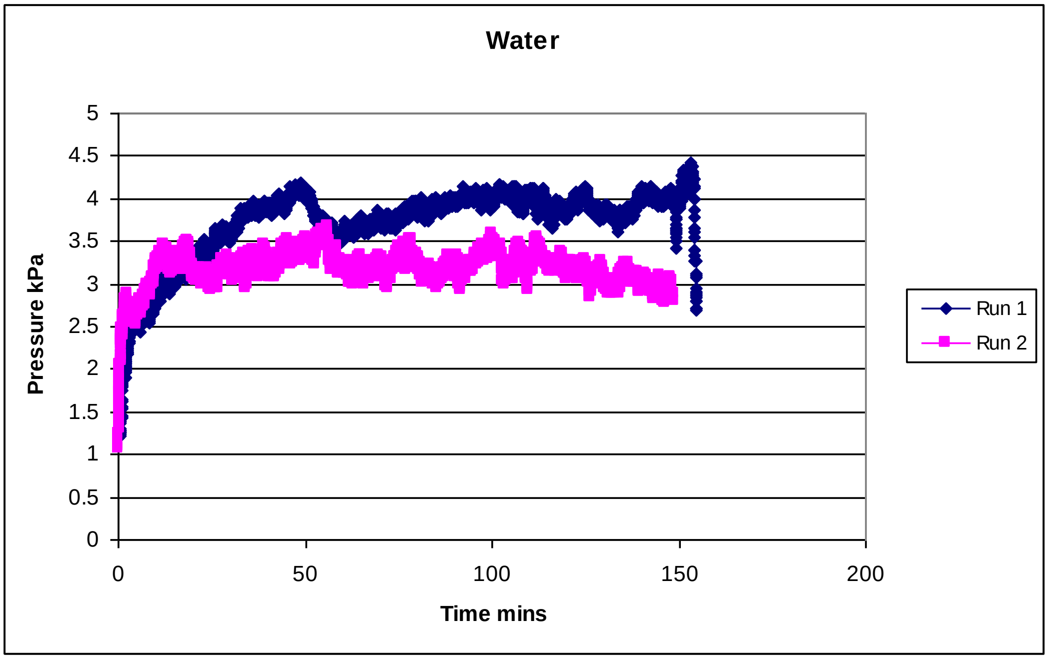

Figure 5-7 Visual cell pressure data for water run 1 & 2

Figure 5-7 shows the pressure data recorded while flooding the visual cell with water. The pressure drop produced is quite low due to the lower viscosity of water compared to the mineral oil with a recorded maximum of 4.5 kPa.

0 mins 30 mins 60 mins

90 mins 120 mins 150 mins

Figure 5-8 Time lapse photos of water flood

Figure 5-8 clearly shows the water bypassing certain sections of the dyed mineral. This results in the uneven pattern seen. The lower viscosity of the water causes fingering through the mineral oil which bypasses some of the oil in the visual cell. This is supported by the low recovery results of Tables 5-7 and 5-8.

5.5 Water followed by CGA Fluid

These experiments look into tertiary recovery mechanisms and were conducted in two stages. After saturation, the visual cell was flooded using de-ionized water. The water injection was stopped after 150 mins, as at this time there was little produced oil. After this, the visual cell was flooded using the CGA fluid and the same parameters recorded. Table 5-9 and Figure 5-5 show the results. This experiment was conducted four times with leakage occurring in three of these experiments. Therefore only one set of data was collected but due to the repeatability with experiments it was seen as accurate.

Table 5-9 Oil recovery using water followed by CGA fluid – experiment run 1

Time	Vol. of Fluid Injected	Vol. of Oil Produced	Cumulative Oil Produced	Vol. of Water Produced
0	0	0	0	0
10	3	3	3	0
20	6	3	6	0
30	9	3	9	0
40	12	3	12	0
50	15	3	15	0
60	18	3	18	0
70	21	3	21	0
80	24	2	23	1
90	27	2	25	1
100	30	1	26	1
110	33	2	28	1
120	36	1	29	2
130	39	1	30	2
140	42	1	31	2
150	45	1	32	3
160	48	1	33	1
170	51	0	33	1
180	54	1	34	1
190	57	0	34	1
200	60	0	34	1
210	63	1	35	1
220	66	1	36	1
230	69	0	36	1
240	72	1	37	1
250	75	1	38	1
260	78	0	38	1
270	81	1	39	1
280	84	1	40	1
290	87	1	41	0
300	90	1	42	1
310	93	1	43	0
320	96	1	44	0
330	99	2	46	1
340	102	2	48	0
350	105	2	50	1
360	108	2	52	0
370	111	2	54	0
380	114	2	56	1
390	117	2	58	0
400	120	2	60	1
410	123	2	62	0
420	126	2	64	1

430	129	2	66	0
440	132	2	68	1
450	135	1	69	1
460	138	2	71	1
470	141	1	72	2
480	144	1	73	2
490	147	1	74	1
500	150	1	75	2
510	153	0	75	1
520	156	1	76	2
530	159	0	76	0
540	162	0	76	0
Breakthrough Time = 75 mins (water)			**Pore Volume = 82 ml**	
Breakthrough Time = 370 mins (CGA Fluid)			**Oil Recovery = 39% (water)**	
Injected Fluid Retention Time = 150 mins (water)			**Oil Recovery = 54% (aphron)**	
Injected Fluid Retention Time = 390 mins (CGA Fluid)			**Total Oil Recovery = 93%**	

Table 5-9 shows good total oil recovery at 93% with breakthrough times of 75 mins and 370 mins.

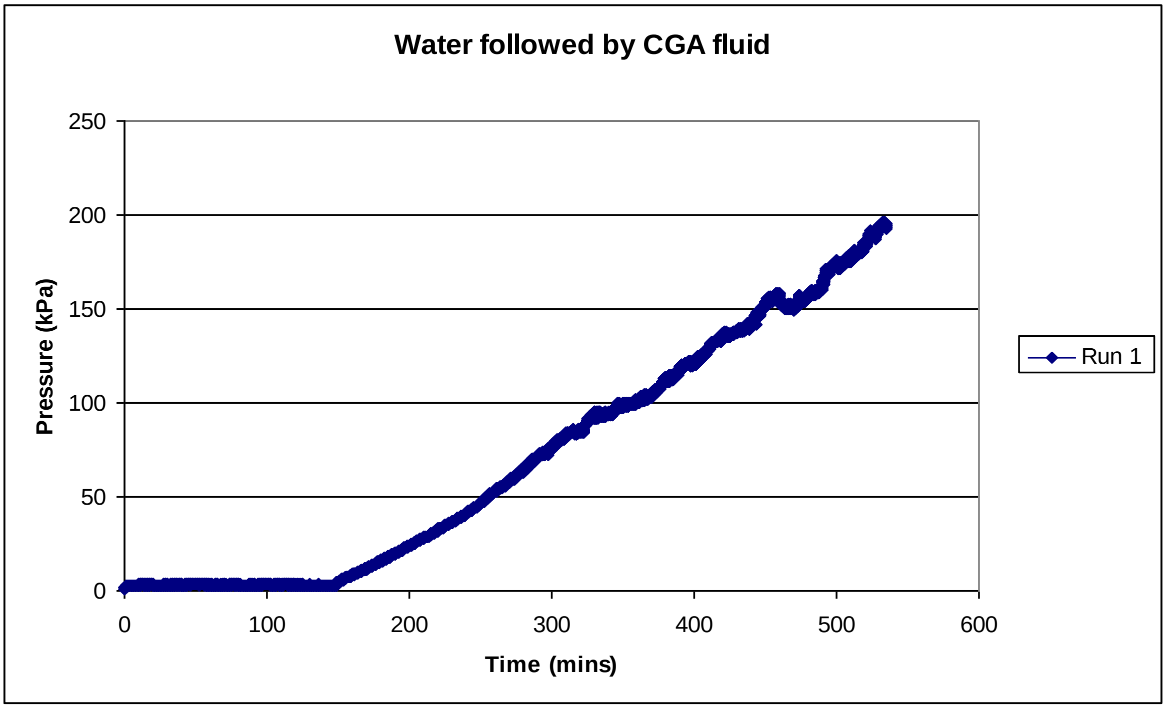

Figure 5-9 Visual cell pressure data for water followed by CGA fluid – experiment run 1

The pressure data seen in Figure 5-9 shows two distinct parts. From the beginning of the experiment to 150 mins the pressure is very low as compared to the rest of the graph. This is the result of waterflooding. After this the CGA fluid is injected and there is a corresponding constant increase in pressure which is a result of the bridging behaviour of aphrons as they move into the pore spaces. The maximum pressure drop was 200 kPa.

0 mins

30 mins

60 mins

90 mins

120 mins

150 mins

180 mins

210 mins

240 mins

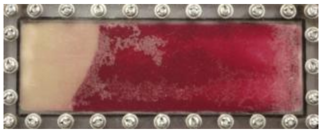

270 mins

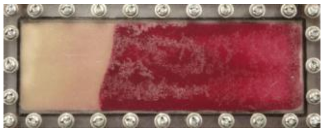

300 mins

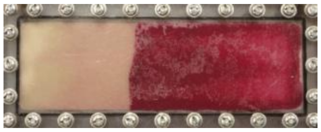

330 mins

360 mins

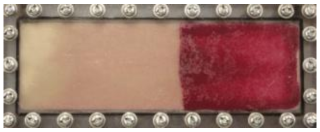

390 mins

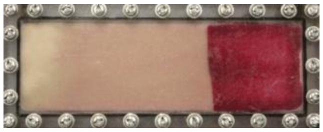

420 mins

450 mins 480 mins 510 mins

540 mins

Figure 5-10 Time lapse photos of water followed by CGA fluid flood

Figure 5-10 shows water fingering from 0 to 150 mins as water is injected. As the less viscous water moves through the visual cell and bypasses the mineral oil an uneven pattern is seen. There is greater oil displacement towards the left end of the visual model as this is the location of the injection port. After 150 mins the CGA fluid is injected and a stable fluid front is soon formed. This front steadily moves forward displacing the dyed mineral oil and leading to good recovery results.

5.6 Water followed by polymer

Polymer flooding is another tertiary recovery method and this was investigated as a comparison to the tertiary recovery results of the CGA fluid. The results are seen in Table 5-10 and 5-11 while Figure 5-6 shows the pressure data.

Table 5-10 Oil recovery using water followed by polymer – experiment run 1

Time	Vol. of Fluid Injected	Vol. of Oil Produced	Cumulative Oil Produced	Vol. of water Produced
0	0	0	0	0
10	3	2	2	0

20	6	3	5	0
30	9	3	8	0
40	12	3	11	0
50	15	3	14	0
60	18	3	17	0
70	21	3	20	0
80	24	2	22	1
90	27	2	24	2
100	30	1	25	3
110	33	1	26	2
120	36	1	27	1
130	39	1	28	2
140	42	1	29	2
150	45	1	30	3
160	48	0	30	0
170	51	1	31	0
180	54	2	33	2
190	57	2	35	1
200	60	2	37	1
210	63	2	39	0
220	66	2	41	1
230	69	2	43	1
240	72	2	45	1
250	75	2	47	1
260	78	2	49	1
270	81	2	51	1
280	84	2	53	1
290	87	2	55	0
300	90	2	57	1
310	93	2	59	1
320	96	3	62	1
330	99	2	64	0
340	102	3	67	1
350	105	2	69	1
360	108	1	70	1
370	111	2	72	1
380	114	1	73	1
390	117	1	74	2
400	120	0	74	2
410	123	0	74	1
420	126	1	75	1
430	129	0	75	0
440	132	0	75	1
450	135	0	75	1
460	138	1	76	1
470	141	0	76	0
Breakthrough Time = 71 mins (water)			**Pore Volume = 85 ml**	
Breakthrough Time = 310 mins			**Oil Recovery = 37% (water)**	

(polymer)	
Injected Fluid Retention Time = 150 mins (water)	**Oil Recovery = 57% (polymer)**
Injected Fluid Retention Time = 320 mins (polymer)	**Total Oil Recovery = 94%**

Table 5-11 Oil recovery using water followed by polymer – experiment run 2

Time	Vol. of Fluid Injected	Vol. of Oil Produced	Cumulative Oil Produced	Vol. of water Produced
0	0	0	0	0
10	3	2	2	0
20	6	3	5	0
30	9	3	8	0
40	12	3	11	0
50	15	3	14	0
60	18	3	17	0
70	21	3	20	0
80	24	3	23	0
90	27	2	25	1
100	30	1	26	2
110	33	1	27	2
120	36	1	28	2
130	39	1	29	2
140	42	1	30	2
150	45	1	31	3
160	48	0	31	0
170	51	0	31	0
180	54	1	32	0
190	57	1	33	0
200	60	1	34	0
210	63	1	35	1
220	66	1	36	1
230	69	1	37	1
240	72	2	39	1
250	75	2	41	0
260	78	1	42	2
270	81	2	44	1
280	84	1	45	1
290	87	2	47	1
300	90	2	49	1
310	93	2	51	1
320	96	2	53	1
330	99	1	54	1
340	102	2	56	1
350	105	2	58	1
360	108	2	60	1

370	111	2	62	1
380	114	2	64	1
390	117	2	66	0
400	120	0	66	1
410	123	1	67	0
420	126	2	69	1
430	129	1	70	1
440	132	1	71	1
450	135	1	72	1
460	138	1	73	2
470	141	1	74	1
480	144	1	75	1
490	147	1	76	1
500	150	1	77	1
510	153	1	78	1
520	156	1	79	0
Breakthrough Time = 81 mins (water)			**Pore Volume = 85 ml**	
Breakthrough Time = 348 mins (polymer)			**Oil Recovery = 37% (water)**	
Injected Fluid Retention Time = 150 mins w. **Injected Fluid Retention Time = 370 mins p.**			**Oil Recovery = 57% (polymer)** **Total Oil Recovery = 94%**	

Tables 5-10 and 5-11 both show 94% total oil recovery with 37% due to water and 57% due to the polymer solution. The water breakthrough times are similar at 71 and 81 mins. There is a difference in the polymer breakthrough times which may be a result of increased polymer adsorption. This increased adsorption may slow the movement of the polymer solution across the visual cell and delay breakthrough time.

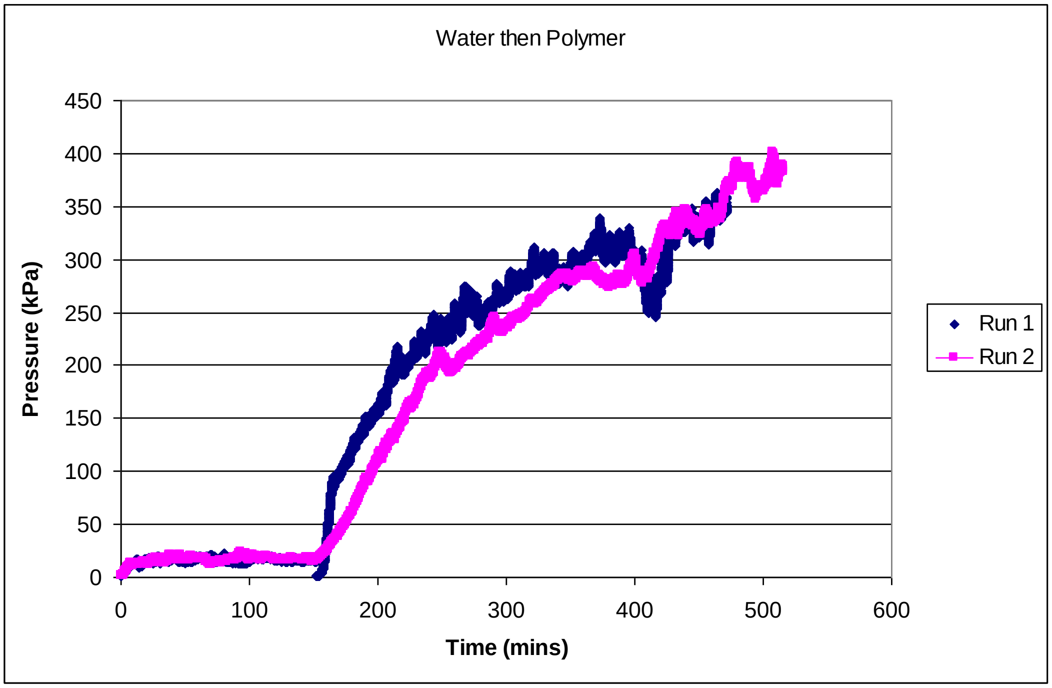

Figure 5-11 Visual cell pressure data for water followed by polymer – experiment run 1 & 2

Figure 5-11 show similar pressure drop data for both water followed by polymer solution experiments. The pressure data from 0 to 150 mins corresponds to the injection of water while 150 mins onwards shows the effect of the injection of the polymer solution. The maximum pressure drop seen was 400 kPa.

0 mins

30 mins

60 mins

90 mins

120 mins

150 mins

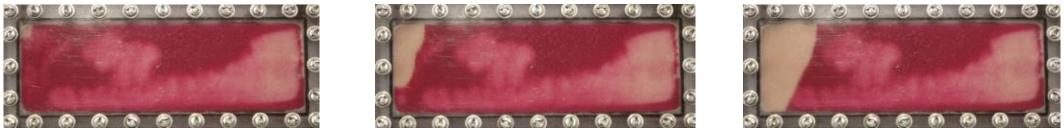

180 mins 210 mins 240 mins

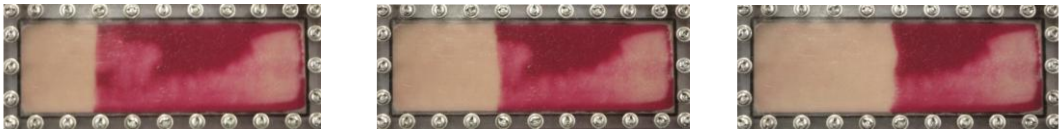

270 mins 300 mins 330 mins

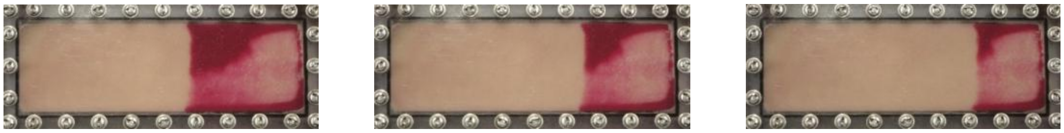

360 mins 390 mins 420 mins

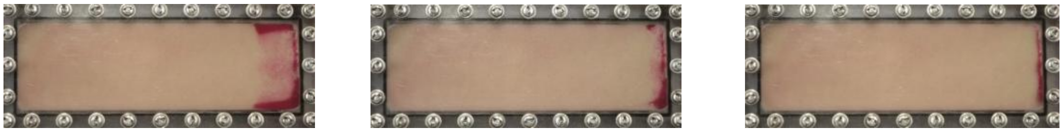

450 mins 480 mins 510 mins

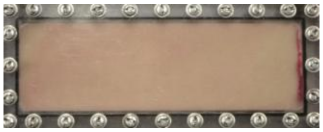

520 mins

Figure 5-12 Time lapse photos of water followed by polymer flood

Figure 5-12 shows no distinct fluid front from 0 to 150 mins when waterflooding is used and much of the mineral oil is still trapped in the porous media. After injection of the polymer solution starts a distinct fluid front develops. At 240 mins the polymer front spans the width of the visual cell and at 270 mins it is linear.

From 270 mins the front progresses quickly and displaces most of the dyed mineral oil.

5.7 Comparison of Results

Table 5-12 Summary of visual cell oil recovery

	Total Oil Recovery (%)		**Breakthrough Time (mins)**		**Oil Recovery at Breakthrough (%)**		**Max. Injected Pressure (kPa)**
Recovery Fluid	**Run 1**	**Run 2**	**Run 1**	**Run 2**	**Run 1**	**Run 2**	
CGA Fluid	89	90	406	402	88	89	200
Polymer	94	94	327	284	89	90	360
Surfactant and Polymer	91	94	302	317	89	93	547
Water	40	39	75	77	26	25	4.5
Water followed by CGA Fluid	93		75/370		26/93		200
Water followed by Polymer	94	94	71/310	81/348	24/93	27/89	400

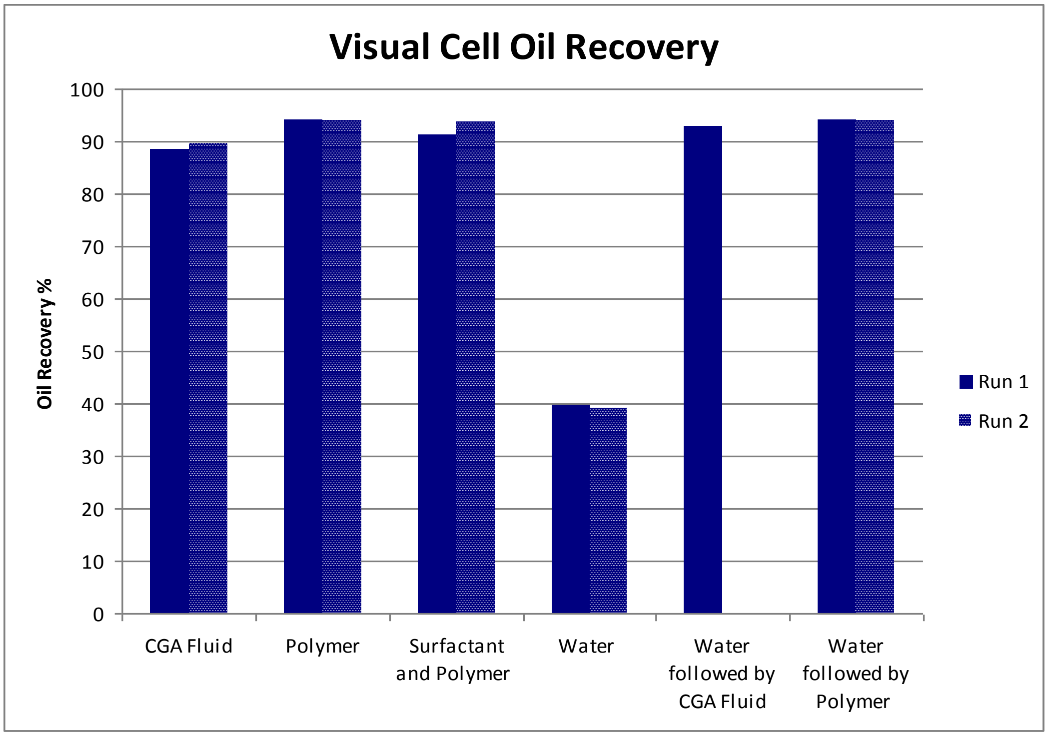

Figure 5-13 Summary of visual cell oil recovery

Using Table 5-12 and Figure 5-13 the fluid which produced the best recovery results was the aqueous xanthan gum polymer solution This fluid had 94% oil recovery when it was used solely or when it was used after water flooding. The surfactant and polymer mix was close behind and there was a 3% difference between experiments. This mixture also generated high pressures. The CGA fluid also preformed very well with recovery being between 89 and 90% using the CGA fluid alone while using water followed by the CGA fluid had a recovery of 93%. Water had the lowest recovery as expected and was 39 to 40%.

Even though there was a difference in recovery between using the CGA fluid and the polymer solution this was quite small especially in the experiments preceded by water flooding. Therefore the CGA fluid and polymer could be described as comparable in terms of their abilities as recovery fluids. The CGA fluid may be even more advantageous when additional factors are considered. The viscosity of the CGA fluid is lower than that of the polymer and this may prove easier to pump than the polymer. This is important for field applications. Table 5-12 shows that the maximum injected pressure for the CGA fluid is much lower at 200 kPa when compared to the polymer solution at 360 kPa. This is also seen in the recovery experiments using CGA fluid and the aqueous polymer solution preceded by water with the maximum injected pressure being 200 kPa for CGA fluid and 400 kPa for the polymer solution.

Figures 5-2 and 5-4 show the time lapse photos taken for the CGA fluid and polymer solution experiments. It is easily apparent that the polymer flood progresses at a faster pace than the CGA fluid experiments. At 60 mins the front of the CGA fluid is not yet linear while the polymer front is already linear and progressing well. This is seen even more at 150 mins, the polymer front is halfway through the model with the CGA fluid front much behind. At 310 mins the polymer front has made its way completely across the model while the CGA fluid takes 420 mins. Figure 5-6 shows the time lapse photos for the polymer/surfactant mix. These photos show a fluid front that is behind that of the polymer in Figure 5-4 but still ahead that of the CGA fluid in Figure 5-2 at 150 mins. The water flooding time lapse photos are seen in Figure 5-8 and show no distinct frontal movement. There is also much of the oil still in place seen by the dark pink mineral oil in uneven patches.

Figure 5-10 and 5-12 show the time lapse images of the CGA fluid and polymer after each was preceded by a water flood. These photos show that both the behaviour of the CGA fluid and the polymer solution was not affected by the prior injected water. The major difference is in the time taken for these two part experiments with the water followed by the CGA fluid taking 540 mins while the water followed by polymer took 520 mins. Using the recovery data, maximum injected pressure and time lapse photos the CGA fluid had the best overall performance as a recovery fluid.

5.8 Effect of gravity

To determine if gravity had an effect on the recovery results the orientation of the apparatus was changed. In the previous experiments the model was placed laterally which was changed to a vertical arrangement for the following experiments. The effect of gravity on oil recovery was conducted using the CGA fluid and the aqueous polymer solution. This was investigated as there was difference in density between the two fluids. The density of the CGA fluid was 0.66 g/cm^3 and the polymer solution was 0.99 g/cm^3. It was thought that due to this difference the CGA fluid might separate into two distinct phases with the colloidal gas aphrons above the polymer base. It was found that this did not occur. These results are seen in Table 5-12 and 5-13 while the pressure data is showed in Figures 5-14 and 5-15.

Table 5-13 Oil recovery using CGA fluid (vertical orientation)

Time	Vol. of Fluid Injected	Vol. of Oil Produced	Cumulative Oil Produced	Vol. of CGA Fluid Produced
0	0	0	0	0
10	3	0	0	0
20	6	0	0	0
30	9	0	0	0
40	12	1	1	0
50	15	1	2	0
60	18	0	2	0
70	21	1	3	0
80	24	0	3	0
90	27	1	4	0
100	30	0	4	0
110	33	1	5	0
120	36	0	5	0
130	39	1	6	0
140	42	1	7	0
150	45	2	9	0
160	48	2	11	0
170	51	2	13	0
180	54	2	15	0
190	57	2	17	0
200	60	2	19	0
210	63	2	21	0
220	66	2	23	0
230	69	2	25	0
240	72	2	27	0
250	75	2	29	0
260	78	2	31	0
270	81	3	34	0
280	84	3	37	0
290	87	3	40	0
300	90	2	42	0
310	93	3	45	0
320	96	2	47	0
330	99	2	49	0
340	102	3	52	0
350	105	2	54	0
360	108	3	57	0
370	111	2	59	0
380	114	2	61	0
390	117	3	64	0
400	120	3	67	0
410	123	2	69	0
420	126	3	72	0
430	129	2	74	0

440	132	2	76	1
450	135	0	76	3
Breakthrough Time = 436 mins			**Pore Volume = 81 ml**	
Injected Fluid Retention Time = 450 mins			**Total Oil Recovery = 94%**	

Table 5-13 shows a total recovery of 94% with a breakthrough time of 436 mins while Table 5-1 shows a breakthrough time of 406 mins and recovery of 89%. The vertical placement of the visual cell lengthened the breakthrough and experiment time but did not hamper the total oil recovered.

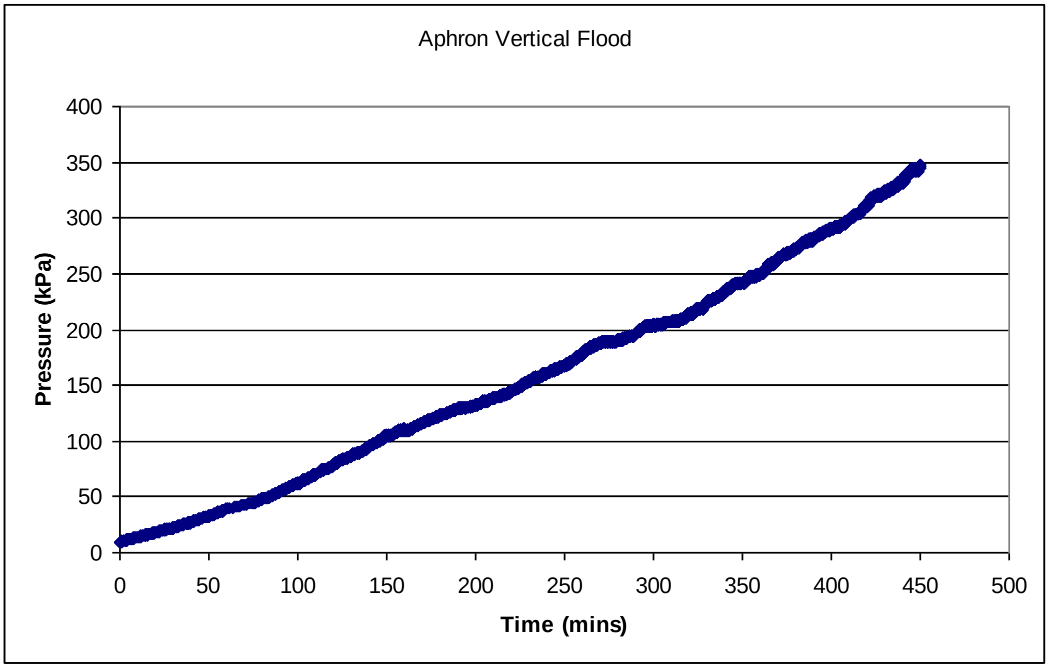

Figure 5-14 Visual cell pressure data for CGA fluid (vertical orientation)

Figure 5-14 shows the pressure data recorded for the CGA fluid when the visual cell was placed vertically. There is a slow pressure buildup throughout the experiment. This is again explained by the blocking ability of colloidal gas aphrons. The aphrons are entering pore spaces and bridging them causing an increase in pressure. Figure 5-14 shows the same trend as Figure 5-1 but with a higher maximum pressure drop of 350 kPa compared to 200 kPa.

Table 5-14 Oil recovery using polymer (vertical orientation)

Time	Vol. of Fluid Injected	Vol. of Oil Produced	Cumulative Oil Produced	Vol. of Polymer Produced
0	0	0	0	0
10	3	0	0	0
20	6	2	2	0
30	9	2	4	0
40	12	2	6	0
50	15	2	8	0
60	18	3	11	0
70	21	3	14	0
80	24	3	17	0
90	27	2	19	0
100	30	3	22	0
110	33	3	25	0
120	36	2	27	0
130	39	3	30	0
140	42	3	33	0
150	45	3	36	0
160	48	2	38	0
170	51	3	41	0
180	54	3	44	0
190	57	3	47	0
200	60	3	50	0
210	63	3	53	0
220	66	3	56	0
230	69	3	59	0
240	72	3	62	0
250	75	3	65	0
260	78	3	68	0
270	81	3	71	0
280	84	2	73	0
290	87	1	74	2
Breakthrough Time = 280 mins			**Pore Volume = 79 ml**	
Injected Fluid Retention Time = 290 mins			**Total Oil Recovery = 94%**	

Table 5-14 shows a total oil recovery of 94% with a breakthrough time of 280 mins. This data is quite similar to that of Table 5-4 which shows a total oil recovery of 94% as well with a breakthrough time of 284 mins.

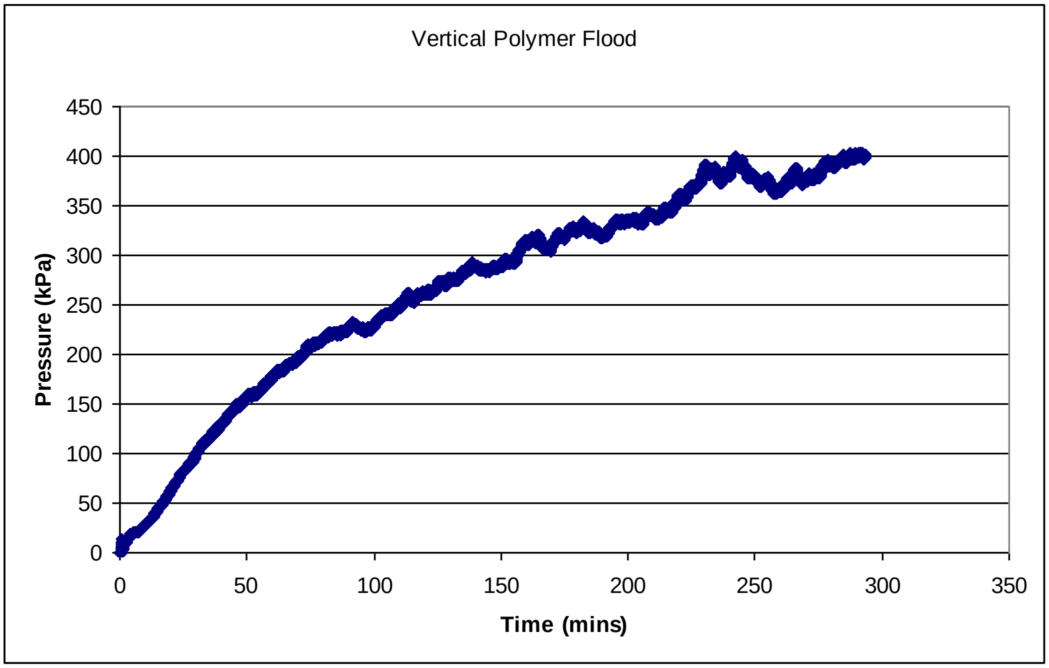

Figure 5-15 Visual cell pressure data for polymer (vertical orientation)

Figure 5-15 shows the pressure data using the aqueous polymer solution to flood the vertical visual cell. This figure shows the same behaviour seen in Figure 5-3 with a similar maximum pressure drop of 400 kPa.

Table 5-15 Oil Recovery using lateral and vertical orientations

	Total Oil Recovery (%)	
Recovery Fluid	Lateral Placement	Vertical Placement
CGA Fluid	90	94
Polymer	94	94

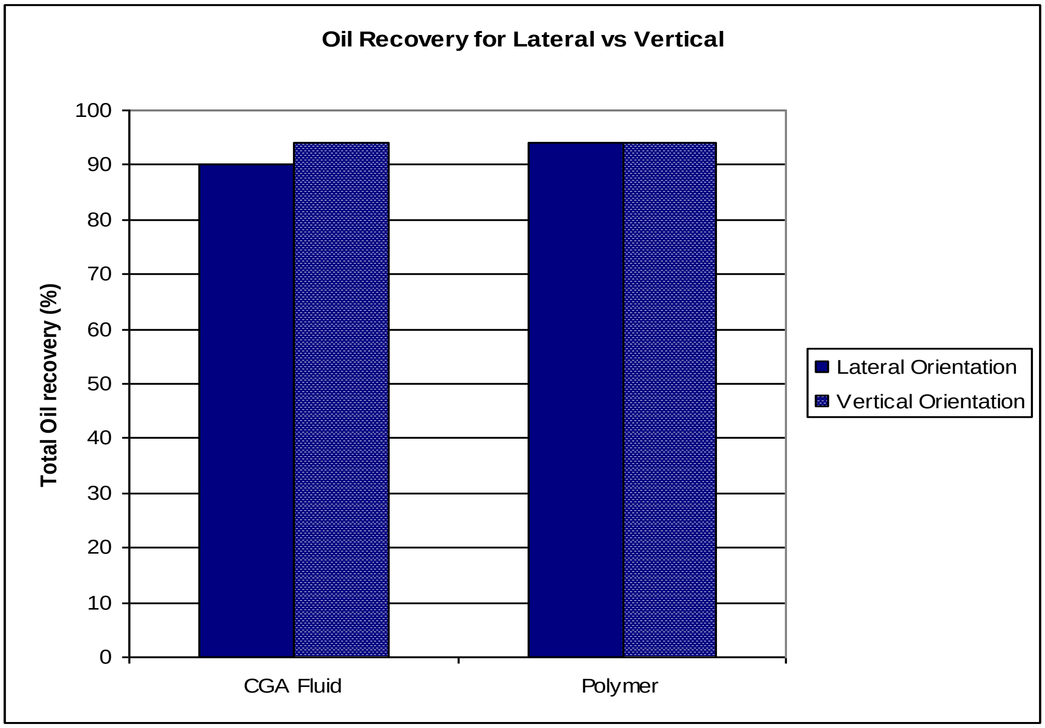

Figure 5-16 Oil Recovery using lateral and vertical orientation

As mentioned before due to the difference in the densities between the two fluids it was thought that gravity may have had an effect on the CGA fluid. However it was seen that gravity had little effect on the CGA fluid as it did not separate into two phases as seen in Figure 5-17. These photos show a stable linear front which moved uniformly across the visual cell. If separation of the CGA fluid did occur then the front would not have been a straight line. A difference of 30 mins was seen in the injected fluid time, however this did not seem to affect the total oil recovery. The recovery of the CGA fluid placed laterally was 90% while than in the vertical orientation was 94%. If separation of the CGA fluid occurred then the recovery would have been less than 90%. The oil recovery using the polymer solution for both the vertical and lateral experiments was 94% so gravity had no effect. The experiment time was also less than that of the lateral experiment, so gravity did not increase this factor. Figure 5-18 shows a smooth stable polymer front as it moves through the visual cell similar to Figure 5-4.

CGA Fluid (Vertical orientation)


0 mins


30 mins


60 mins


90 mins


120 mins


150 mins


180 mins


210 mins


240 mins


270 mins


300 mins

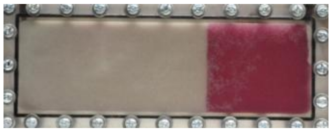
330 mins


360 mins


390 mins


420 mins


450 mins

Figure 5-17 Time lapse photos of CGA fluid flood vertical orientation

Polymer (Vertical orientation)

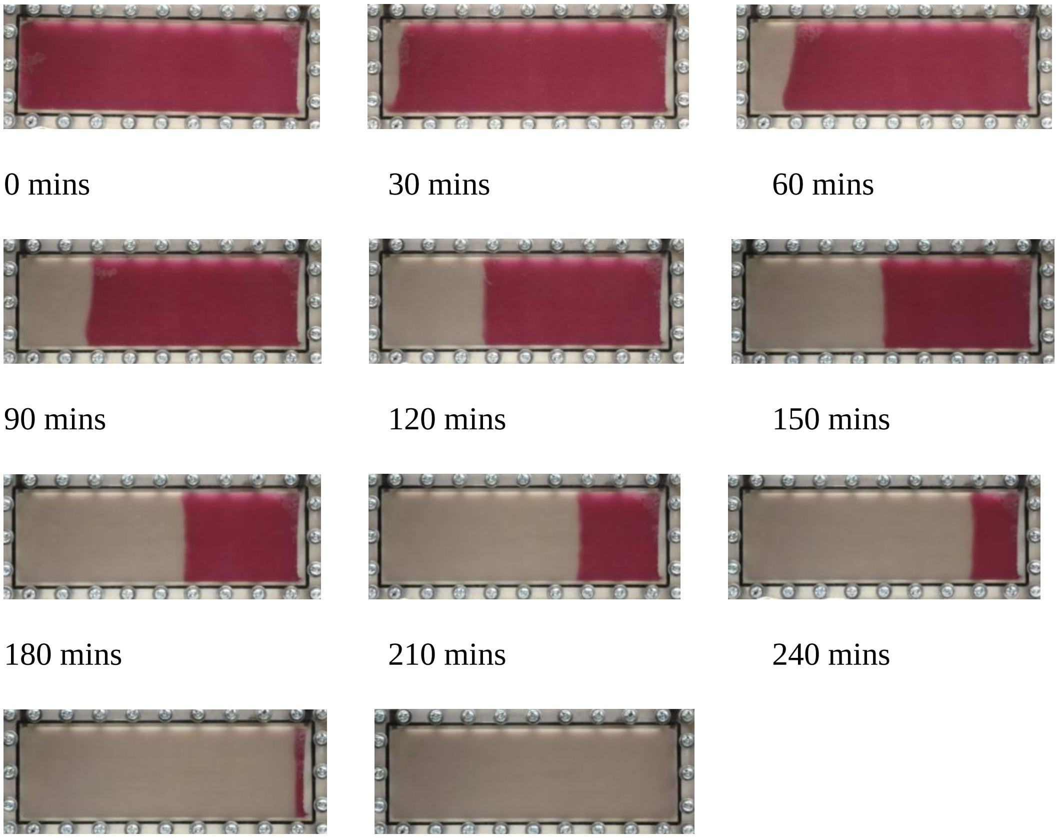

0 mins 30 mins 60 mins

90 mins 120 mins 150 mins

180 mins 210 mins 240 mins

270 mins 290 mins

Figure 5-18 Time lapse photos of polymer flood vertical orientation

6. RADIAL CELL

In the previous chapter the performance of the CGA fluid as a recovery fluid was tested using the 2-D visual cell experiments. In this section the CGA fluid is further tested in a radial cell to determine its suitability as a recovery fluid. The radial cell is made up of a steel hollow cylinder with two removable ends. One of these ends contains three ports: one is used for injection and the other two for production. The cylinder was tightly packed with glass beads and saturated with dyed mineral oil. The porosity was 35% and permeability was 0.15 D. The CGA fluid was then injected into the radial cell at a rate of 4 ml/min and total oil recovery, breakthrough time and fluid injection time was recorded. The procedure is described in Chapter 3.

The injection rate of 4 ml/min was based on work done by Veerabhadrappa et al. (2011). In this investigation Equation 6-1 suggested by Christopher and Middleman (1965) was used as well as the material constant suggested by Chauveteau (1982) to determine the injection rate.

$$\Gamma = \{(3n+1) / 4n\} \times \{(4Q) / (A\ (8k\phi)^{0.5})\} \qquad \text{Equation 6-1}$$

Γ is the shear rate (s^{-1}), $(3n+1) / 4n$ is the non-Newtonian correction factor for power-law fluids, Q is the flow rate (cm^3s^{-1}), A is the cross sectional area of the core (cm^2), k is the permeability (cm^2) and ϕ is porosity. The material constant of $\alpha = 1.7$ for glass beads is used as suggested by Chauveteau (1982) and Equation 6-1 is rewritten in terms of Q to give Equation 6-2 (Veerabhadrappa et al. 2011).

$$Q = (A\gamma\ (8k\phi)^{0.5}\ ) / 4\alpha \qquad \text{Equation 6-2}$$

This resulted in a flow rate of 4 ml/min which was found to correspond to shear rates of 10-100 s^{-1}. This shear rate range represents the flow conditions experienced in water flooding experiments in typical oil reservoirs.

The pressure profile of the CGA fluid across the radial cell was observed and recorded along with other fluids. These other fluids were used to compare the recovery performance as in the visual cell experiments. The radial cell experiments were conducted using a) aqueous CGA fluid b) aqueous polymer solution c) water d) water followed by aqueous CGA fluid and e) water followed by aqueous polymer solution. As this apparatus was tightly sealed each fluid was tested once except water followed by aqueous CGA fluid. This experiment was completed twice to ensure accurate data.

6.1 CGA Fluid

These experiments were conducted using the CGA fluid. As before this fluid was comprised of a base fluid of de-ionized water and 2 lb/bbl xanthan gum (Barazan D) polymer with 1 lb/bbl DDBS (Sodium Dodecyl Benzene Sulfonate) surfactant. The results for this experiment are seen in Table 6-1 and Figure 6-1.

Table 6-1 Oil recovery using CGA Fluid

Time	Vol. of CGA Fluid Injected	Vol. of Oil Produced	Cumulative Oil Produced	Vol. of CGA Fluid Produced
0	0	0	0	0
10	40	5	5	0
20	80	20	25	0
30	120	26	51	0
40	160	29	80	0
50	200	27	107	0
60	240	35	142	0
70	280	34	176	1

80	320	30	206	1
90	360	36	242	1
100	400	8	250	3
110	440	9	259	2
120	480	12	271	5
130	520	11	282	18
140	560	18	300	20
150	600	19	319	23
160	640	17	336	21
170	680	8	344	30
180	720	7	351	32
190	760	7	358	33
200	800	0	358	19
210	840	3	361	4
220	880	4	365	26
230	920	3	368	16
240	960	4	372	36
250	1000	4	376	69
Breakthrough Time = 66 mins			**Pore Volume = 500 ml**	
Injected Fluid Retention Time = 250 mins			**Total Oil Recovery = 75%**	

Table 6-1 shows a total oil recovery of 75% from a pore volume of 500 ml. In the first 90 mins the amount of oil produced was much greater than after 90 mins. The breakthrough time was 66 mins which was much earlier than the breakthrough times seen for the visual cell in Chapter 5.

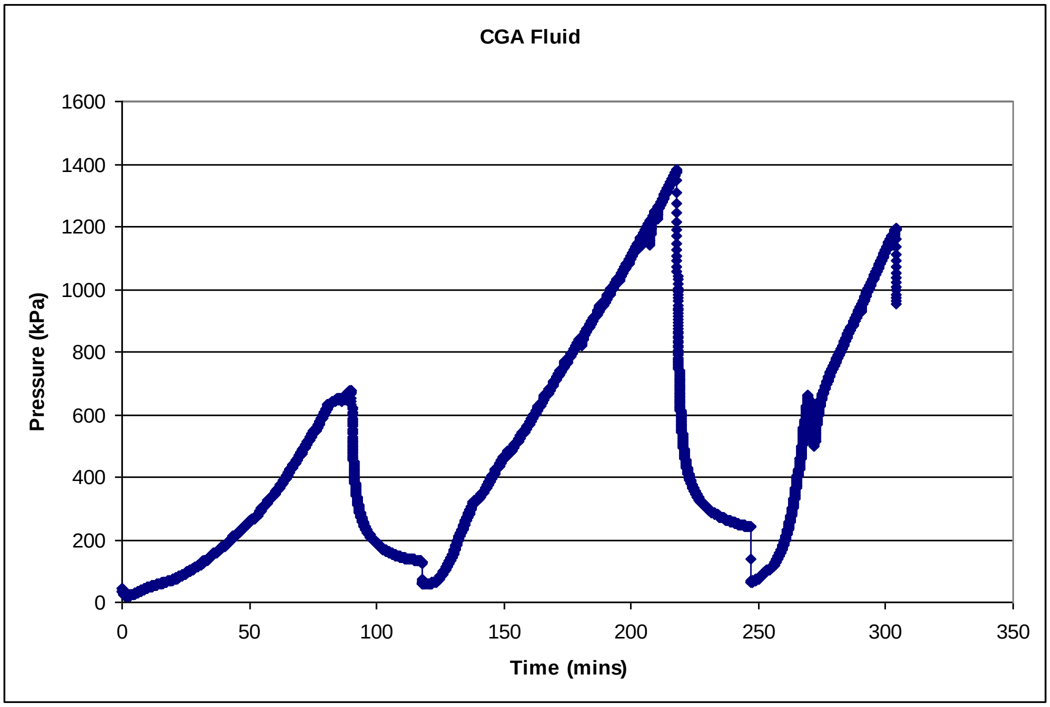

Figure 6-1 Radial cell pressure data for CGA fluid

Figure 6-1 shows the pressure drop recorded for the CGA fluid as it was injected into the radial cell. The steep fall in pressure was due to the stopping of the experiment to refill the pump. Figure 6-1 shows a smooth continual rise in pressure which can be attributed to aphron buildup. As more of the CGA fluid is injected into the radial cell more aphrons enter the pore spaces and bridge them which increases the pressure drop. The maximum pressure drop was 1,400 kPa.

6.2 Aqueous Polymer Solution

The polymer containing base solution was used in this experiment. The solution was made up of 2 lb/bbl xanthan gum polymer mixed into de-ionized water. Table 6-2 and Figure 6-2 show the results of the polymer flood.

Table 6-2 Oil recovery using polymer

Time	Vol. of Polymer Injected	Vol. of Oil Produced	Cumulative Oil Produced	Vol. of Polymer Produced
0	0	0	0	0
10	40	28	28	0
20	80	26	54	0
30	120	38	92	0
40	160	32	124	0
50	200	35	159	1
60	240	11	170	13
70	280	8	178	26
80	320	33	211	20
90	360	34	245	20
100	400	21	266	12
110	440	19	285	16
120	480	20	305	22
130	520	18	323	20
140	560	18	341	22
150	600	14	355	22
160	640	15	370	28
170	680	7	377	30
180	720	10	387	26
190	760	8	395	32
200	800	12	407	22
210	840	6	413	40
220	880	5	418	28
230	920	2	420	40
240	960	2	422	32
250	1000	3	425	38
Breakthrough Time = 48 mins			**Pore Volume = 500 ml**	
Injected Fluid Retention Time = 250 mins			**Total Oil Recovery = 85%**	

Table 6-2 shows an oil recovery of 85% from a pore volume of 500 ml. The majority of the oil was produced from 0 to 160 mins with a significant decrease occurring after 160 mins. The breakthrough time was 48 mins.

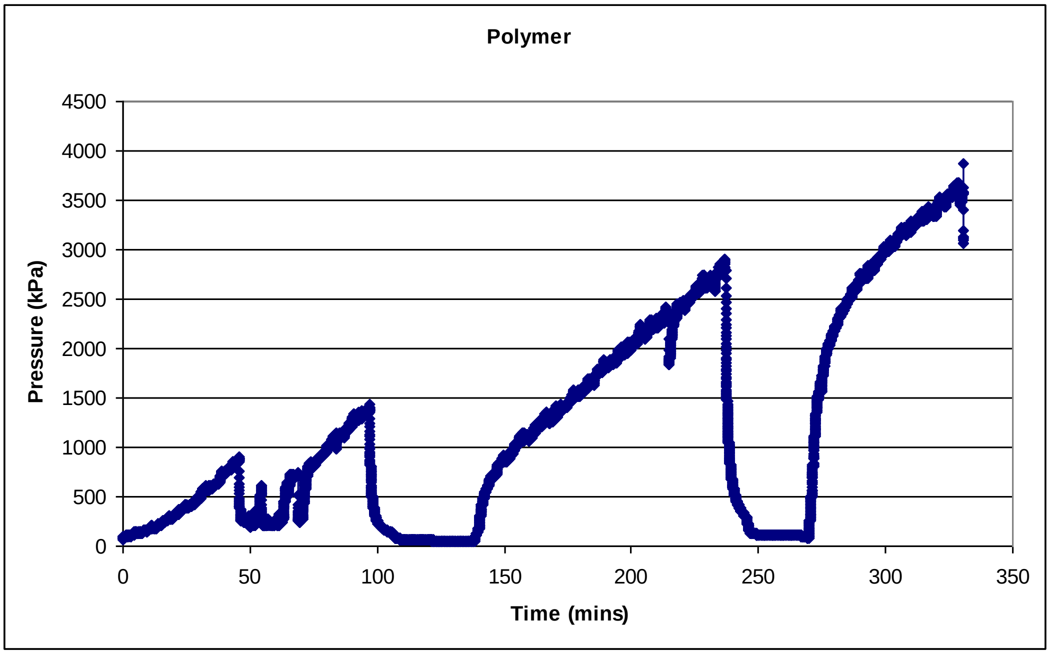

Figure 6-2 Radial cell pressure data for polymer

Figure 6-2 shows the pressure drop recorded while injecting the aqueous polymer solution. The sharp decreases in pressure are again due to the stopping of the pump to refill the polymer solution. The pressure drop is very steep with a maximum pressure of 3,700 kPa. This large increase in pressure could be due to adsorption where the polymer solution clings to the pore walls.

6.3 Water

De-ionized water was also used to conduct a water flood as in the visual cell. Table 6-3 show the oil recovery results and Figure 6-3 shows the pressure profile.

Table 6-3 Oil recovery using water

Time	Vol. of Water Injected	Vol. of Oil Produced	Cumulative Oil Produced	Vol. of Water Produced
0	0	0	0	0
10	40	0	0	0
20	80	23	23	0
30	120	11	34	3
40	160	20	54	13
50	200	18	72	22
60	240	17	89	24
70	280	14	103	29
80	320	10	113	27
90	360	10	123	32
100	400	8	131	32
110	440	8	139	32
120	480	10	149	64
Breakthrough Time = 24 mins			**Pore Volume = 500 ml**	
Injected Fluid Retention Time = 120 mins			**Total Oil Recovery = 30%**	

Table 6-3 shows a low total oil recovery of 30% from a pore volume of 500 ml. The breakthrough time is also low at 24 mins. This is due to the lower viscosity of water as compared to the mineral oil. The difference in viscosity causes water fingering in the sand pack. This results in sections of the sand pack being bypassed by the water and so large amounts of residual oil.

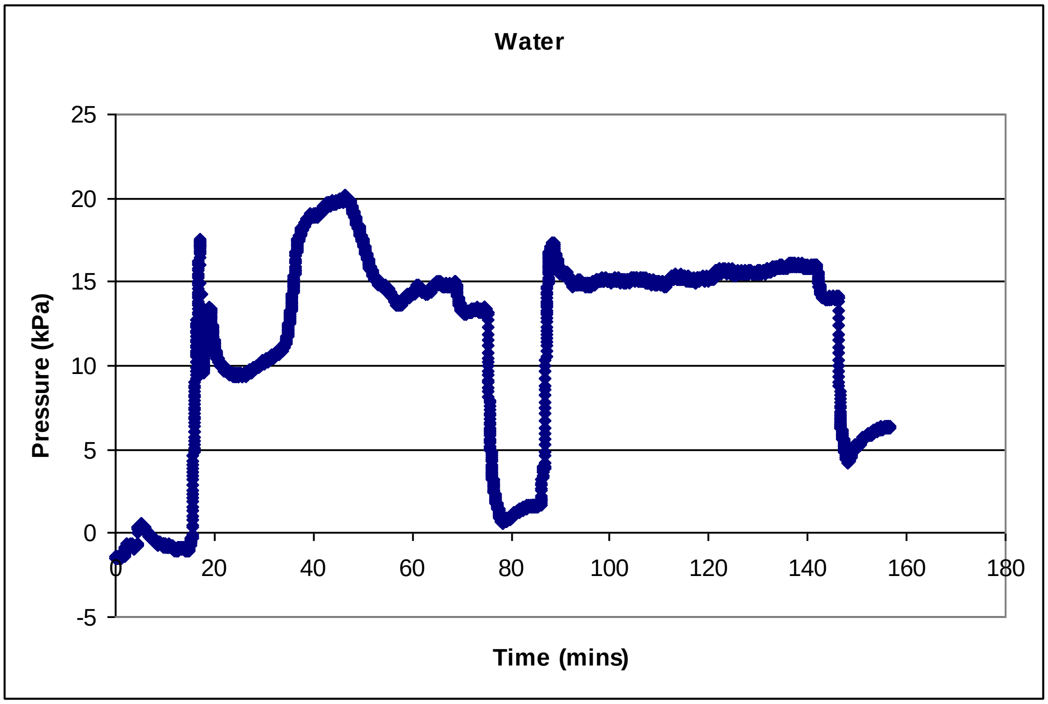

Figure 6-3 Radial cell pressure data for water

Figure 6-3 shows the recorded pressure drop while water was injected. The maximum injected pressure was 20 kPa which was quite low as compared to the other fluids.

6.4 Water followed by CGA Fluid

As in the visual cell, tertiary radial cell recovery experiments were done to further test the CGA Fluid. These experiments were done in two stages. Firstly water was used as the recovery fluid for 120 mins and then followed by the CGA fluid for 250 mins. These times were used due to the low oil production relative to the water produced if the experiment was continued. This experiment was conducted twice to ensure the data was accurate. The results are seen in Tables 6-4 and 6-5 and Figure 6-4.

Table 6-4 Oil recovery using water followed by CGA fluid experiment 1

Time	Vol. of Fluid Injected	Vol. of Oil Produced	Cumulative Oil Produced	Vol. of Water Produced	Vol. of CGA Fluid Prod
0	0	0	0	0	0
10	40	13	13	0	0
20	80	27	40	4	0
30	120	22	62	12	0
40	160	10	72	18	0
50	200	13	85	26	0
60	240	13	98	28	0
70	280	9	107	30	0
80	320	10	117	30	0
90	360	7	124	34	0
100	400	7	131	32	0
110	440	8	139	32	0
120	480	8	147	32	0
130	520	7	154	32	0
140	560	11	165	10	0
150	600	10	175	16	0
160	640	12	187	14	0
170	680	14	201	22	0
180	720	9	210	16	0
190	760	15	225	10	10
200	800	15	240	0	26
210	840	14	254	0	14
220	880	14	268	0	24
230	920	2	270	0	12
240	960	9	279	0	10
250	1000	17	296	0	14
260	1040	8	304	0	32
270	1080	8	312	0	30
280	1120	8	320	0	38
290	1160	6	326	0	32
300	1200	6	332	0	32
310	1240	6	338	0	36
320	1280	4	342	0	44
330	1320	4	346	0	8
340	1360	4	350	0	28
350	1400	3	353	0	40
360	1440	3	356	0	40
370	1480	2	358	0	33

Breakthrough Time = 18 mins (water)	**Pore Volume = 500 ml**
Breakthrough Time = 64 mins (CGA Fluid)	**Oil Recovery = 29% (water)**
Injected Fluid Retention Time = 120 mins (water)	**Oil Recovery = 43% (CGA Fluid)**
Injected Fluid Retention Time = 250 mins (CGA Fluid)	**Total Oil Recovery = 72%**

Table 6-4 shows a total oil recovery of 72% from a pore volume of 500 ml. Using water 29% of the oil was recovered while 43% was recovered using the CGA fluid. The breakthrough times were 18 mins for water and 64 mins for the CGA fluid.

Table 6-5 Oil recovery using water followed by CGA fluid experiment 2

Time	Vol. of Fluid Injected	Vol. of Oil Produced	Cumulative Oil Produced	Vol. of Water Produced	Vol. of CGA Fluid Produced
0	0	0	0	0	0
10	40	0	0	0	0
20	80	20	20	0	0
30	120	13	33	2	0
40	160	20	53	14	0
50	200	19	72	22	0
60	240	18	90	24	0
70	280	14	104	28	0
80	320	10	114	28	0
90	360	10	124	30	0
100	400	10	134	32	0
110	440	8	142	30	0
120	480	8	150	68	0
130	520	8	158	0	0
140	560	6	164	8	0
150	600	12	176	15	0
160	640	10	186	24	0
170	680	12	198	18	13
180	720	16	214	22	9
190	760	10	224	8	6
200	800	14	238	0	12
210	840	13	251	0	30
220	880	12	263	0	28
230	920	15	278	0	7
240	960	3	281	0	15
250	1000	10	291	0	20

260	1040	16	307	0	30
270	1080	7	314	0	48
280	1120	8	322	0	38
290	1160	7	329	0	38
300	1200	6	335	0	36
310	1240	5	340	0	39
320	1280	6	346	0	37
330	1320	4	350	0	15
340	1360	4	354	0	8
350	1400	3	357	0	29
360	1440	2	359	0	36
370	1480	2	361	0	60
Breakthrough Time = 22 mins (water)				**Pore Volume = 500 ml**	
Breakthrough Time = 48 mins (CGA fluid)				**Oil Recovery = 30% (water)**	
Injected Fluid Retention Time = 120 mins (water)				**Oil Recovery = 42% (CGA fluid)**	
Injected Fluid Retention Time = 250 mins (CGA fluid)				**Total Oil Recovery = 72%**	

Table 6-5 also shows a total oil recovery of 72% with 30% from water injection and 42% from injecting the CGA fluid. The breakthrough times were 22 mins for water and 48 mins for the CGA fluid. Tables 6-4 and 6-5 both show similar total oil recovery at 72% while the breakthrough times are also similar.

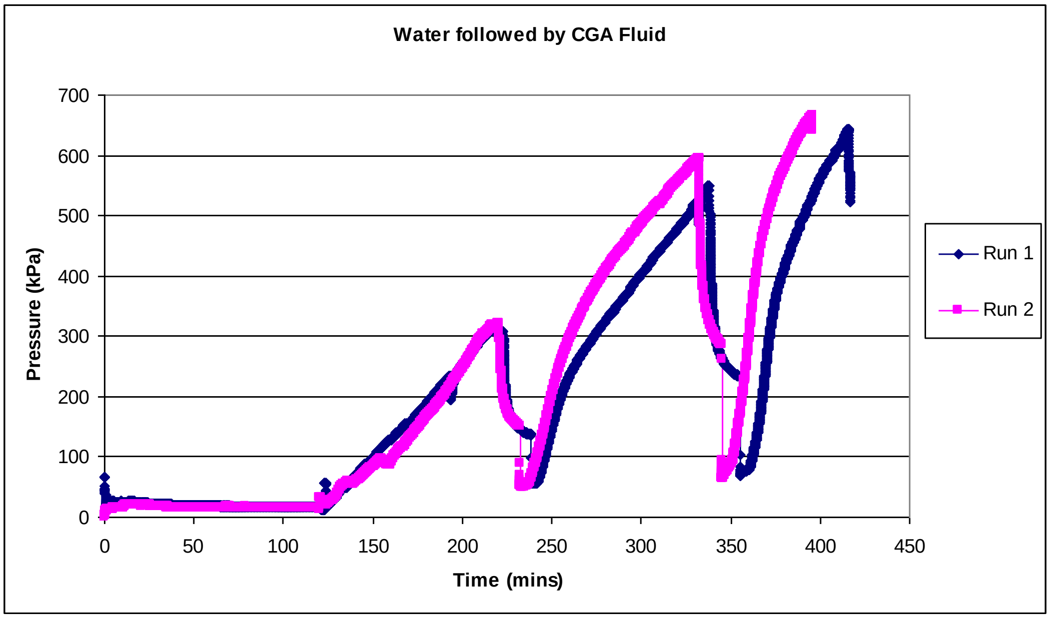

Figure 6-4 Radial cell pressure data for water followed by CGA fluid experiment 1 and 2

Figure 6-4 shows the pressure drop for the two experiments using water followed by the aqueous CGA fluid. From 0 to 120 mins the pressure is low due to water injection but this quickly rises as the CGA fluid is introduced. As with Figure 6-1 there is a smooth increase in pressure due to the aphron bridging. The maximum pressure drop was 660 kPa for experiment 1 and 670 kPa for experiment 2.

6.5 Water followed by polymer

Water followed by polymer was also used in comparison to the water followed by CGA fluid. These results are seen in Table 6-6 and Figure 6-5.

Table 6-6 Oil recovery using water followed by polymer

Time	Vol. of Fluid Injected	Vol. of Oil Produced	Cumulative Oil Produced	Vol. of Water Produced	Vol. of Polymer Produced
0	0	0	0	0	0
10	40	4	4	0	0
20	80	20	24	0	0
30	120	13	37	15	0
40	160	10	47	26	0
50	200	8	55	26	0
60	240	9	64	36	0
70	280	8	72	33	0
80	320	6	78	32	0
90	360	6	84	36	0
100	400	6	90	34	0
110	440	4	94	36	0
120	480	5	99	34	0
130	520	4	103	28	0
140	560	13	116	27	0
150	600	9	125	21	0
160	640	16	141	22	0
170	680	20	161	18	0
180	720	24	185	15	0

190	760	21	206	18	0
200	800	28	234	5	0
210	840	19	253	0	8
220	880	22	275	0	18
230	920	20	295	0	19
240	960	17	312	0	21
250	1000	2	314	0	2
260	1040	4	318	0	8
270	1080	14	332	0	16
280	1120	2	334	0	12
290	1160	8	342	0	22
300	1200	7	349	0	32
310	1240	5	354	0	28
320	1280	10	364	0	28
330	1320	13	377	0	32
340	1360	9	386	0	32
350	1400	8	394	0	24
360	1440	9	403	0	40
370	1480	0	403	0	0
380	1520	8	411	0	62
390	1560	4	415	0	4
400	1600	2	417	0	34
410	1640	4	421	0	41
420	1680	3	424	0	73
Breakthrough Time = 22 mins (water)				**Pore Volume = 500 ml**	
Breakthrough Time = 83 mins				**Oil Recovery = 20% (water)**	
Injected Fluid Retention Time = 120 mins (water)				**Oil Recovery = 65% (polymer)**	
Injected Fluid Retention Time = 250 mins (polymer)				**Total Oil Recovery = 85%**	

Table 6-6 shows a total recovery of 85 % with 20% due to water injection and 65% from injecting the aqueous polymer solution. The breakthrough times were 22 mins for water and 83 mins for the polymer solution.

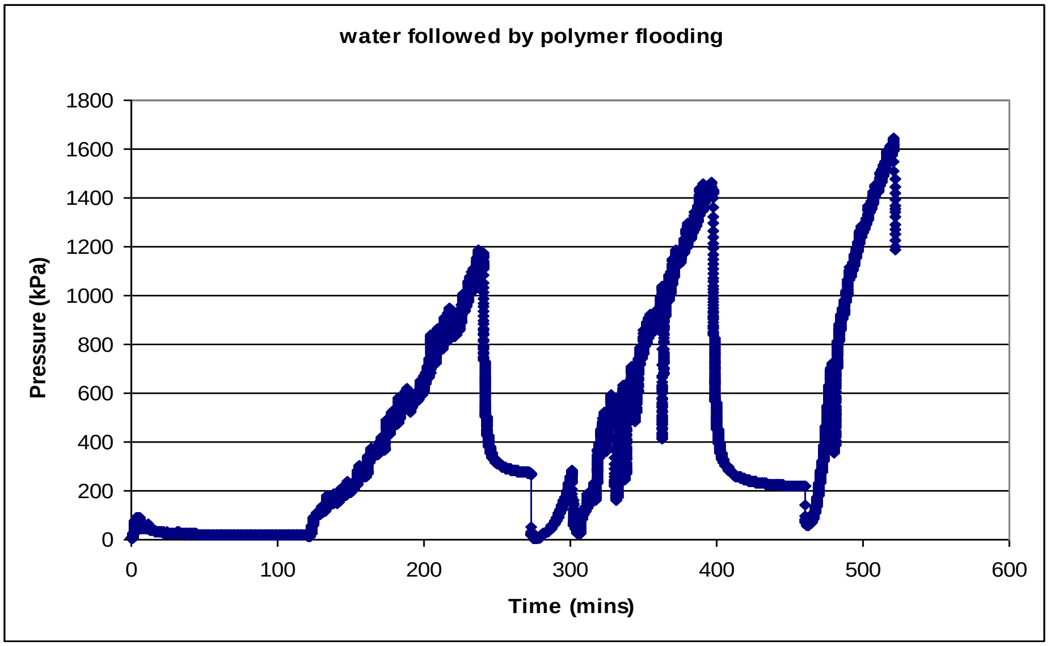

Figure 6-5 Radial cell data for water followed by polymer

Figure 6-5 shows a maximum pressure drop of 1650 kPa. The low pressure values recorded from 0-120 mins occurred during water injection. After 120 mins there is a steep rise in pressure as the polymer solution was injected.

Table 6-7 Summary of radial cell recovery

Recovery Fluid	Oil Recovery (%)	Breakthrough Time (mins)	Oil Recovery at BT (%)	Max. Injected Pressure (kPa)
CGA Fluid	75	66	28.2	1400
Polymer	85	48	24.8	3700
Water	30	24	4.6	20
Water followed by CGA Fluid	72	18/64 22/48	2.6/42 4.6/35.2	660/670
Water followed by Polymer	82	22/83	4.8/46.8	1650

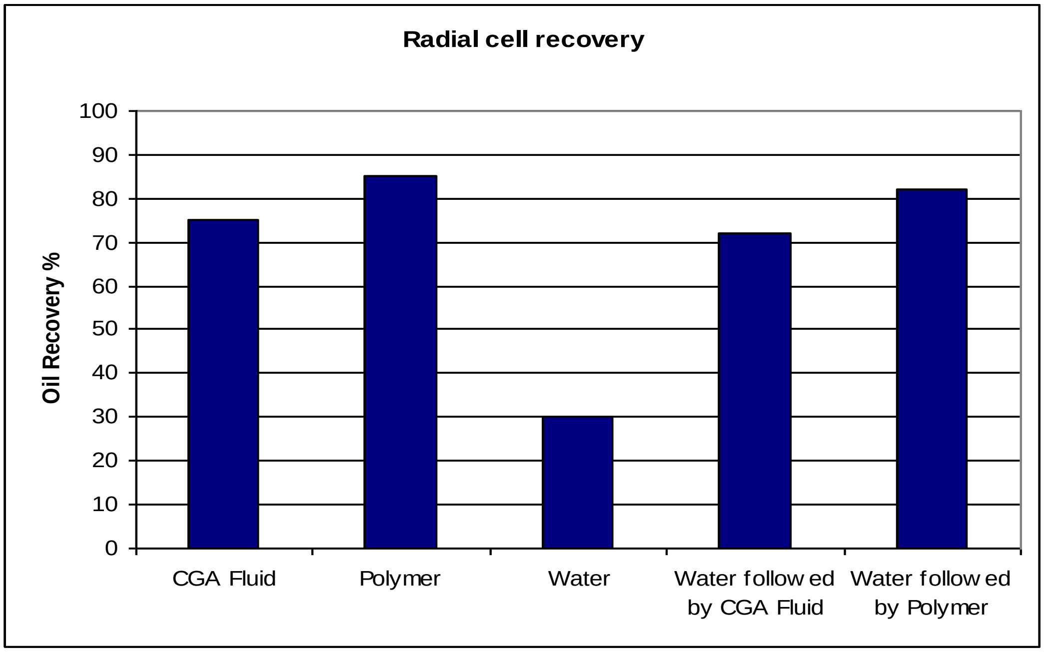

Figure 6-6 Summary of radial cell recovery

The oil recovery results of the tested fluids can be seen in Table 6-7 and Figure 6-6 with water having the lowest recovery at 30%. As in the visual cell the polymer showed the best total oil recovery at 85%. The CGA fluid recovered 75% of the original oil in place while for both fluids preceded by water the recovery was lower. The water followed by polymer recovered 82% while the water followed by CGA Fluid recovered 72%, in both cases there was a reduction of 3%. Therefore there was more residual oil in these experiments as compared to those using only CGA fluid or aqueous polymer solution. This differed from the visual cell where the experiments preceded by water had the same total recovery as those using only CGA fluid or aqueous polymer solution.

The breakthrough times differed for the experiments conducted with water, polymer and CGA fluid with water having the earliest breakthrough and the CGA fluid having the latest breakthrough time. This changed in the tertiary recovery experiments with water as the polymer took longer to breakthrough than the CGA fluid. Looking at the breakthrough times in the visual cell experiments the CGA fluid consistently took the longest time to breakthrough. This is also reflected in the radial cell experiments. Oil recovery at breakthrough was 28.2% of the original oil in place using the CGA fluid as compared to 24.8% using the polymer solution. Using the breakthrough times for the polymer solution and CGA fluid and upscaling this to a longer time span shows that for a 10 year project the polymer solution would breakthrough in 1.9 years as compared to 2.6 years for the CGA fluid. Therefore using the polymer solution may be more costly than the CGA fluid as polymer will be produced earlier and separation of the produced fluids will be expensive.

Table 6-7 shows the maximum injected pressure for each fluid. The polymer flood experiment had the highest pressure drop of about 3700 kPa. The CGA fluid had a maximum pressure drop of about 1400 kPa which was approximately a third of that of the polymer. This is quite a large pressure difference and will favour the use of the CGA fluid as a recovery fluid in preference to the polymer solution. This difference of about a third was also seen in the water followed by CGA fluid and water followed by polymer experiments. Water showed the lowest pressure drop of approximately 20 kPa. The sharp drops in the pressure graphs where the pressure decreases to 0 kPa was due to the stopping of the pump to refill the injection fluid.

7. CONCLUSIONS AND RECOMMENDATIONS

Conclusions

At the beginning of this study two main objectives were identified which were the development and characterization of the aqueous CGA fluid and the evaluation of its stability and performance as an enhanced recovery fluid. The following section summarizes the major conclusions reached based on the experimental investigation conducted in this study.

The three surfactants used in this study were: DDBS (anionic), CTAB (cationic) and Tergitol (non-ionic), among these the anionic surfactant DDBS was found to be the most suitable for CGA formulation. This anionic surfactant (DDBS) yielded the smallest bubble sizes (d_{50}= 53 μm) and better CGA stability (d_{50}=248 μm) after 6 hours. Bubble size and stability also varied with surfactant concentration. This helped determine the optimum anionic surfactant concentration which was found to be 1 lb/bbl.

The different polymers tested were: Xanthan gum (Barazan D), Carboxymethylcellulose (CMC), Hydroxyethylcellulose (Liqui-Vis EP), Xanthan gum (N-Vis) and a cellulose derived polymer (Quik-Trol). Low shear rate viscosity (LSRV) of the polymer solutions was identified as the most important parameter influencing CGA stability. Among the tested polymers only xanthan gum (Barazan D) was found to yield LSRV higher than the minimum required LSRV of 40,000 cP. Using the bubble size diameter and bubble size distribution as the selection criterion the optimum concentration of xanthan gum was found to be 2 lb/bbl.

The effect of mixing procedure on the CGA bubble size and stability was also examined. Smaller, more stable aphrons were produced when the surfactant was added to a prepared base solution of the polymer and then mixed (d_{50}= 100 µm at 0 mins and 240 µm at 6 hours). Immediate mixing of all the CGA fluid components produced larger, less stable aphrons (d_{50}= 200 µm at 0 mins and 290 µm at 6 hours). The optimum CGA formulation was then determined to be a base fluid of de-ionized water and 2 lb/bbl xanthan gum mixed with 1 lb/bbl DDBS (anionic) surfactant.

In the visual cell experiments the xanthan gum polymer solution had the highest total oil recovery of 94% in both experiments. This was followed closely by the surfactant and polymer mixture with total oil recoveries of 91% and 94%. The total oil recovery for the CGA fluid was 89% and 90% while water had the lowest total oil recovery at 39% and 40%. In the experiments preceded by water the polymer solution had a total oil recovery of 94%. The CGA fluid preceded by water had a total oil recovery of 93%.

The polymer solution also produced 4-5% of the total oil recovered after breakthrough as compared to 1-2% by the CGA fluid. This means that the cost of separating the produced fluids will be more for the polymer solution than the CGA fluid.

The maximum injected pressure measured for each fluid differed with the surfactant and polymer mix having the highest injected pressure of 547 kPa. The water followed by polymer solution had a maximum injected pressure of 400 kPa closely followed by the polymer solution at 360 kPa. The experiments using the CGA fluid and water followed by the CGA fluid both had a maximum injected pressure of 200 kPa. Water had the lowest maximum injected pressure at 4.5 kPa.

The time lapse photos show that the polymer solution, surfactant and polymer mix, CGA fluid all had stable linear moving fronts. The effect of gravity on the total oil recovery using the polymer solution and CGA fluid was also investigated. The total oil recovery did not decrease for either fluid and there was no gravitational separation of the CGA fluid. Therefore gravity had no effect.

In the radial cell experiments the polymer solution again had the highest total oil recovery of 85%, followed by the CGA fluid at 75%. Water as expected, had the lowest total oil recovery of 30%. In the experiments preceded by water the polymer solution had the higher total oil recovery of 82% as compared to the CGA fluid at 72%.

In these experiments the CGA fluid had a higher oil recovery of 28.2% at breakthrough as compared to 24.8% by the polymer solution as the polymer solution had a shorter breakthrough time. This influences the economic cost as a shorter breakthrough time will result in the need for earlier separation of the produced fluids which can be costly.

The maximum injected pressure was 3,700 kPa using the polymer solution. The CGA fluid had a maximum injected pressure of 1,400 kPa which was about a third of that of the polymer solution. This pattern continued in the experiments preceded by water. The polymer solution had a maximum injected pressure of

1,650 kPa while the CGA fluid had a maximum injected pressure of 670 kPa. Water had the lowest maximum injected pressure at 20 kPa.

The CGA fluid has proved to be a possible recovery fluid in this study. The polymer solution had higher oil recovery but also had the highest maximum injected pressure and shorter breakthrough time. The CGA fluid had a significantly lower maximum injected pressure and longer breakthrough time which could compensate for its lower oil recovery.

Recommendations

- Reservoir pressures and temperatures are quite different to those used in this investigation. The effect of pressure and temperature on average bubble size, bubble size distribution and yield could be studied to determine how aphrons would respond to reservoir conditions.
- The oil recovery experiments conducted in this study were done under laboratory conditions. If oil recovery experiments were done under simulated reservoir conditions this would give a better idea of its performance as a recovery fluid under field conditions.
- Recovery experiments could be conducted in the presence of brine to determine the effect of formation water on the CGA fluid.
- As temperature will affect the rheology of the CGA fluid an additive such as a thermal stabilizer may be used and its effect on bubble size and stability studied.

- The oil recovery experiments using the CGA fluid could be repeated using a larger scale visual cell and with less permeable glass beads.
- These recovery experiments were conducted using mineral oil and should be repeated using heavy oil.
- The CGA fluid could be used on an actual core sample to measure oil recovery in comparison to the glass beads used in this experimental study.
- The air contained in the aphron core of this CGA fluid could be replaced with carbon dioxide/flue gas. This would then be useful for carbon sequestration with the added benefit of acting as a recovery fluid.

8. REFERENCES

Ali, S.M.F. and Thomas, S. (1996) The Promise and Problems of Enhanced Oil Recovery Techniques. Paper 96-07-07, The Journal of Canadian Petroleum Technology, September 1996, Volume 35, Number 7, Pages 57-63.

Alkafeef, S.F. and Zaid, A.M. (2007) Review of and Outlook for Enhanced Oil Recovery Techniques in Kuwait Oil Reservoirs. IPTC 11234, 2007 International Petroleum Technology Conference, December 4-6, Dubai, U.A.E.

Baroid® Product Data Sheets for Polymers: Barazan D, Liqui-Vis and N-Vis.

Belkin, A., Irving, M., O'Connor, R., Fosdick, M., Hoff, T., Growcock, F.B. (2005) How Aphron Drilling Fluids Work, SPE 96145, 2005 SPE Annual Technical Conference and Exhibition, October 9-12, Dallas, TX.

bioWORLD® Product Data Sheet for Surfactant CTAB.

Bjorndalen, N., and Kuru, E. (2005) Physico-Chemical Characterization of Aphron Based Drilling Fluids, Paper 2005-050, 2005 Petroleum Society's 6th Canadian International Petroleum Conference (56th Annual Technical Meeting), June 7-9, Calgary, AB.

Bjorndalen, N., and Kuru, E. (2006) Stability of Microbubble Based Fluids Under Downhole Conditions, Paper 2006-079, 2006 Petroleum Society's 7th Canadian International Petroleum Conference (57th Annual Technical Meeting), June 13-15, Calgary, AB.

Bjorndalen N., Jossy, E., Alvarez, J.M. and Kuru, E. (2007) Reducing Formation Damage with Microbubble Based Drilling Fluid: Understanding the Blocking Ability, Paper 2007-091, 2007 Petroleum Society's 8th Canadian International Petroleum Conference (58th Annual Technical Meeting), June 12-14, Calgary, AB.

Bjorndalen N., Jossy, E., Alvarez, J.M. and Kuru, E. (2010) A Laboratory Investigation of the Factors Controlling Filtration Loss when Drilling with Colloidal Gas Aphrons (CGA) Fluids. 2010 SPE International Symposium and Exhibition on Formation Damage Control, February 10-12, Lafayette, LA.

Bjorndalen, N. (2011) A Study of the Rheology, Stability and Pore Blocking Ability of Aqueous Colloidal Gas Aphron Drilling Fluids. PhD thesis. University of Alberta, Edmonton, 2010.

Brookey, T. (1998) "Microbubble": New Aphron Drill-In Fluid Technique Reduces Formation Damage in Horizontal Wells. SPE 39589, 1998 SPE

International Symposium on Formation Damage Control, February 18-19, Lafayette, LA.

Chapalkar, P.G., Valsaraj, K.T. and Roy, D. (1994) Separation Science and Technology (1994), Volume 28 Issue 6, Page 1287.

Chauveteau, G. (1982) Rodlike Polymer Solution Flow through Fine Pores: Influence of Pore Size on Rheological Behaviour, Journal of Rheology, Volume 26 Issue 2, Pages111-142.

Christopher, R.H. and Middleman, S. (1965) Power-Law Flow through a Packed Tube, Industrial and Engineering Chemistry Fundamentals, Volume 4 Issue 4, Pages 422-426.

Feng, W., Singhal, N. and Swift, S. (2009) Drainage Mechanism of Microbubble Dispersion and Factors Influencing its Stability. Journal of Colloid and Interface Science, Issue 337 (2009), Pages 548-554.

Fisher Scientific® Product Data Sheet for Mineral Oil.

Gardescu, I.I. (1930) Behaviour of Gas Bubbles in Capillary Spaces. AIME Technology Publication, 306.

Gaurina-Medimuric N. and Pasic, B. (2009) Aphron Based Drilling Fluids: Solution for Low Pressure Reservoirs, Rudarsko-geolosko-naftni zbornik (Zagreb, 2009), Volume 21, Pages 65-72.

Growcock, F.B., Khan, A.M., and Simon, G.A. (2003) Application of Water-Based and Oil-Based Aphrons in Drilling Fluid. SPE 80208, 2003 SPE International Symposium on Oilfield Chemistry, February 5-7, Houston, TX.

Growcock, F.B., Simon, G.A., Rea, A.B., Leonard, R.S., Noello, E. and Castellan, R. (2004) Alternative Aphron-Based Drilling Fluid. IADC/SPE 87134, 2004 IADC/SPE Drilling Conference, March 2-4, Dallas, TX.

Growcock, F. (2005) Enhanced Wellbore stabilization and Reservoir Productivity with Aphron Drilling Fluid Technology. Final Report, DPE Award Number DE-FC26-03NT42000, October.

Growcock F.B., Belkin, A., Fosdick, M., Irving, M., O'Connor, B. and Brookey, T. (2007) Recent Advances in Aphron Drilling-Fluid Technology. SPE 97982, SPE Drilling and Completion Journal June 2007, Volume 22 Number 2, Pages 74-80.

Halliburton® Product Data Sheet for Quik-Trol.

Hashim, M.A., Dey, A., Hasan, S. and Gupta, B.S. (1999) Mass Transfer Correlation in Flotation of Palm Oil by Colloidal Gas Aphrons. Bioprocess Engineering Volume 21 (1999), Pages 401-404, Springer-Verlag 1999.

Hashim, M.A., Kumar, S.V. and Gupta, B.S. (2000) Particle Bubble Attachment in Yeast Flotation by Colloidal Gas Aphrons. Bioprocess Engineering Volume 22 (2000), Pages 333-336, Springer-Verlag 2000.

He Xiaoqing (2010) The Past, Present and Future of Aphron Based Drilling Fluids. SPE 141136. 2010 SPE Annual Technical Conference and Exhibition, September 19-22, Florence, Italy.

Ivan, C.D., Quintana, J.L., Blake, L.D. (2001) Aphron Base Drilling Fluid: Evolving Technologies for Lost Circulation Control. SPE 71377, 2001 SPE Annual Technical Conference and Exhibition, September 30-October 3, New Orleans, LA.

Jauregi, P. and Varley, J. (1996) Lysozome Separation by Colloidal Gas Aphrons. Progess in Colloid and Polymer Science (1996), Volume 100, Pages 362-367.

Jauregi, P., Golmour, S. and Varley, J. (1997) Characterization of Colloidal Gas Aphrons for Subsequent Use for Protein Recovery. The Chemical Engineering Journal, Volume 65, Pages 1-11.

Leica Microsystems, Leica DM 6000 User Manuals.

MacPhail, W.F., Cooper, R.C., Brookey, T. and Paradis, J. (2008) Adopting Aphron Fluid Technology for Completion and Workover Applications. SPE 112439, 2008 SPE International Symposium and Exhibition on Formation Damage Control, February 13-15, Lafayette, LA.

Malverne Instruments, User Manual Bohlin CVOR.

Matsushita, K., Mollah, A.H., Stuckey, D.C., Del Cerro, C. and Bailey, A.I. (1992) Colloids Surface. Volume 69 (1992), Page 65.

Oliveira, R.C.G., Oliviera, J.F., and Moudgil, B.M. (2004) Optimizing Micro-foam Rheology for Soil Remediation. Progress in Colloid and Polymer Science (2004), Issue 128, pages 298-302.

Polytron User Manual for PT 6100.

Puerto, M., Hirasaki, G.J., Miller, C.A., and Barnes, J.R. (2010) Surfactant Systems for EOR in High-Temperature, High-salinity Environments. SPE 129675. 2010 Improved Oil Recovery Symposium, April 24-28, Tulsa, OK.

Ramirez, F., Greaves, R. and Montilva, J. (2002) Experience Using Microbubbles-Aphron Drilling Fluid in Mature Reservoirs of Lake Maracaibo. SPE 73710. 2002 International Symposium and Exhibition on Formation Damage Control, February 20-21, Lafayette, LA.

Rea, A.B., Alvis, E.C., Paiuk, B.P., Climaco, J.M., Vallerjo, M., Leon, E. and Inojosa, J. (2003) Application of Aphrons Technology in Drilling Depleted Mature Fields. SPE 81082. 2003 SPE Latin American and Caribbean Petroleum Engineering Conference, April 27-30, Port-of-Spain, Trinidad.

Samanta, A., Ojha, K., Sarkar, A., and Mandal, A. (2011) Surfactant and Surfactant-Polymer Flooding for Enhanced Oil Recovery. CS Canada Advances in Petroleum Exploration and Development, Volume 2, Number 1, Pages 13-18.

Save, S.V and Pangarkar, V.G. (1993) Characterization of Colloidal Gas Aphrons. Chemical Engineering Communications, Volume 127, Pages 35-54.

Schaneman, B.D., Jones, T., and Rea, A.B. (2003) Aphrons Technology- A Solution, AADE-03-NTCE-41. 2003 AADE National Technology Conference- Practical Solutions for Drilling Challenges, April 1-3, Houston, TX.

Sebba, F. (1985) An Improved Generator for Micron-sized Bubbles. Chemistry and Industry. February 4, Pages 91-92.

Sebba, F. (1987) Foams and Bilquid Foams-Aphrons, John Wiley and Sons, Toronto. 236 pages.

Shivhare, S. and Kuru, E. (2010) Physico-Chemical Characterization of Non-Aqueous Colloidal Gas Aphron Based Drilling Fluids. SPE 133274. 2010 Canadian Unconventional Resources and International Petroleum Conference, October 19-21, Calgary, AB.

Shivhare, S. (2011) A Study of the Rheology, Stability and Pore Blocking Ability of Non Aqueous Colloidal Gas Aphron Drilling Fluids. MS thesis. University of Alberta, Edmonton, 2011.

Sigma-Aldrich® Product Data Sheets for Surfactants DDBS and Tergitol

Spinelli, L.S., Neto, G.R., Freire, L.F.A., Monteiro, V., Lomba, R., Michel, R. and Lucas, E. (2010) Synthetic Based Aphrons: Correlation between Properties and Filtrate Reduction Performance. Colloids and Surfaces A: Physicochemical Engineering Aspects 353 (2010), Pages 57-63.

Veerabhadrappa, S.K., Urbinissova, T.S., Trivedi, J. and Kuru, E. (2011) Polymer Screening Criteria for EOR Application- A Rheological Characterization

Approach. SPE 144570. 2011 SPE Western North American Regional Meeting, May 7-11, Anchorage, AK.

Xu, Q., Nakajima, M., Ichikawa, S., Nakamura, N., Roy, P., Okadome, H. and Shiina, T. (2009) A Comparative Study of Microbubble Generation by Mechanical Agitation and Sonication. Journal of Colloid and Interface Science 332 (2009), Pages 208-214.

Zhao, J., Pillai, S. and Pilon, L. (2009) Rheology of Colloidal Gas Aphrons (Microfoams) made from Different surfactants. Colloids and Surfaces A: Physicochemical Engineering Aspects 348 (2009), Pages 93-99.